

AD _____

Award Number:

W81XWH-o8-2-0157

TITLE:

Glyburide – Novel Prophylaxis and Effective Treatment for Traumatic Brain Injury

PRINCIPAL INVESTIGATOR:

J. Marc Simard, M.D., Ph.D.

CONTRACTING ORGANIZATION:

University of Maryland, Baltimore
Baltimore, MD 21201

REPORT DATE:

UNCLASSIFIED

TYPE OF REPORT:

Final

PREPARED FOR: U.S. Army Medical Research and Materiel Command
Fort Detrick, Maryland 21702-5012

DISTRIBUTION STATEMENT: Approved for Public Release;
Distribution Unlimited

The views, opinions and/or findings contained in this report are those of the author(s) and should not be construed as an official Department of the Army position, policy or decision unless so designated by other documentation.

REPORT DOCUMENTATION PAGE				Form Approved OMB No. 0704-0188	
Public reporting burden for this collection of information is estimated to average 1 hour per response, including the time for reviewing instructions, searching existing data sources, gathering and maintaining the data needed, and completing and reviewing this collection of information. Send comments regarding this burden estimate or any other aspect of this collection of information, including suggestions for reducing this burden to Department of Defense, Washington Headquarters Services, Directorate for Information Operations and Reports (0704-0188), 1215 Jefferson Davis Highway, Suite 1204, Arlington, VA 22202-4302. Respondents should be aware that notwithstanding any other provision of law, no person shall be subject to any penalty for failing to comply with a collection of information if it does not display a currently valid OMB control number. PLEASE DO NOT RETURN YOUR FORM TO THE ABOVE ADDRESS.					
1. REPORT DATE September 2014		2. REPORT TYPE Final		3. DATES COVERED 7 Jul 2008 - 30 Jun 2014	
4. TITLE AND SUBTITLE Glyburide – Novel Prophylaxis and Effective Treatment for Traumatic Brain Injury				5a. CONTRACT NUMBER	
				5b. GRANT NUMBER W81XWH-08-2-0157	
				5c. PROGRAM ELEMENT NUMBER	
6. AUTHOR(S) J. Marc Simard, M.D., Ph.D. E-Mail: msimard@smail.umaryland.edu				5d. PROJECT NUMBER	
				5e. TASK NUMBER	
				5f. WORK UNIT NUMBER	
7. PERFORMING ORGANIZATION NAME(S) AND ADDRESS(ES) University of Maryland, Baltimore Baltimore, MD 21201				8. PERFORMING ORGANIZATION REPORT NUMBER	
9. SPONSORING / MONITORING AGENCY NAME(S) AND ADDRESS(ES) U.S. Army Medical Research and Materiel Command Fort Detrick, Maryland 21702-5012				10. SPONSOR/MONITOR'S ACRONYM(S)	
				11. SPONSOR/MONITOR'S REPORT NUMBER(S)	
12. DISTRIBUTION / AVAILABILITY STATEMENT Approved for Public Release; Distribution Unlimited					
13. SUPPLEMENTARY NOTES					
14. ABSTRACT Addressing specific objectives of the project we developed, constructed and implemented a cranium only blast injury apparatus (COBIA) for production of standardized and reliable rat model of “dose dependent” blast-TBI (bTBI) to study the direct transcranial effects of blast on the brain, independent of indirect transthoracic effects Detailed anatomical evaluation revealed that cranium only blast impacts brain-blood barrier transiently, immediately after the blast. Long term impact of the blast is manifested predominantly in the brain tissues at the density boundaries, with elevated markers of the neuroinflammation, neurodegeneration and neuronal cell death. COBIA bTBI resulted in the transient vestibulomotor abnormalities and long term spatial memory deficits. After COBIA bTBI Sur1 and TRPM4 RNA and protein up-regulation was detected as early 4 hours after the blast consistent with de-novo expression of the SUR1 regulated NC _{Ca} -ATP channel Studies (including GLP-compliant protocol) with chronic administration of the SUR1 antagonist showed that post-bTBI Glyburide does not alter blast-induced long term cognitive deficits but improves anxiety-like behavior. In contrast prophylactic treatment with Glyburide improved performance in spatial memory task related to the hippocampal function. Study on the human volunteers showed that Glyburide is safe drug to be used for potential prophylaxis against blast –TBI.					
15. SUBJECT TERMS blast-TBI, sulfonylurea receptor					
16. SECURITY CLASSIFICATION OF:			17. LIMITATION OF ABSTRACT UU	18. NUMBER OF PAGES 75	19a. NAME OF RESPONSIBLE PERSON USAMRMC
a. REPORT U	b. ABSTRACT U	c. THIS PAGE U			19b. TELEPHONE NUMBER (include area code)

Table of Contents

	Page
	<hr/>
Introduction.....	4
Body.....	4
Objectives	5
Objective 1a.....	5
Objective 1b.....	12
Objective 1c.....	16
Objective 2a.....	20
Objective 2b.....	27
Objective 3a.....	31
Objective 3b.....	36
Summary of animal use.....	38
Objective 4	39
Key Research Accomplishments.....	43
Reportable Outcomes.....	44
Conclusion.....	46
References.....	47
Supporting data.....	49

INTRODUCTION: Narrative that briefly (one paragraph) describes the subject, purpose and scope of the research.

Explosive munitions cause more than half of all injuries sustained in military combat, and are responsible for an increasing number of civilian casualties ((1-6)). Traumatic brain injury due to an explosive blast (blast-TBI or bTBI) is one of the most serious wounds suffered by warfighters in modern conflicts. bTBI can range from overt injuries marked by soft tissue damage to the face and scalp complicated by open brain injury, to more insidious injuries with no external physical damage that manifest as persistent neurocognitive or psychological abnormalities ((2, 7-12)). Tremendous progress has been made in understanding the pathophysiology of blast injury (BI) to the brain that is caused by the intense transient overpressure of the blast wave generated by an explosion. Importantly, the so-called “thoracic mechanism” has come to be recognized, whereby the brain is believed to be injured indirectly by a blast wave that impacts the gas-filled thoracic cavity and is transmitted to the brain by way of major blood vessels in the neck ((7, 13-15)). Preclinical work has confirmed the importance of protecting against the thoracic mechanism of BI to the brain ((15, 16)).

The sulfonylurea receptor 1 (SUR1)-regulated NCCa-ATP channel is a 30-pS channel that conducts monovalent but not divalent cations ((17)). This channel is not constitutively expressed, but is newly upregulated in neurons, astrocytes, and capillary endothelial cells after central nervous system (CNS) ischemia or trauma. The channel is inactive when expressed, but becomes activated when intracellular ATP is depleted, with activation leading to cell depolarization, cytotoxic edema, and oncotic cell death ((18-20)). Pathological involvement of the channel in capillaries results in formation of ionic and vasogenic edema ((20-22)), has been postulated to predispose to hemorrhagic transformation in the context of ischemia ((23)), and has been shown to be responsible for secondary hemorrhage following spinal cord trauma ((24)). In rodent models of ischemic stroke, subarachnoid hemorrhage, spinal cord injury, and hemorrhagic contusion of the brain, block of the SUR1-regulated NCCa-ATP channel by glibenclamide or other SUR1 inhibitors results in significant improvements in edema, lesion volume, neurological function, and mortality ((20, 22, 24)). In humans with diabetes mellitus, use of sulfonylureas before and during hospitalization for stroke is associated with significantly better stroke outcomes ((25)).

NOTE: This final report covers all animal research activity throughout the period of the grant awarded, which reflects requested modification of the grant to extend project for one more year without additional funds.

BODY: This section of the report shall describe the research accomplishments associated with each task outlined in the approved Statement of Work. Data presentation shall be comprehensive in providing a complete record of the research findings for the period of the report. Provide data explaining the relationship of the most recent findings with that of previously reported findings. Appended publications and/or presentations may be substituted for detailed descriptions of methodology but must be referenced in the body of the report. If applicable, for each task outlined in the Statement of Work, reference appended publications and/or presentations for details of result findings and tables and/or figures. The

report shall include negative as well as positive findings. Include problems in accomplishing any of the tasks. Statistical tests of significance shall be applied to all data whenever possible. Figures and graphs referenced in the text may be embedded in the text or appended. Figures and graphs can also be referenced in the text and appended to a publication. Recommended changes or future work to better address the research topic may also be included, although changes to the original Statement of Work must be approved by the Army Contracting Officer Representative. This approval must be obtained prior to initiating any change to the original Statement of Work.

Background: In humans TBI following an area-blast is a complex multi-faceted disease. Pathophysiologically, blast-TBI results in brain edema, swelling, hemorrhage, neuronal injury, degeneration, and death, leading to severe neurological and neuropsychological deficits and possibly death. The primary blast injury in itself is complex, and is believed to occur by way of two distinct mechanisms: (i) direct transcranial propagation of the blast wave; (ii) indirect transmittal via vasculature following blast to the thorax. All the existing work on blast-TBI exposes the subject's total body to an area-blast. Whereas this approach appropriately simulates the real-world combat experience, it does not permit assessment of direct blast injury to the brain in isolation of indirect injury to the brain due to blast injury to other organs, especially the lungs and major vessels within the thorax. The transmission of a blast wave through the skull to the brain has long been postulated ((10)), but this "direct" mechanism of injury has garnered less attention than the "indirect" thoracic mechanism, owing perhaps to the impression that the brain is protected from direct injury by the relatively rigid skull. However, it has been shown that a blast wave can traverse the cranium of the rat almost unchanged ((26)). Numerical simulations that take into account the physical properties of the skull and other tissues of the head exposed to an explosive blast predict that a nonlethal blast can interact with CNS tissues to cause brain injury ((27, 28)). In principle, a blast wave may induce sufficient flexure of the skull to generate damaging loads within the brain, or it may deposit kinetic energy at boundaries between tissues of different density. Despite such observations and considerations, the effects of an explosive blast overpressure directly impacting the head are poorly understood. Prior to our work that we reporting in the first section, no animal model existed to examine the direct transcranial mechanism of blast-TBI, independent of the indirect transthoracic mechanism. Compression driven and blast driven shock tubes have been used to apply blast waves to test subjects and materials. Both typically have diameters too large to isolate the blast exposure to a single anatomical area, to study separately tissue and cellular in each organ (head, thorax).

Objectives.

The overall subject of this research project is direct cranial blast-traumatic brain injury (dcBI-TBI) and the role of the SUR1-regulated NCCa-ATP channel in secondary injury following dcBI. The specific objectives of this research project may be summarized as follows:

- (1) Develop standardized rat model of direct cranial blast-TBI,
 - a) Establish the usable working range for the "intensity-response" relationship between blast intensity and outcome in our blast-TBI model (**Objective 1a**)

- b) Assess the model through various (short and long term) behavioral tests **(Objective 1b)**
 - c) Assess the model through histology (edema, hemorrhage, tissue sodium) in the brain of the rats **(Objective 1c)**.
- (2) Using this rat model, determine the specific role of the SUR1-regulated NCCa-ATP channel in blast-TBI, the time course for SUR1 and TRPM4 upregulation and downregulation after blast-TBI.
 - a) SUR1 and TRPM4 upregulation after blast-TBI **(Objective 2a)**
 - i) immunohistochemistry
 - ii) immunoprecipitation/western blot
 - iii) qualitative PCR
 - b) Short and long term pathologic changes in different brain regions; evaluation of different apoptotic and neurodegenerative protein expressions **(Objective 2b)**.
- (3) Evaluate the treatment effect of Glibenclamide: including testing whether block of SUR1 using glibenclamide would show a beneficial effect in blast-TBI. Assess through short and long term behavioral, cognitive and memory tests.
 - a. Glibenclamide treatment after mild and severe Blast-TBI **(Objective 3a)**.
 - b. Pre-treatment with glibenclamide rats undergoing Blast-TBI **(Objective 3b)**.
- (4) In normal human volunteers, determine the safety of oral glibenclamide as it might be used as prophylaxis against blast-TBI **(Objective 4)**.

Objective 1a: establish the usable working range for the “intensity-response” relationship between blast intensity and outcome in our blast-TBI model

Our aim in this objective was to develop a standardized rodent model for direct cranial blast, a postulated mechanism, “direct transcranial”, which is less studied than the transthoracic.

We developed and validated a direct transcranial blast model. A detailed description and validation of the **Cranium Only Blast Injury Apparatus (COBIA)** to deliver blast overpressures generated by detonating .22 caliber cartridges of smokeless powder was published (2011) in *J. Neurotrauma*. ((29))(Fig. 1)

COBIA: Blast is powered by detonating a .22 caliber blank shot [Remington, power level 2 or power level 4 shots; weight of powder (means±S.D.): 0.128±0.003 or 0.179±0.003gm, respectively] inside the firing chamber of a gun (ITW Ramset, Model RS22, Glenview IL; with piston removed). The blast is directed down the barrel of the gun, which interfaces with one of a variety of interchangeable, 2 sets with two different diameters (2.05cm, and 2.54 cm) of custom-made blast dissipation chambers (BDC), all with the same cylindrical shape but with different lengths. Due to different differences in length/volume, different BDC yield different magnitude of blast intensity (Table 1) delivered to the cranium. The BDC terminates in a BDC-cranium interface (BDCCI), which directly contacts the scalp of the dorsal cranium of the rat. The BDCCI is fitted with an O-ring constructed of a soft material that forms a gentle seal with the scalp. The dorsum of the rat’s head (shaved scalp) is lifted into place against the O-ring by use of

an inflatable pillow positioned beneath the mandible that is inflated to 75 mm Hg to form the seal. The entire assembly of gun, BDC, BDCCI and the platform used to support the rat, is held vertically with the aid of two vertically adjustable stages, the upper one of which fixes the gun and neutralizes its safety, and the other of which allows accommodating different sizes (lengths) of BDCs. (Fig.1)

Blast Overpressure Measurements:

Blast pressure measurements were made using a pressure transducer and charge amplifier (model 100P and 4601, respectively; Columbia Research Labs, Woodlyn, PA), with the output recorded using a D-A converter (Digidata 1200 data acquisition system, Axon Instruments). Typical recordings of blast waveform, with the transducer placed where the rat's head would be, show an initial large transient overpressure, followed by smaller transient under- and overpressures which are fully damped after ~2 sec. (Fig. 3). At high temporal resolution, the initial overpressure is seen to be quite complex, including a "quasi-static" pressure component (Fig. 3B). Notably, the initial complex overpressure waveforms generated by the COBIA resemble closely the published recordings of blast overpressure waveforms recorded in an armored vehicle penetrated by shaped charge munitions (Fig. 3B). Initial peak overpressure measurements recorded with different BDCs are given in Table 1 for power level 2 and level 4 shots. The plots of these shots are in Fig. 3C.

Pressure-step generator. Although the charge amplifier was factory calibrated, we sought to independently verify the calibration for the range of pressures that we would be studying. We constructed a device to generate pressure steps of known magnitude that could be recorded by the pressure measuring system. The pressure-step generator consisted of two chambers, a source chamber and a test chamber, separated by a solenoid-operated valve (#8262G202 120/60, normally closed; Asco, Florham Park, NJ; Fig. 2A). The source chamber (22,712 mL) was pressurized using an air compressor (6 gallon, Model #C2002-WK; Porter-Cable, Jackson, TN), with the exact pressure adjusted to the desired value using a bleed valve, and measured using a factory-calibrated, precision static pressure gauge (4001 heavy duty 4-inch; 0.5% accuracy full scale; Precision Instrument Co., Kennesaw, GA). The test chamber (15 mL) included a valve to allow decompression of the test chamber after each test cycle, and an endcap to interface with the piezoelectric pressure transducer being tested. The apparatus was capable of generating pressure steps from 0 to 600 kPa with a rise time (from 10–90%) of * 9 msec. Generating a pressure step did not result in any measureable drop in pressure in the source chamber, due to the large difference in volume between the chambers.

Validating the pressure measuring system. Pressure steps from 0 to 137.9–551.6 kPa, in increments of 68.9 kPa, were generated using the pressure-step generator, and was recorded using the pressure measuring system. All measurements were repeated in triplicate. Because the pressure measuring system acts like a second-order bandpass filter, measurements of steady-state pressures were not possible and some ringing of the peak was observed (Fig. 2B). Therefore the decay phases of the recorded waveforms (from the peak out to 1000 msec) were fit with a second-order exponential equation (s_1 , 230–300 msec; s_2 , 50–90 msec) to estimate the peak pressure. Values from the fits were plotted against the steady-state input pressure, showing excellent agreement; a least-squares fit of the data yielded a slope of 1.025 and an intercept of - 7.1 kPa (Fig. 2C), confirming proper calibration of the pressure measuring system.

Figure 1: Cranium Only Blast Injury Apparatus (COBIA).

(A) Photo of the COBIA showing the vertically-oriented gun interfacing with the blast dissipation chamber (BDC), which connects in turn to the BDC-cranium interface (BDCCI). (B–D) Views of the BDCCI before (B) and after (C and D) positioning the intubated, anesthetized rat; note the uninflated balloon in B, which when inflated to 10 kPa, promotes contact between the scalp and the O-ring of the BDCCI, resulting in reproducible positioning of the head before injury, and which partially cushions the head during downward acceleration from the blast wind. (E) Photo of several of the BDCs used, identified by the numbers referred to in Table 1; to the left is shown the brass coupler that interfaces between the barrel of the gun, the BDC, and the BDCCI.

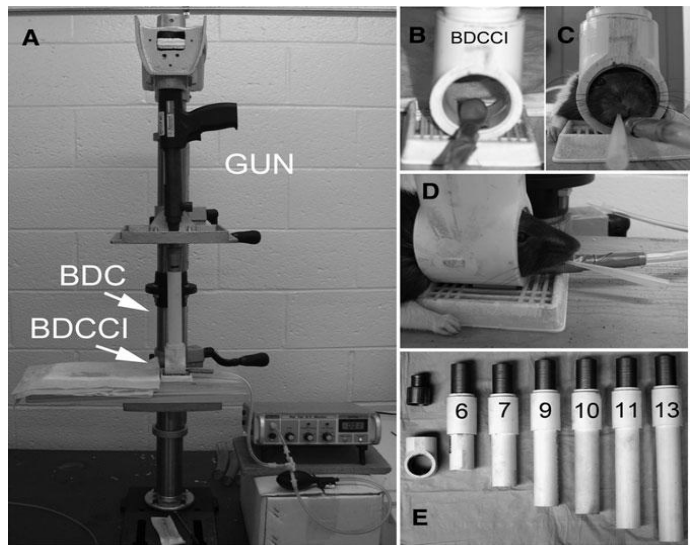


Figure 2: Validation of the pressure measuring system. (A) The pressure step generator used to validate the pressure measuring system (see methods section for description). (B) The input pressure step (above) and the output waveform recorded during a validation test run (below); the inset shows the peak of the recorded waveform to illustrate ringing, and the double exponential fit used to estimate the peak value. (C) Plot of the steadystate input pressures versus the measured peak pressures estimated from double exponential fits; a least-squares-fit of the data indicated a slope of 1.025 and an intercept of - 7.1 kPa, confirming proper calibration of the pressure measuring system.

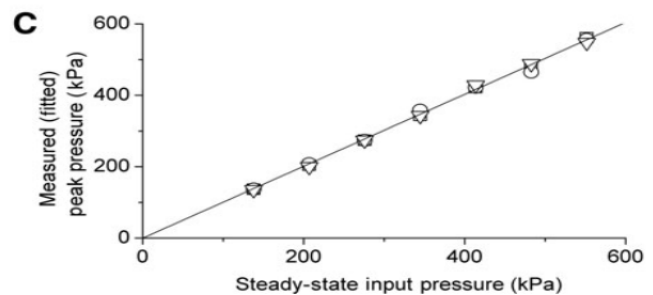
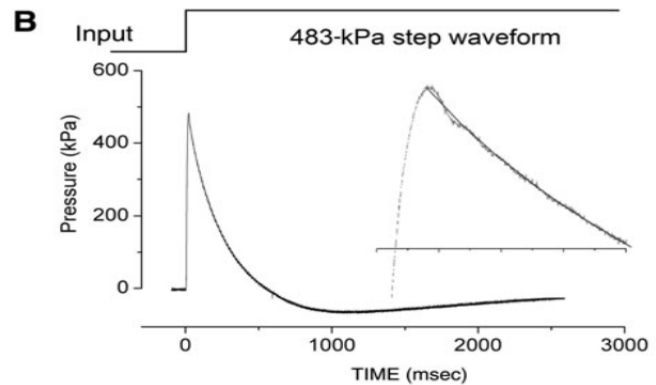
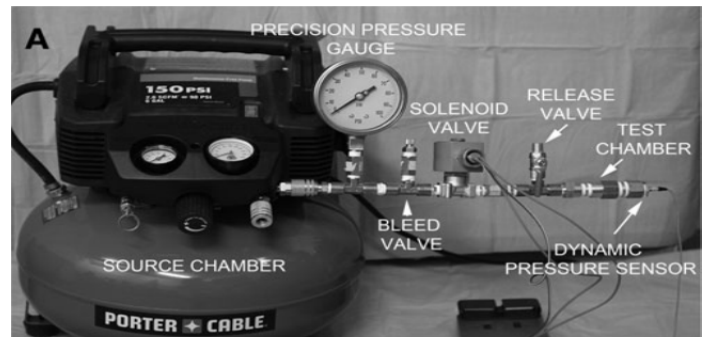


Table 1. Peak Overpressure with Various Blast Dissipation Chambers (BDCs)

BDC	Length of BDC (with BDC-cranium interface) (cm)	Diameter of BDC (cm)	Peak overpressure power level 2 (kPa)	Peak overpressure power level 4 (kPa)
1	9.5	2.05	579	1372
2	10.5	2.05	545	1054
2	14.5	2.05	483	869
4	19	2.05	414	655
5	30	2.05	303	483
6	14	2.54		
7	17	2.54	421	669
8	19.5	2.54	365	655
9	22	2.54	317	545
10	23.25	2.54	303	531
11	24.5	2.54	290	517
12	27	2.54	262	462
13	28.25	2.54	276	448
14	29.5	2.54	269	427

The values shown are the means of 5-10 test firings

Figure 3. Positioning of the head inside the Cranium Only Blast Injury Apparatus (COBIA), and absence of significant inward flexure of the skull by the blast. (A) Photograph of a rat skull and a clear cylinder (2.54 cm diameter), demonstrating the position of the skull inside the COBIA; note that the external occipital crest (arrow) is situated * 1/3 of the way inside the inner circumference of the cylinder, allowing this strong ridge of bone to buttress the skull against inward flexure during the blast. (B and C) Photographs from above of a rat skull (B) and of a live rat head (C) positioned inside the blast dissipation chamber-cranium interface (BDCCI) of the COBIA; note the position of the external occipital crest (arrows), which is visually apparent in B, and which is marked on the scalp with black ink in (C), snout facing downward. (D and E) Photographs of the thin glass strain gauge glued to the exposed skull over the lambda, before (D) and after (E) exposure to an explosive blast of 517 kPa; note the absence of fractures in the glass in E, indicating that if inward flexure of the skull occurred, it was < 200 μ m at the lambda (see methods section for details), snout facing downward.

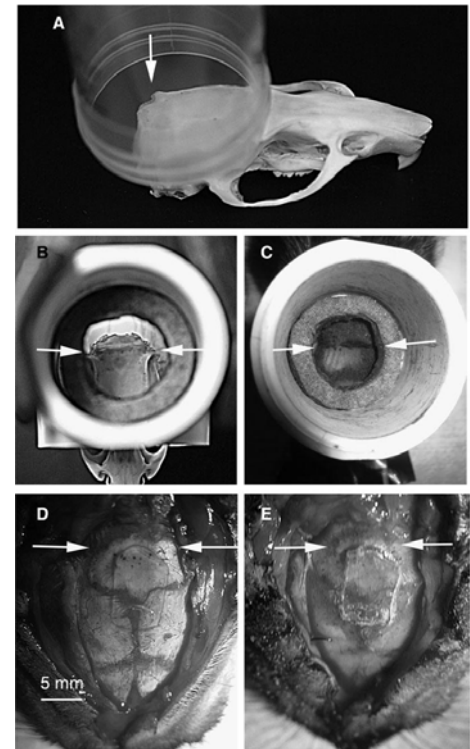
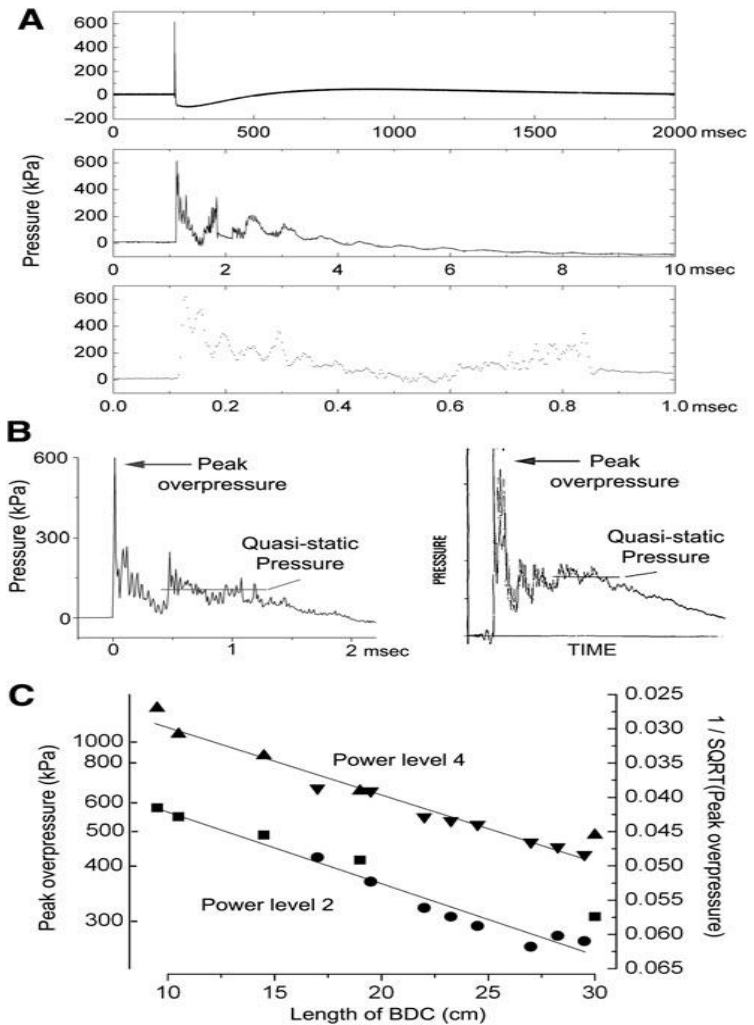


Figure 3: Pressure waveforms generated by the Cranium Only Blast Injury Apparatus (COBIA). (A) Pressure waveforms generated by the COBIA shown at three temporal resolutions, with the lowest resolution showing the typical appearance of a Friedlander wave. (B) Comparison of a pressure waveform generated by the COBIA (left), and a published waveform of a blast recorded inside an armored vehicle penetrated by a shaped-charge munition (right; adapted from Stuhmiller et al., 1991). (C) Plot of the inverse of the square root (SQRT) of the peak overpressures (right-sided ordinate) generated using blast dissipation chambers (BDCs) of different lengths and cartridges of different power levels, versus the length of the BDC, demonstrating the linear relationship expected for the inverse square law; the values of the peak overpressures are given on the left-sided ordinate (data from Table 1).



Blast (COBIA) Injury Model: All procedures were approved by the Institutional Animal Care and Use Committee of the University of Maryland School of Medicine. This research was conducted in compliance with the Animal Welfare Act Regulations and other federal statutes relating to animals and experiments involving animals, and adheres to the principles set forth in the Guide for the Care and Use of Laboratory Animals, National Research Council, 1996. Male Long-Evans rats (300±10 g; Harlan, Indianapolis, IN) were anesthetized (60 mg/kg ketamine plus 7.5 mg/kg xylazine, IP), intubated with an endotracheal tube, and were allowed to breathe air spontaneously. Core temperature was maintained at 37°C using an isothermal pad (Deltaphase; Braintree Scientific, Braintree, MA). The hair was clipped from the dorsum of the head.

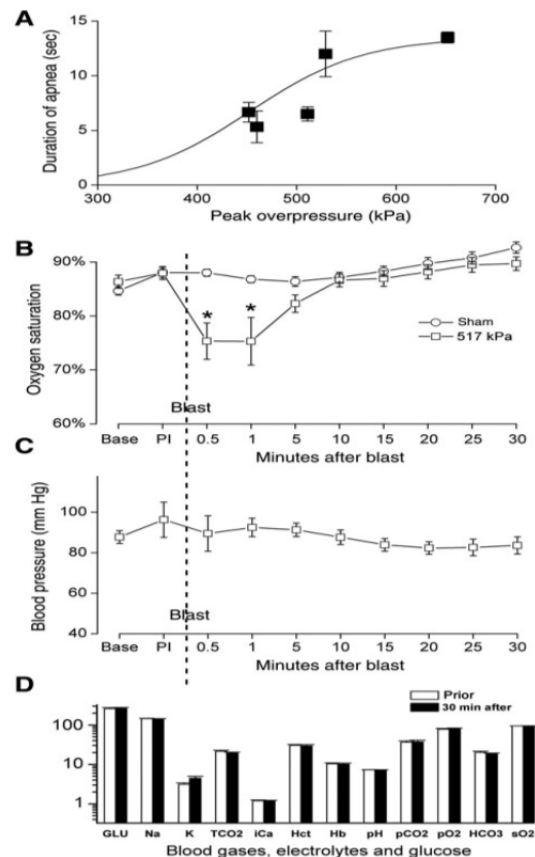
The rat was positioned prone with the vertex carefully placed against the O-ring of the BDCCI (Fig. 1D). The head was positioned so that when viewed from above, the external occipital crest was $\approx 1/3$ of the way inside the inner circumference of the BDCCI (Fig. 1B–C). Just prior to detonation, a small balloon under the rat's lower jaw was inflated to 10 kPa to promote contact between the scalp and the O-ring, resulting in reproducible positioning of the head inside the COBIA before the blast. The balloon

beneath the jaw also served to cushion (but not prevent) the head from downward acceleration during the blast.

Positioning the head as described above reduced the exposure to blast of the thin parietal and frontal bones, and of the weakest structures, the sutures between these bones, and allowed the external occipital crest to act as a buttress to prevent inward flexure of the skull during the blast. We assessed for possible inward flexure of the skull, which has been reported in other models ((16)), using a thin piece of glass as a strain gauge spanning the sutures exposed to the blast (Fig. 3XD). In separate measurements, the glass strain gauge (a cover-slip 0.15mm thick) was found to fracture by deflecting 0.2mm midway over a span of 10mm (n = 6). After exposing the dorsum of the skull of an anesthetized rat, the glass strain gauge was glued to the skull, centered over lambda, using alpha cyanoacrylate adhesive (Fig. 3XD). The scalp incision was sutured and the rat was exposed to a blast overpressure (517 kPa), as detailed above. After the blast, examination of the glass strain gauge revealed no fracture (Fig. 3XE), indicating that if inward flexure occurred, it was < 200 μ m at the lambda.

In the usual blast injury procedure, after the blast, the rat was removed from the apparatus and was observed for apnea. If spontaneous respiration did not resume within 10 sec, the endotracheal tube was connected to a ventilator (Micro- Vent gas, compressed air; Hallowell, Pittsfield, MA), and ventilatory support as well as chest massage were instituted and maintained until either spontaneous cardiopulmonary function resumed or until cardiac arrest was deemed to be irreversible. Survivors were nursed on a heating pad until they recovered spontaneous movements. For sham injury, all of the above was performed except for detonating the cartridge.

Figure 4: Sub-lethal direct cranial blast injury (dcBI). (A) Plot of the duration (mean – standard error) of apnea versus peak overpressure; data are from 3–12 rats at each point; 30 rats total. (B) Plot of the oxygen saturation during the initial 30 min following sub-lethal dcBI (517 kPa) in 13 sham and 17 injured rats (*p < 0.05). (C) Plot of systolic blood pressure during the initial 30 min following sub-lethal dcBI (427–517 kPa; 26 rats). (D) Bar graphs comparing blood gases, serum electrolytes, and serum glucose before and 30 min after dcBI (427–517 kPa; 17 rats); all values were normal before injury, and except for potassium, were not significantly affected by injury; the slight elevation in potassium was attributed to hemolysis due to clotting in the indwelling catheter (GLU, glucose; Na, sodium; K, potassium; TCO₂, total carbon dioxide; iCa, ionized calcium; Hct, hematocrit; Hb, hemoglobin; pCO₂, partial carbon dioxide pressure; pO₂, partial oxygen pressure; HCO₃, bicarbonate; sO₂, oxygen saturation).



Objective 1b: Assessment of the model through different vestibulomotor behavior, and cognitive and memory tests.

Neurofunctional testing

Vertical Exploration: Neurobehavioral function is assessed by quantifying the total time spent in vertical exploration during a 3-min period of observation. Vertical exploration involves not only complex, coordinated sensorimotor performance, as does the Roto Rod test, but in addition, it involves sophisticated voluntary cognitive behavior(30, 31) not required by the Roto Rod test. Animals are placed in the transparent 24" in vertical cylinder 15" diameter and spontaneous activity is calculated by time spent in vertical position.

Beam Balance: Rats are evaluated on a thin rod for their balancing ability and they are scored according to the limb position and ability to stay on the rod. Scores are from 0 to 4, (0) means all 4 limbs are on the rod, (1) at least one limb is on the side, (2) if two or more limbs are on the side, (3) if the animal slips while balancing on the rod, and (4) if not able to stay on the rod.

Beam Walk: Rats are trained to walk a distance of 3 feet on a narrow rod to enter a dark box with a small opening on the other side of the rod, while escaping a noisy discomfort above their head while walking. The time to pass the three feet will be recorded. Three trials will be conducted each test day with a 5 minute rest time in between trials.

Accelerating Rotorod: The accelerating Rotorod test is used to assess coerced locomotor activity (Hamm, 2001). The rats are placed on the drum of the accelerating Rotorod (starting at 4 rpm, accelerating at a rate of 2 rpm every 5 sec up to a maximum of 45 rpm; IITC, Life Science, Woodland Hills, CA), with 3 trials separated by 20 min administered on each day of testing. We report the average latency to falling off of the drum.

Cognitive and memory testing

Morris Water Maze

Rats are maintained in the animal facility under standard laboratory conditions (lights on at 0600 and off at 1800), housed in pairs or triplets, and having access to food and water ad libitum after surgical procedures and throughout MWM testing. All MWM trial blocks are conducted at the same time each day.

The maze consists of a circular pool (1.45 m diameter, 0.6 m high) with a black interior filled with water ($20 \pm 1^{\circ}\text{C}$) to a depth of 0.53 m. White Tempera nontoxic paint powder is used to render the water opaque. A clear Plexiglass platform (11 cm in diameter) is submerged 2 cm below the water surface (invisible to the rat) at a distance of 30 cm from the maze periphery during learning trials. The platform is flagged and raised 1 cm above the water surface (visible to the rat) during vision and motor testing trials. The testing room has several extramaze cues (tables, shelf, wall markings, etc). The investigator, dressed in white lab coat, stood in the same location during test trials after releasing the rat into the maze with its face toward the pool wall. A computerized tracking system (ANY-Maze; Stoelting Co) is used to record animal movements during

probe trials and to calculate the average swim speed during vision and motor testing trials.

At 2 weeks after injury or sham injury, rats were evaluated for performance in incremental place learning ((32)). Starting on postinjury day 14, rats were trained to locate the submerged platform in the northwest (NE) quadrant of the pool, based on extramaze cues. Rats underwent 4 trials per day for 5 consecutive days, with an intertrial interval of 30 minutes. Rats started a trial once from each of the 4 possible start locations (north [N], south [S], west [W]), and east [E], and separated by 90 degrees around the maze periphery. Each trial lasted until the rat climbed onto the platform or until 120 seconds had elapsed, whichever occurred first. Rats that failed to locate the escape platform within the allotted time were manually guided to it. All animals remained on the platform for 30 seconds before being placed in a heated drying cage between trials. The rat's latency to reach the platform was recorded for each of the 20 trials, and the average for each day was calculated as a measure of incremental place learning ability.

A memory probe trial for incremental learning ability, with the platform removed from the pool, was run on postinjury day 19. Rats were released from the south start point for the 60-second probe trial. The percent time spent in the NE quadrant was measured only during the first 30 seconds of the trial because animals with good hippocampal function abandon their search in the correct quadrant after this period if no escape platform exists ((33-35)).

Vision and motor abilities were tested on postinjury day 20 with 4 trials per day. The visible platform was located at the same location (NE), as during incremental learning trials. The rats started a trial once from each of the 4 possible start locations. Rats were allowed up to 120 seconds to find the platform, 30 seconds to remain on the platform, and 30 minutes in a heated cage between trials. The animal's escape latency to the visible platform was measured using the tracking software for each of the 4 trials and averaged. At day 21 and day 28 after injury or sham operation, the same rats underwent an adapted version of the reversal and rapid place learning tests ((32, 36)).

On postinjury day 21, rats were given 1 trial (released from SE start site) to learn a new location of the submerged platform in the southeast (NW) quadrant. As before, the animals were allowed up to 120 seconds to find the hidden platform and 30 seconds to remain on the platform. The platform was then removed from the pool, and after a 30-minute intertrial interval in a heated cage, they underwent a memory probe trial for 60 seconds released from the same start site. The percent time spent in the right quadrant during the first 30 seconds of the probe was measured for each rat.

Additional Tests:

Elevated Plus-Maze a sturdy apparatus: Frequently used to measure anxiety levels in rodents, because of its use of natural conditions and stimuli to induce anxiety, such as a fear of new, bright, and open spaces and the fear of balancing on a relatively narrow raised surface. In the EPM test, anxiety-like behavior is measured as a reduction in both the number of entries and the time spent in the open arms, and an increase in the amount of time spent in the closed arms ((37-39)).

Figure 5: Blast exposure to COBIA causes dose-dependent abnormalities in vestibulomotor performance. A: Histogram of the distribution of apnea duration after blast exposure, all using a 24.5 cm BDC, which generates peak overpressures at the cranium of 544 ± 41.7 kPa; note the broad distribution of apnea duration despite the uniformity of blast generation parameters, suggesting that individual biological responses may provide a better measure of blast exposure than the physical parameters of the blast. B–E: Scatter plots of beam walk (B), beam balance (C), accelerating RotaRod (D) and spontaneous rearing (E) 24 hours after blast exposure, plotted against duration of apnea; Pearson’s correlation coefficient (ρ) and statistical significance (p) are also shown; $n=53$ per test.

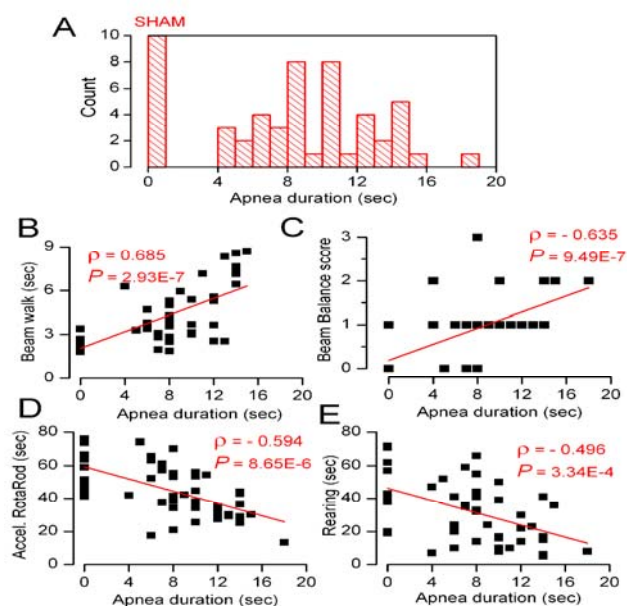


Figure 6: Blast exposure to COBIA causes abnormalities in vestibulomotor performance. A–D: Tests of beam walk (A), beam balance (B), accelerating RotaRod (C) and spontaneous rearing (D) over the course of 7–14 days after blast exposure; $n=10$ sham, 13 blast. (517 kpa)

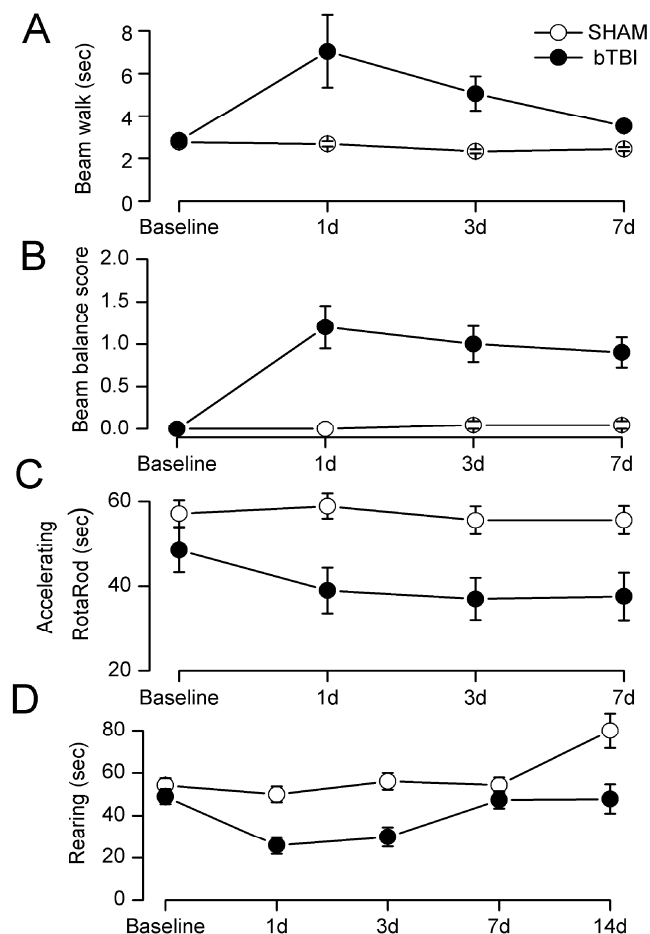


Figure 7: Morris Water Maze memory and cognition tests: A-C: (A) Incremental learning on MWM 14-18 days post injury. (B) Memory probe on day 19 post injury. (C) MWM memory probe vs apnea at blast; n=10 sham, 13 blast.

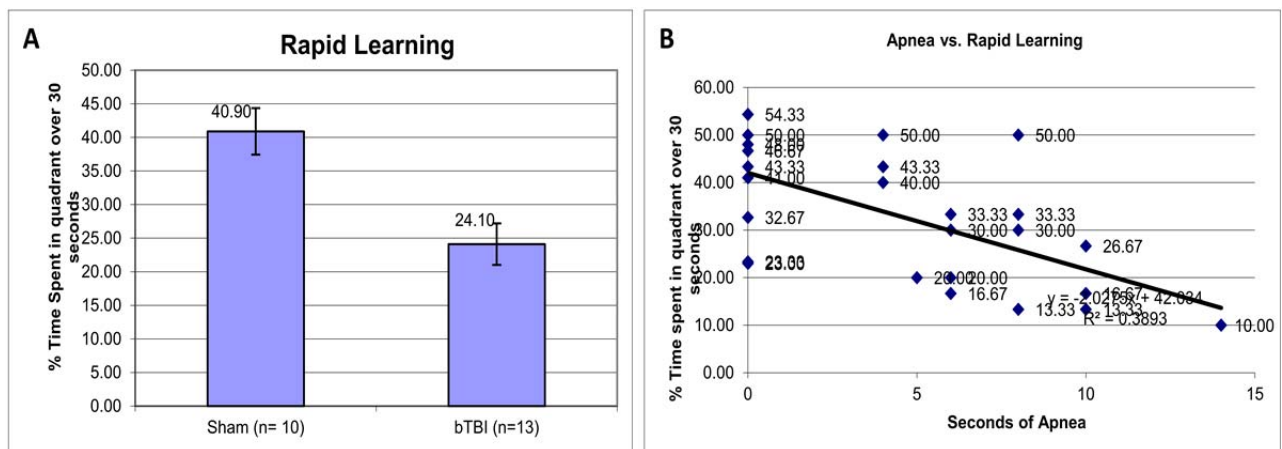
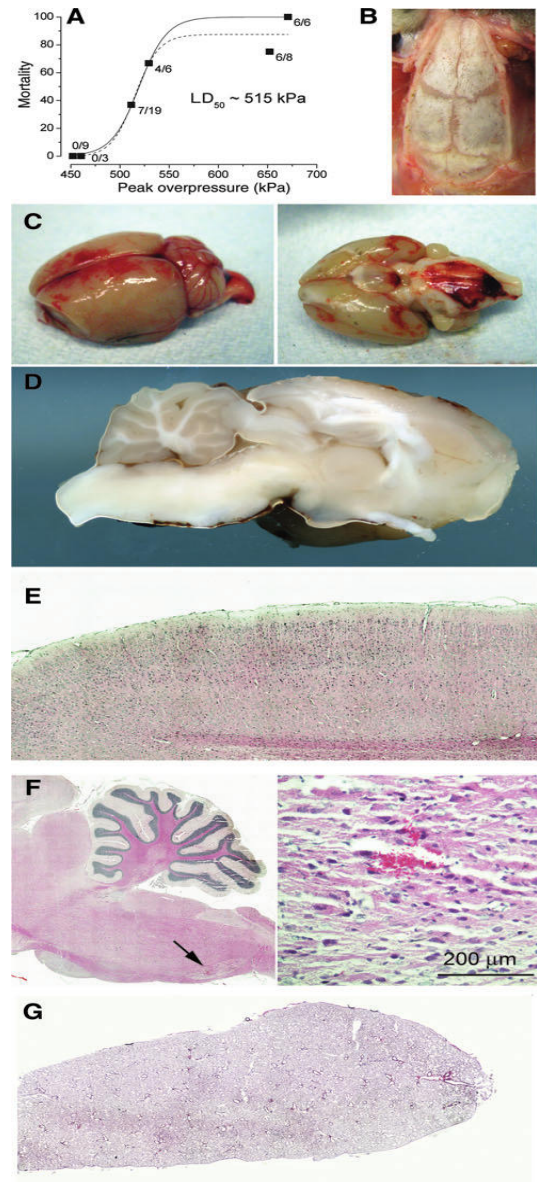


Figure 8: Morris Water Maze (MWM) memory and cognition tests: A,B: (A) Rapid learning test on day 21 post injury. (B) Rapid learning vs apnea at blast; n=10 sham, 13 blast

Objective 1c: Assessment of the model - histology (edema, hemorrhage, tissue sodium) of the rat bTBI brain.

Nissl (cresyl violet) staining: Cresyl violet staining was used to assess cellular and morphological alterations in the blasted areas of the brain. Dead cells were identified morphologically by blebbing of plasma membrane, diffused pallor of eosinophilic background, alterations in size and shape of cells, vacuolation, and condensed nucleus (Fig.10). Nissl staining was conducted on a group of rats with dcBI, (n=10).

Figure 9: Lethal direct cranial blast injury (dcBI). (A) Plot of the percent mortality versus peak overpressure, showing a 50% lethal dose (LD₅₀) of * 515 kPa; data from 51 rats, all obtained with blast dissipation chambers (BDCs) of 2.54 cm internal diameter (series 2). (B) Image of the exposed skull at the site of maximum blast exposure immediately following lethal dcBI, showing no signs of inward flexure or of other injury to the bones or sutures. (C) Images of dorsal and ventral brain surfaces showing extensive subarachnoid hemorrhages following lethal dcBI. (D) Images of unprocessed parasagittal sections of the brain, showing the absence of cortical contusions and of other internal hemorrhages following lethal dcBI. (E) Hematoxylin and eosin (H&E)- stained sections of the parietal cortex in the path of the blast wave, showing an absence of cortical contusions. (F) H&E stained sections of the cerebellum and brainstem following lethal dcBI, mostly confirming the absence of internal brain hemorrhages (left), but occasionally showing one or two microhemorrhages < 200 μ m (arrow on the left image, and magnified view on the right). (G) H&E-stained sections of the lungs following lethal dcBI, showing normal-appearing parenchyma. In all cases, the brains and lungs were harvested and imaged shortly after death, which occurred within 2 min of the blast injury.



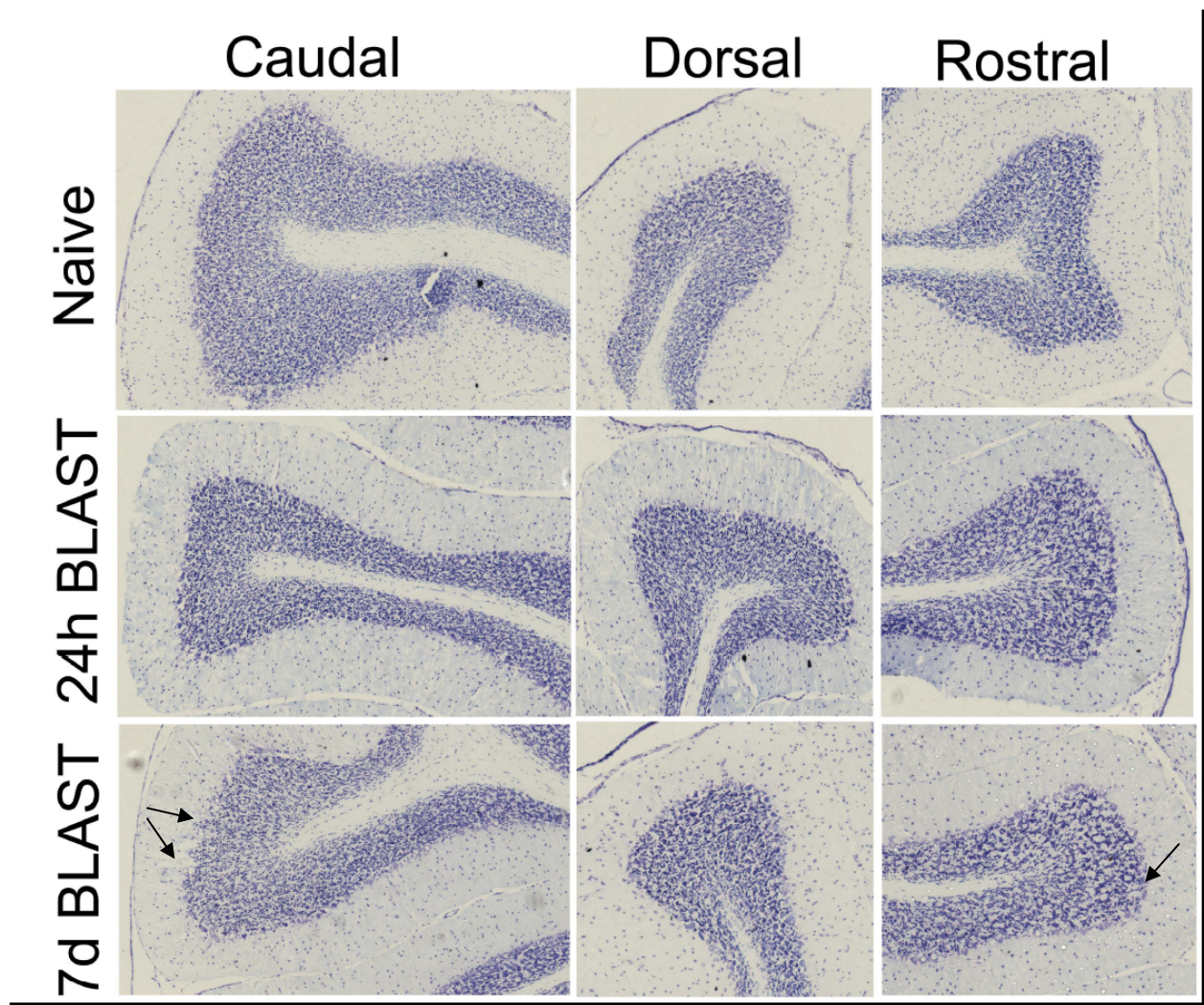


Figure 10: Nissl staining of the cerebellum of dcBI rats, Naïve rat compared with 24hrs and 7 days after dcBI. The caudal is the posterior part of cerebellum, dorsal is the middle superior part and rostral is the anterior part of cerebellum. 7d caudal cerebellar cells show vacuoles, and faded Nissl staining (arrows) compared with Naïve and 24hr corresponding cells.

Tissue Hemoglobin Detection: Lethal direct cranial Blast induced massive subdural and also lethal blasts, some subarachnoid hemorrhage in the brain of blasted rats. Sublethal direct cranial blast induced mainly subdural hemorrhage; we performed tissue Hb detection in a group of sublethal blast-TBI rats (n=5): brain tissue was perfused with normal saline and harvested 24 hrs after sublethal direct cranial blast, brain tissue was sectioned into 5 different parts, frontal (F), cortex (C), cerebellum (CB), thalamus (T), brainstem (BS). Tissues were lysed and the hemoglobin levels were detected by spectroscopy, against predetermined standard levels of Hb.

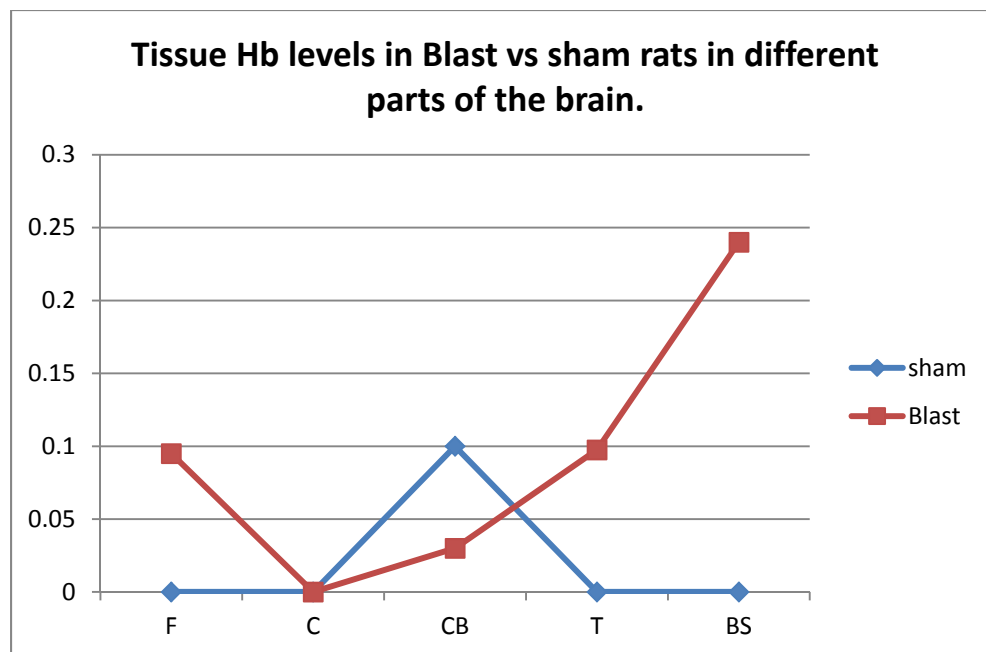


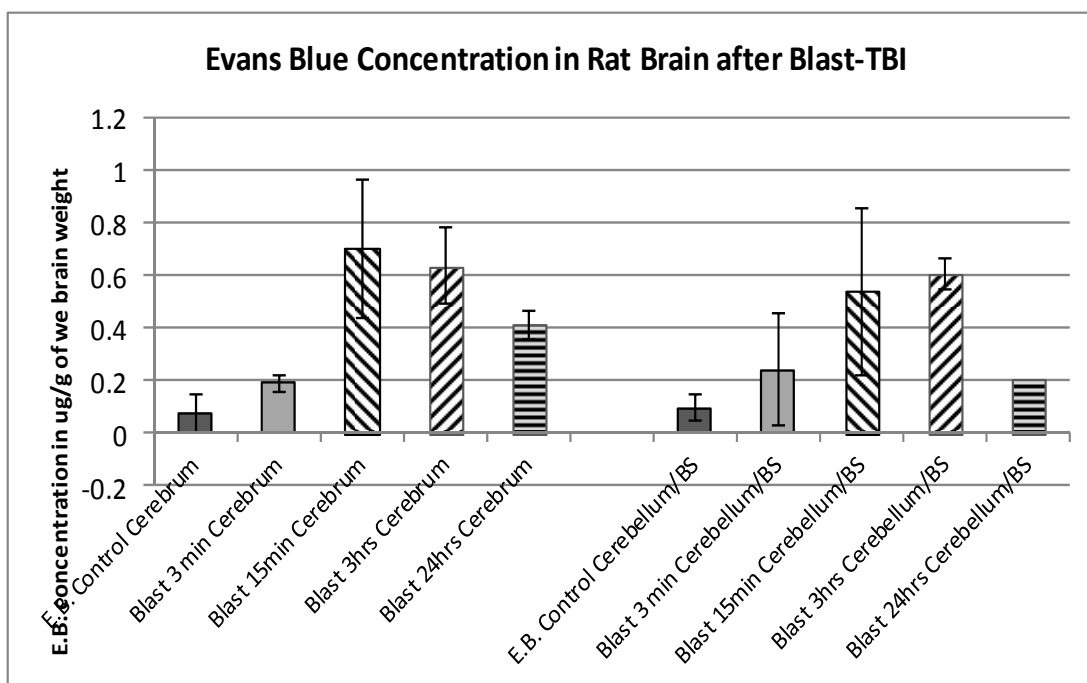
Figure 11: Tissue hemoglobin levels 24 hrs after sub-lethal blast in rats. (n=5) F:frontal cerebral, C: cortex, CB: cerebellum, T: Thalamus, BS: brainstem.

Blood Brain Barrier Disruption:

The extent of extravasation of Evans blue (EB) dye into the brain parenchyma was measured using the method described by Martin et al (Nature Protocols) with some modifications. 3 different time points were chosen for this experiment, 15 min, 3 hrs and 24 hrs after B-TBI. 15 min group were catheterized and E.B. was injected 45 min before blast, while 3 hrs and 24 hrs were injected with E.B. at 2 hrs and 23 hrs post blast respectively. Under general anesthesia, Evans blue dye (50 mg/kg in saline soln) was injected into the rat tail vein through a rat tail vein catheter (Braintree Scientific, Braintree, MA) and allowed to circulate for 60 minutes. Rats were then euthanized by intracardiac perfusion with normal saline, and brains were harvested and divided into two parts, 1) right and left cerebra, and 2) cerebellum with brainstem. The specimens were weighed, covered separately in aluminum foil and dried in the oven for 2 days at 56°C. At 2 days the dry weights were taken and formamide (8 ml/g of dry tissue) was added for each sample in a plastic tube covered with aluminum foil, and then returned to the oven at 56°C for another 2 days. The supernatants were collected and centrifuged at 13200 rpm, and absorbance was detected at 620 nm wavelength using a Thermo Spectronic BioMate3 spectrophotometer (Thermo Fisher Scientific Inc., Waltham, MA). Standards were created at each experiment (0, 0.25, 0.5, 1, 2, 4, and 8 µg/ml). A naïve rat brain was used to deduct the background absorbance, and an uninjured rat brain with E.B. injection was used for control. A key component in understanding the disruption of blood brain barrier (BBB)/vasculature after Blast-TBI is to investigate events of blast injury in the pathology of brain tissue. We hypothesized that elucidating BBB permeability after Blast-TBI in our model may offer very important information about the optimal time window for therapeutic intervention. We examined the BBB permeability after Blast-TBI, as early as 3 min and up to 24 hrs. post-injury. The content of EB in brain tissue increased as early as 3 min post-Blast-TBI, remained high

up to 24 hrs, where there was decrease compared to earlier 15min and 3 hrs data, suggesting a time dependent BBB leakage (Fig. 12A). It reached a peak between 15 min and 3 hrs. post- injury. This BBB leakage was also confirmed with IHC as early as 45min post injury by EB flourodetection and IgG immunofluorescence labelling (Fig. 12D).

A



B



C



D

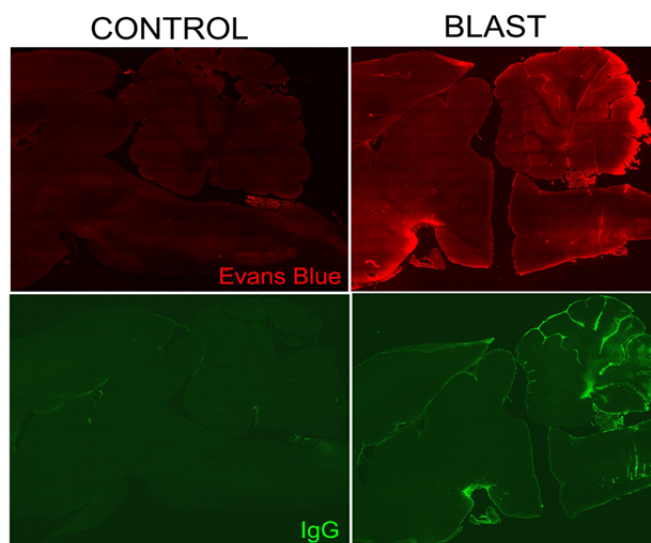


Figure 12: Blood Brain Barrier disruption. (A) Graph of the E.B. concentration in the brain tissue after blast-TBI (ug/g). (B) Blast spot on the head of the rat, notice the blast impact is 4-5mm away from the occipital crest (black mark), (C) macroscopic brain image of rat brain showing the EB leak. (D) Permeability of blood vessels as revealed by Evans blue staining (upper). Diffuse red fluorescence intensity was observed in the brain parenchyma as well as vessels, IgG immunofluorescence labelling (lower).

Objective 2a: determine the time course for SUR1 and TRPM4 upregulation and downregulation post-blast-TBI.

SUR1 and TRPM4 upregulation after COBIA Blast

As early as 2 hours after blast-TBI we can detect SUR1 protein in microvessels in the brain stem and cerebellum by immunohistochemical analysis (Fig. 13,14). Levels of SUR1 expression further increased at 8 and 24 hours after the blast-TBI, with predominant localization in capillaries and larger vessels (Fig. 13,14). Vascular localization of newly expressed SUR1 was confirmed by co-localization with laminin, a protein expressed exclusively in the vascular wall. In addition, at 8 hours after blast-TBI, upregulation of SUR1 was detected in Purkinje neurons of the cerebellar cortex. The neuronal origin of the SUR1-labelled cells was confirmed by co-localization of SUR1 with NeuN protein, which is specific for neurons. TRPM4 protein expression after blast generally followed that of SUR1. Similarly to SUR1, TRPM4 expression after blast-TBI was primarily localized in the caudal parts of the brain with little or no expression in the cerebral cortex, thalamus or hippocampus.

We continued these experiments by performing Western blot and qPCR analysis of the brain tissues impacted by the blast injury. In order to compare data on the levels of expression of SUR1 and TRPM4 RNA and protein, we performed uniform harvest of the tissues from different brain regions (Fig. 20). We focused on the anatomical areas of the brain positioned in the path projected from the BDCCI output, specifically: (i) underlying cortex, (ii) thalamus and hypothalamus, (iii) cerebellum, and (iv) brainstem, as depicted on Fig 10,

Brain tissues were collected from dcBI rats at different time points in triplicates for early times after blast (1/2-24 hours and for later times (3-10 days). Immunohistochemical analysis of these tissues indicates that we can detect significant difference in the SUR1 and TRPM4 protein as early as 4 hours after blast TBI in brain stem (Fig. 11). 24 hours after blast we detect upregulation of the both proteins in brainstem and cerebellum (Fig. 21, 22). This result corroborates data detected immunohistochemically and confirms specificity of the signals detected with SUR1 and TRPM4 antibodies.

Additionally to the data on the COBIA reported in our paper we studied more in detail impact of the cranium-only blast on the neuronal injury in the brain stem. We detected upregulation of both of cleaved caspase-3 (Fig. 25,26), and upregulation of β -APP. Arguably, one of the most intriguing findings was involvement of neurons of the raphe system, which projects 5-HT fibers to cortical and other forebrain regions, and play an important role in neuropsychological function. Cells of the dorsal raphe, identified by their location and by expression of tryptophan hydroxylase, showed upregulation of β -APP (Fig.30), Sur1 (Fig. 31) and TUNEL labeling (Fig. 25B).

We hypothesized that neurons of the raphe system may be selectively vulnerable to blast injury, for the same reason that pial veins appear to be selectively vulnerable – they reside near a CSF-brain boundary. Moreover, raphe neurons located at the rostral

end of the 4th ventricle, where the 4th ventricle joins the aqueduct of Sylvius, may be selectively vulnerable because the “bottleneck” at this location accelerates a hydrodynamic pulse traveling upward from the 4th ventricle, transferring kinetic energy to surrounding tissues. Indeed, immunolabeling for Sur1 showed exactly this phenomenon (Fig. 25). Also, the nearby cluster of large raphe neurons showed distinct upregulation of Sur1 (Fig. 31). The raphe neurons that upregulated Sur1 were identified by their location and by expression of tryptophan hydroxylase (Fig. 31).

These findings of widespread injury to raphe neurons correlates well with data presented below (Fig. 34E) on abnormal thigmotaxis, a measure of anxiety, following blast induced by COBIA. Moreover, the involvement of Sur1 in this pathological response correlates with data presented below that abnormal thigmotaxis following blast induced by COBIA was significantly ameliorated by treatment with glibenclamide.

Table 2: Antibodies/markers used for histology, Immunohistochemistry and immunology

Proteins	Assays	Histology
SUR1 (sulfonylurea-receptor 1) 56	Tunel	H & E
TRPM4 (melastatin transient receptor potential) 35	In situ Hybridization	Nissl
GFAP (Glial fibrillary acidic protein) 10	Immunoprecipitation	
NeuN (neuronal marker) 24	Western blot	
APP (Beta-amyloid precursor protein) 64	qPCR	
Casp 3 (caspase 3) 28	Tissue hemoglobin detection	
SP1 (ischemic, hypoxic marker) 7		
ED1 (microglial marker) 36		
MPO (Myeloperoxidase) 7		
Iba1 (ionized calcium-binding adaptor molecule-1) 7		
TNFα (tumor necrosis factor alpha) 7		
IgG (immune-globulin G) 21		
Lam (Laminin) 19		
5-HT (serotonin) 21		
P65 5		
TPH (tryptophan hydroxylase) 13		
Fluoro-Jade ??? (neurodegenerative marker) 7		
vWF von Willebrand factor (vessel marker) 5		

Figure 13: SUR1 is upregulated in brainstem after blast exposure to COBIA. A–D: Low magnification views of sections of the brainstem immunolabeled for SUR1 in sham injured, and blast-injured rats at the times indicated.

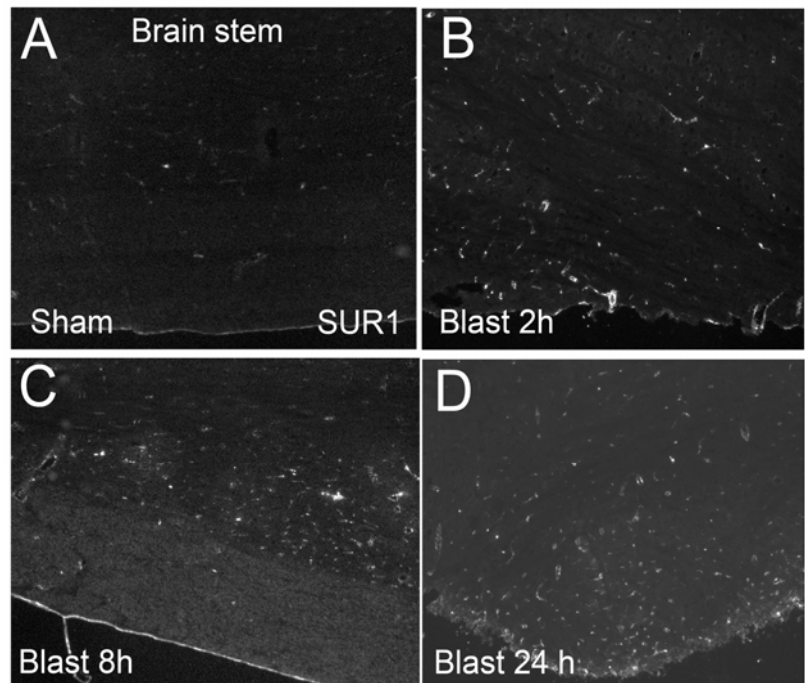


Figure 14: SUR1 is upregulated in cerebellum after blast exposure to COBIA. A–D: Low magnification views of sections of the cerebellum immunolabeled for SUR1 in sham injured, and blast-injured rats at the times indicated.

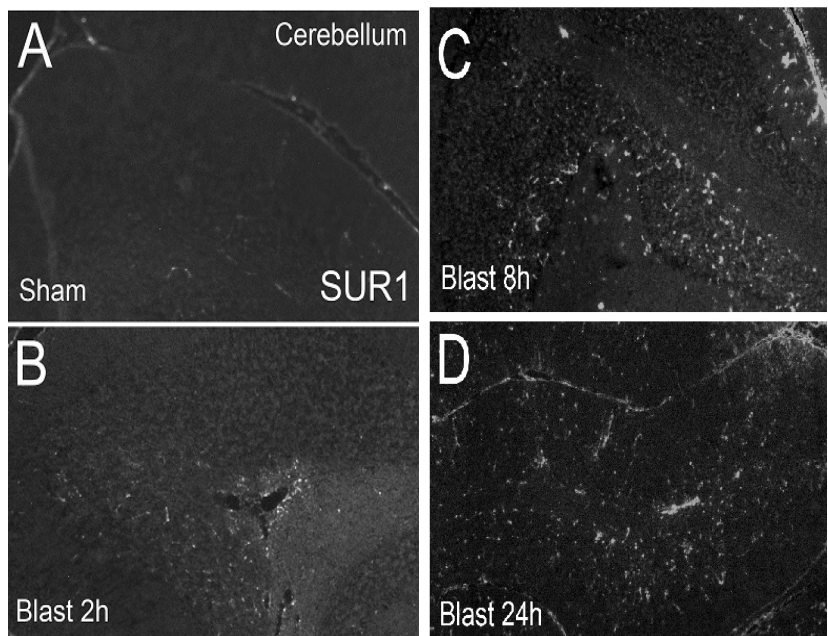


Figure 15: Brain tissues near density boundary show up-regulation of SUR1 after blast. Sagittal sections of the floor and roof of 4th ventricle from control rat brain (**A**) and brain of the rat 24 hours after dcBI (**B,C,D**) labeled for SUR1. (**Aq**-aqueduct, **4V**-4th ventricle, **CL**-cerebellar lobe, **DR**-dorsal raphe nucleus). **B**: Newly expressed SUR1 in DR is demarked by arrows and in ependyma by asterisk. **C**: High power view of the DR showing upregulation of SUR1 in individual neurons. **D**: upregulation of SUR1 in ependyma of the 4th ventricle.

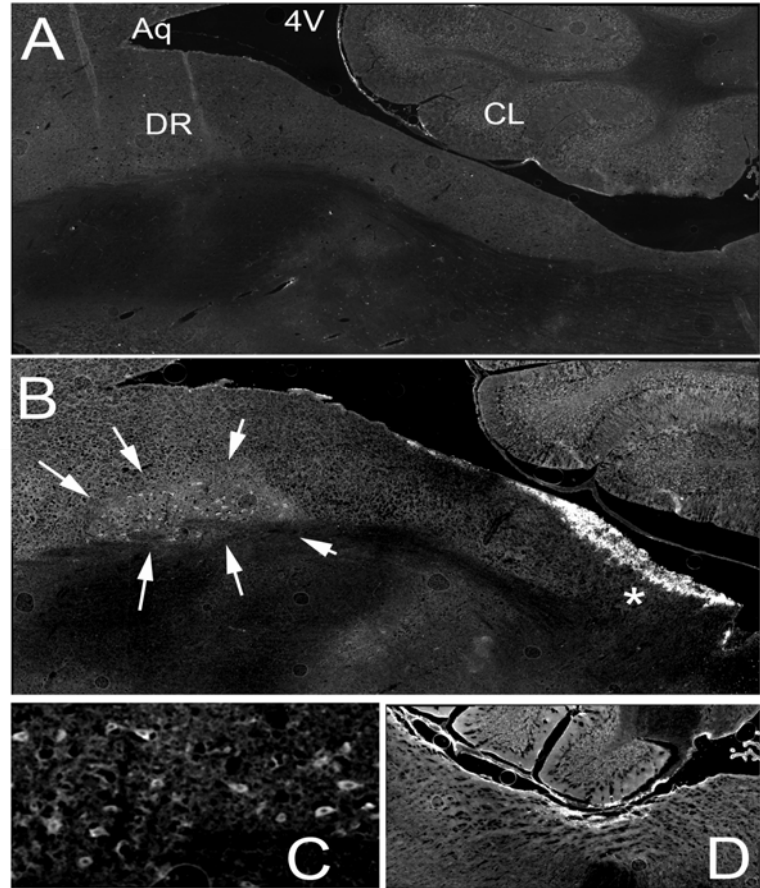


Figure 16: SUR1 is upregulated in microvessels and neurons after blast exposure to COBIA. **A–C**: High magnification views of sections of the brainstem and cerebellum immunolabeled for SUR1 and co-labeled with laminin to show microvessels (**A**), or NeuN to show neurons (**B**), or GFAP to show astrocytes (**C**); note localization of SUR1 in microvessels and neurons, but not astrocytes; panels on the right show the superimposed images from the corresponding images on the left.

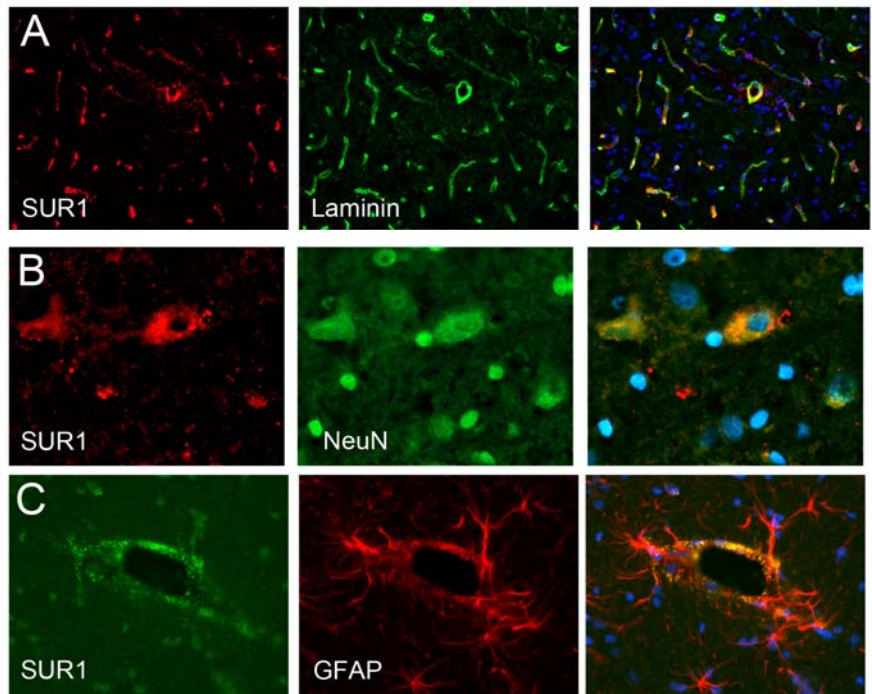


Figure 17: SUR1 is upregulated in choroid plexus and the ependyma after blast exposure to COBIA. A–D: Intermediate magnification views of sections of the ventricles immunolabeled for SUR1 in sham injured (**A,C**), and blast-injured rats (**B,D**); note upregulation of SUR1 in choroid plexus and ependymal lining of the ventricle.

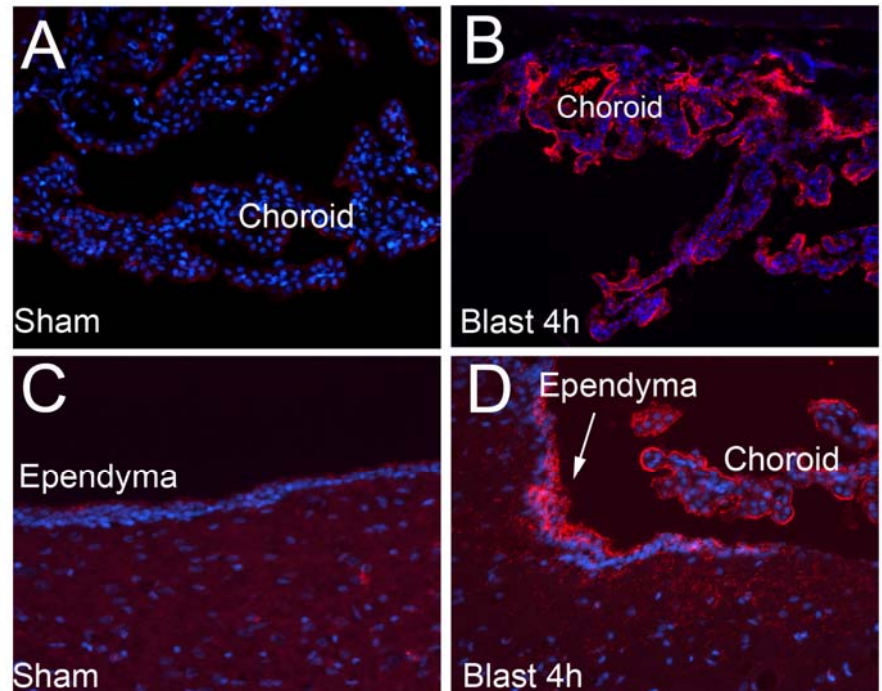
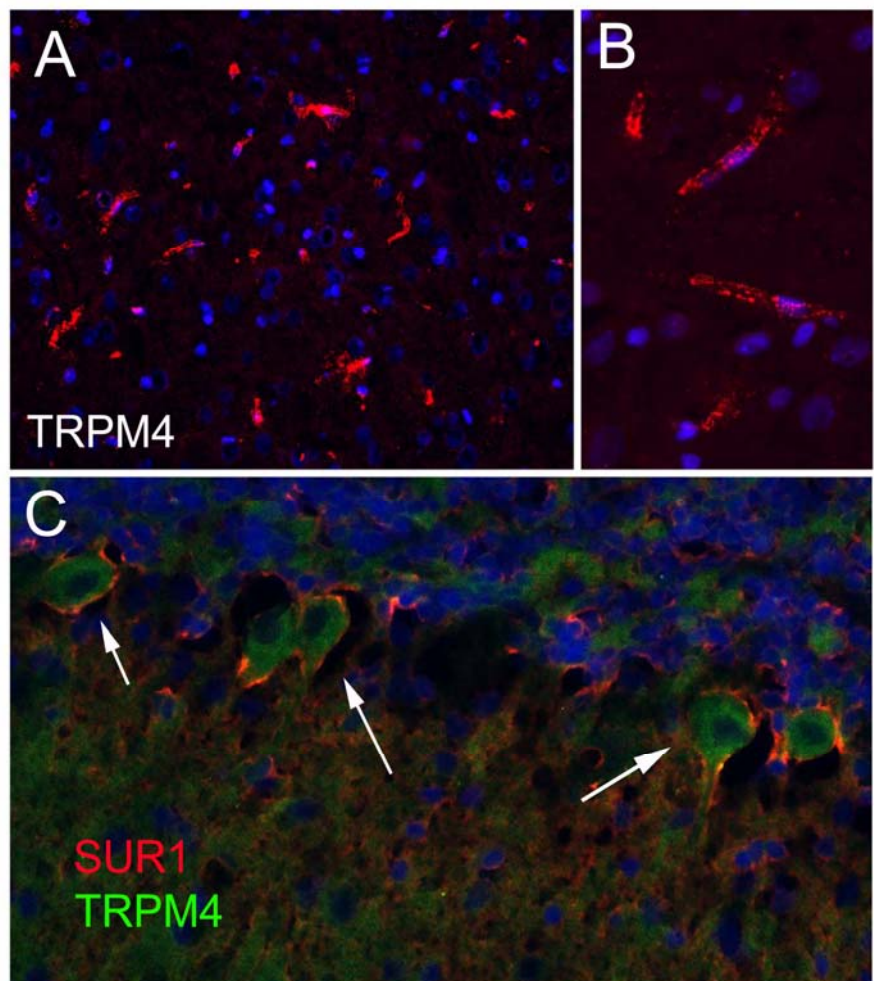


Figure 18: TRPM4 is upregulated in brainstem and cerebellum after blast exposure to COBIA. A,B: Intermediate (A) and high (B) magnification views of sections of the brainstem immunolabeled for TRPM4 in blast-injured rats, showing labeling in microvessels. **C:** High magnification views of sections of the cerebellum immunolabeled for TRPM4 and SUR1 in blast-injured rats, showing colocalization in Purkinje cells (arrows).



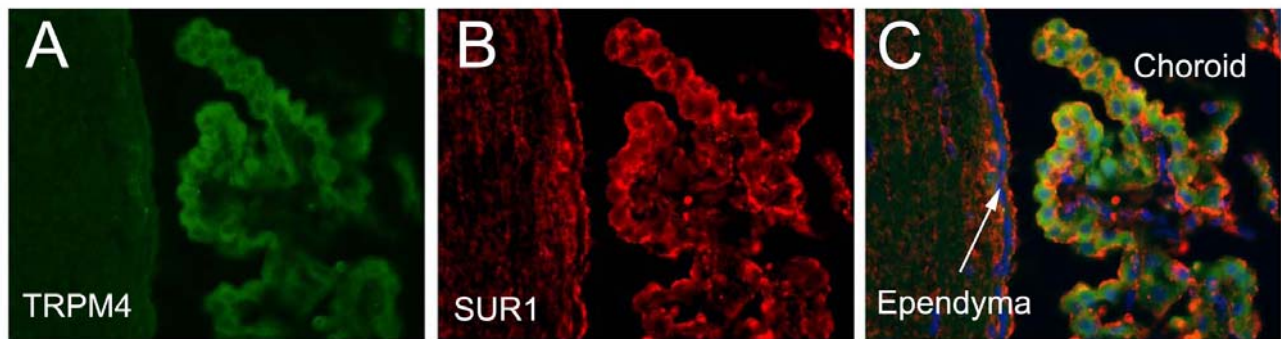


Figure 19: TRPM4 and SUR1 are upregulated in choroid plexus after blast exposure to COBIA. A–C: Intermediate magnification views of sections of the lateral ventricle immunolabeled for TRPM4 (**A**) and SUR1 (**B**) in a blast-injured rat, showing colocalization in the choroid plexus, but not in the ependyma (**C**).

Immunoprecipitation and Western Blot

IP , WB and qPCR (n=18)

Brains of blasted (2 hrs, 4 hrs, 8hrs, 24hrs) and sham rats were perfused with cold PBS and harvested. Tissues of blasted and sham rats were dissected into 4 parts according to the figure below (fig 16), tissues were lyzed with lysis buffer and immunoprecipitated overnight with SUR1 and TRPM4 antibodies covered beads. Then separated and the lyzates were run on an electrophoresis gel and incubated with SUR1 and TRPM4 antibodies. We found SUR1 protein over-expression in the cerebellum and brainstem after dcBI and TRPM4 protein overexpression in the brainstem as early as 4 hours and up to 24 hrs after dcBI. Which corresponds and confirms with our immunohistochemical data.

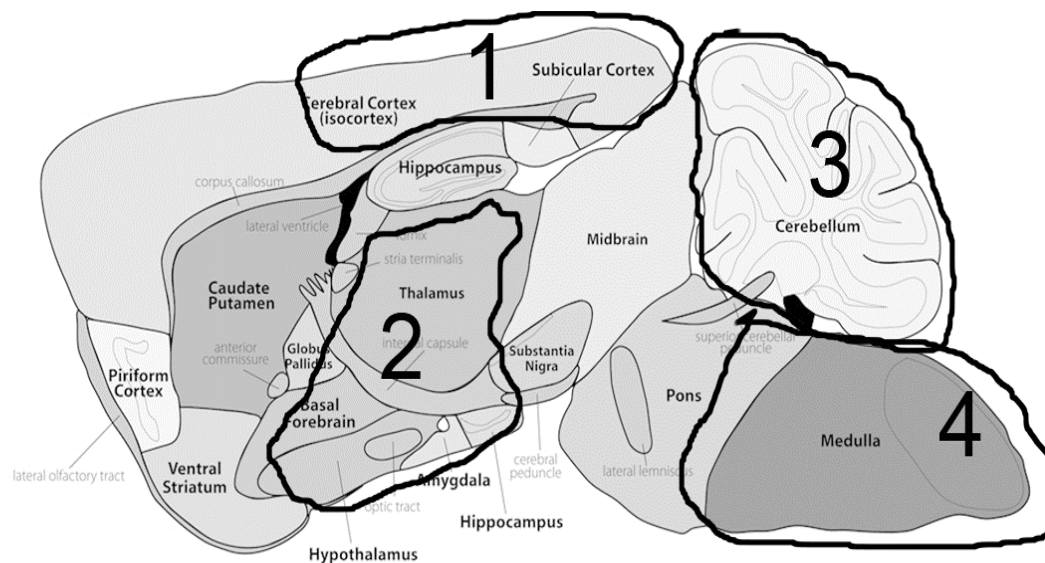


Figure 20: Rat brain anatomical regions dissected after blast injury for Western blot and PCR analysis. 1- Cortex (CTX), 2-Thalamus and Hypothalamys (Tha/HT), 3- Cerebellum (CRBL), and Brain stem (BStem).

Figure 21. Western blot of the brain tissues dissected 4 hours after Blast injury. Tissues from cortex(CTX), Thalamus and Hypothalamus (Tha/HT), Cerebellum (CRBL) and Brain stem (BStem) were homogenized in RIPA buffer, run on electrophoretic gel and blotted using antibodies specific for Sulfonylurea receptor-1 (SUR1), and control proteins HSC-70 and β -actin. Note upregulation of SUR1 in brain

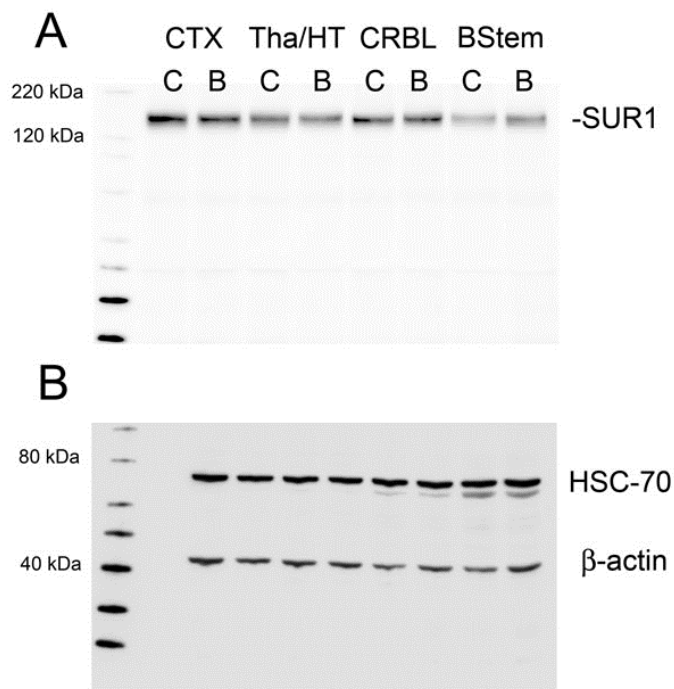
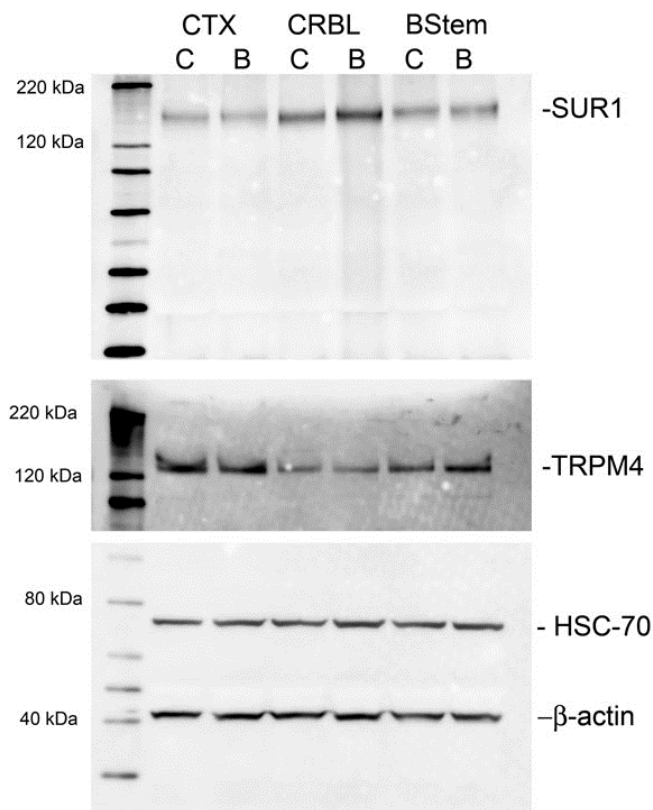


Figure 22: Western blot of the brain tissues dissected 24 hours after Blast injury. Tissues from cortex (CTX), Cerebellum (CRBL) and Brain stem (BStem) were homogenized in RIPA buffer, run on electrophoretic gel and blotted using antibodies specific for SUR1, TRPM4 and control proteins HSC-70 and β -actin. Note upregulation of SUR1 in Cerebellum and Brain stem, and upregulation of SUR1 in Brain stem.



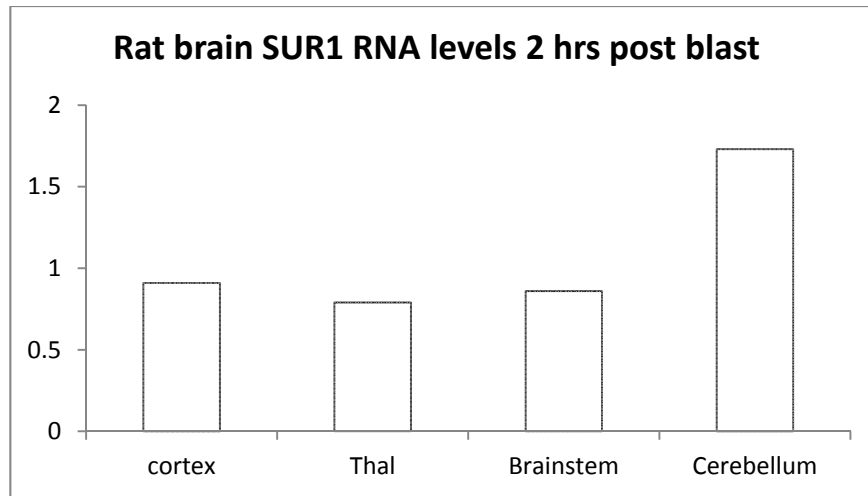
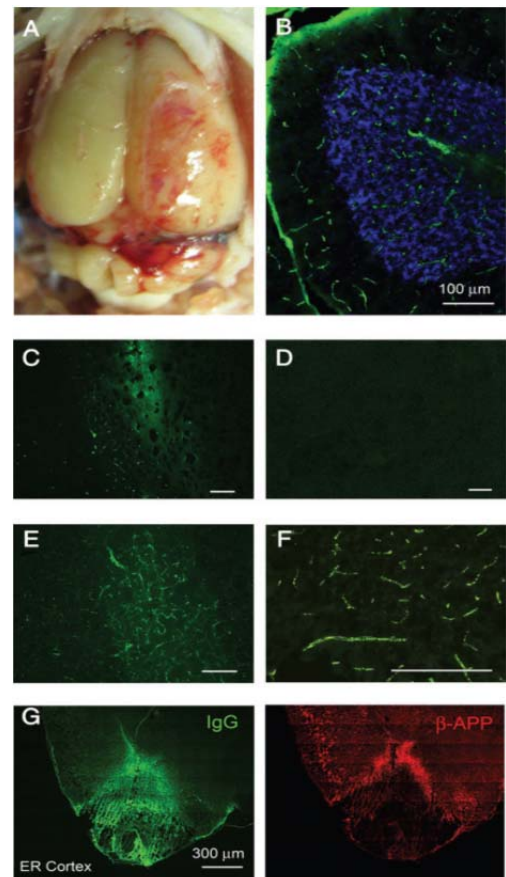


Figure 23: qPCR of the brain tissues dissected 2 hours after Blast injury. Tissues from cortex, thalamus (Thal), brainstem, and cerebellum were prepared for qPCR for SUR1. Note upregulation of SUR1 in different brain parts. These were matched with naïve rat tissues from the same part of the brain.

Objective 2b: Short and long term pathologic changes in different brain regions; evaluation of different apoptotic and neurodegenerative protein expression.

Figure 24: Sub-lethal direct cranial blast injury (dcBI): microvascular abnormalities and contrecoup injury. (A) Image of the dorsal surface of the brain 24 h after sublethal dcTBI (427 kPa), showing the presence of subarachnoid hemorrhage involving the cerebellum and parietal lobe in the path of the blast wave, but sparing the rostral cortex outside of the path. (B–F) Cryosections of cerebellum (B–D) and thalamus (E and F) immunolabeled for rat IgG 24 h after sub-lethal dcBI (517 kPa in B, C, E, and F), or following sham injury (D), showing no labeling in uninjured controls (D), a diffuse pattern of labeling suggestive of vasogenic edema (C and E), or distinct microvascular labeling consistent with stasis or thrombosis (B and F). (G) Cryosection of entorhinal cortex (ER Cortex) immunolabeled for rat IgG and co-labeled for b-amyloid precursor protein (b-APP), showing contrecoup injury at the ventral tip with surrounding penumbral vasogenic edema and b-APP upregulation 24 h after sublethal dcBI (517 kPa).



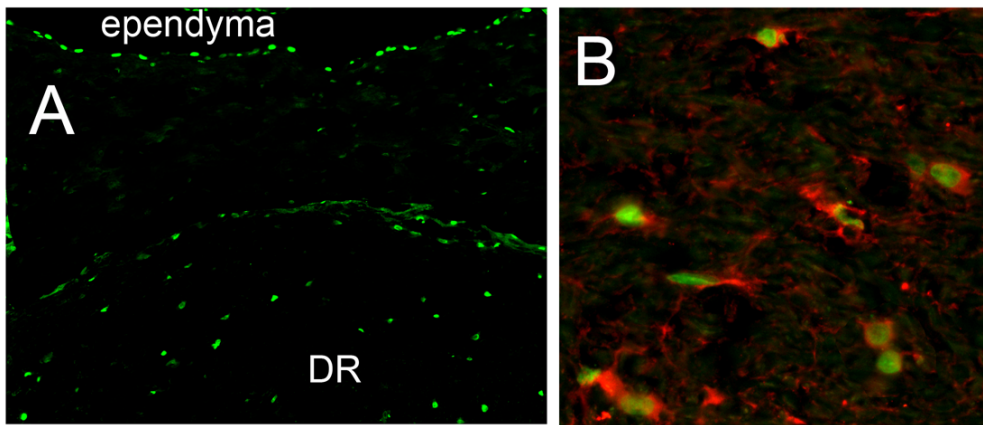


Figure 25: dcBI causes cell death in tissues near density boundary. **A:** Cell death 24 h after dcBI detected in ependyma of 4th ventricle and dorsal raphe nucleus (DR) using TUNEL labeling. **B:** TUNEL labeling (green) in serotonergic neurons from DR labeled for Tryptophan hydroxylase (red).

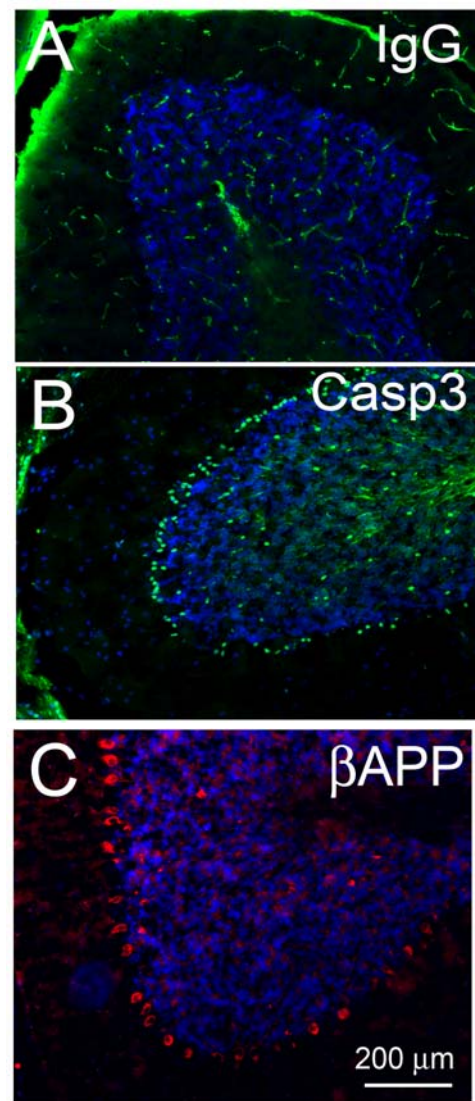


Figure 26: Immunohistochemistry after blast-TBI. A-C: Immunolabeling of cerebellum for IgG (A, green), activated caspase 3 (B, green) and β -amyloid precursor protein (β -APP) (C, red); in all cases, the nuclei were labeled with DAPI (blue); note the extensive Purkinje cell labeling with IgG in A, and the extensive Purkinje cell labeling for activated caspase 3 and β -APP in B and C; brains perfused to remove intravascular blood. Labeling of control uninjured brains showed no signal (data not shown).

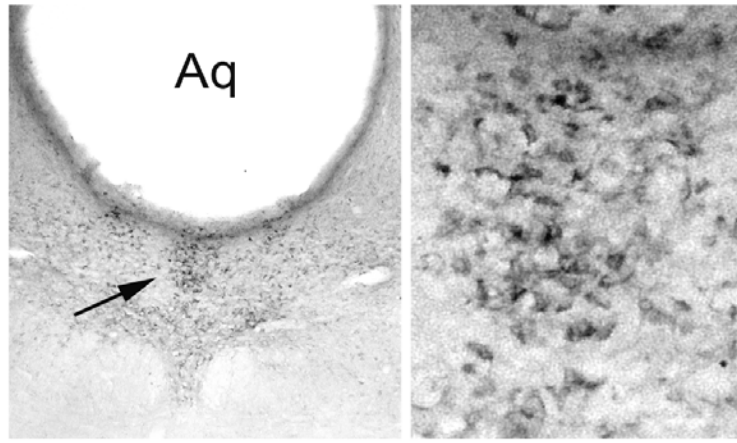


Figure 27: Brain tissues near density boundary show abnormal up-regulation of β -APP after blast (dcBI). Low power view (*Left*) of the peri-aqueduct tissues shows prominent up-regulation of the β -APP in neuron-like cells. *Right*: higher power view of the area point to by arrow in left panel. Tissues labeled with anti- β -APP antibody and developed using DAB chromogen

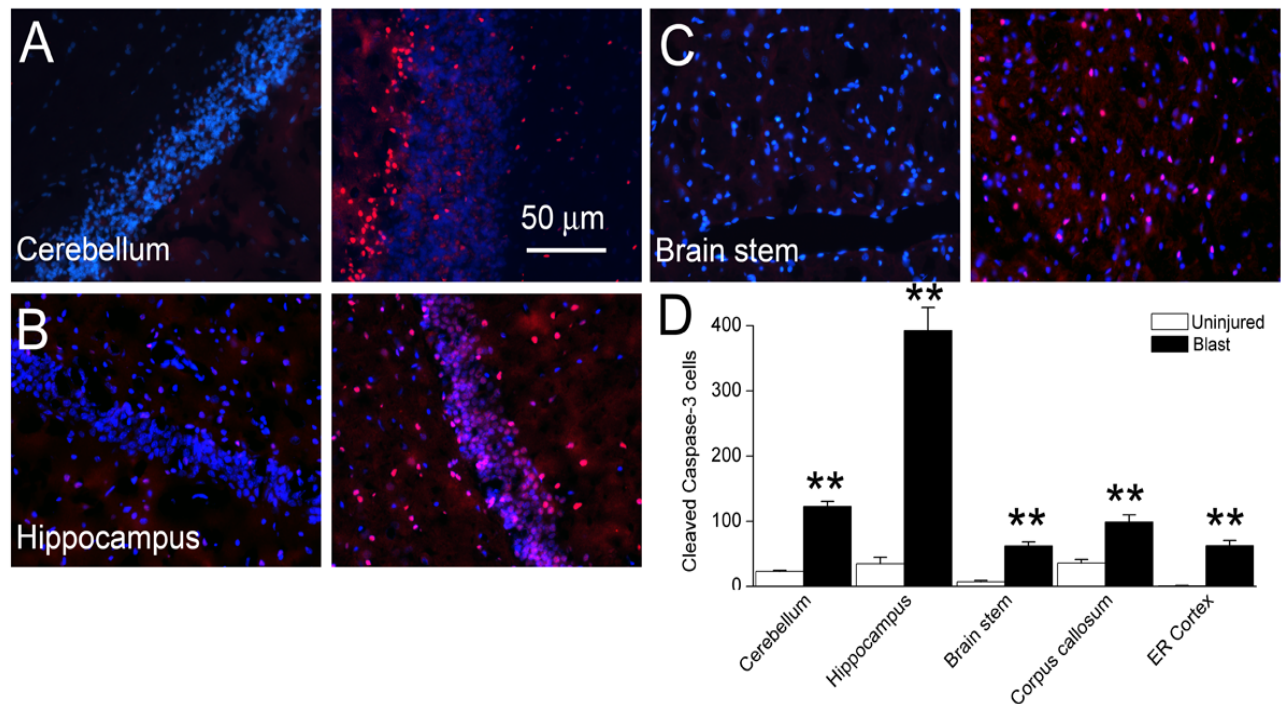


Figure 28: Sub-lethal direct dcBI– cleaved caspase-3. **A–C:** Sections of cerebellum, hippocampus, and brain stem from uninjured rats (left) and from rats 24 hours after sublethal dcBI, immunolabeled for cleaved caspase-3 (red) and stained with DAPI (blue). **D:** Counts of nuclei with cleaved caspase-3 in various brain regions including the entorhinal cortex (ER), from uninjured rats (empty bars) and from rats 24 hours after sublethal dcBI (filled bars); counts were obtained in “regions of interest” (ROI) 400 x 400 μ m for each area for each of 5 rats **, $P < 0.01$.

Figure 29: Sub-lethal direct cranial blast injury (dcBI): axonal and neuronal abnormalities and neurological dysfunction. (A) Cryosections immunolabeled for β -amyloid precursor protein (β -APP) (visualized with diaminobenzidine), showing axonal disruption in deep white matter. (B) Cryosections immunolabeled for b-APP (visualized with fluorescent secondary antibody), showing upregulation in cerebellar Purkinje cells and hippocampal neurons. (C and D) Cryosections stained with Fluoro-Jade C, showing positive labeling in cerebellar Purkinje cells and hippocampal neurons from injured rats (right) but not in uninjured rats (left); all scale bars = 25 μ m.

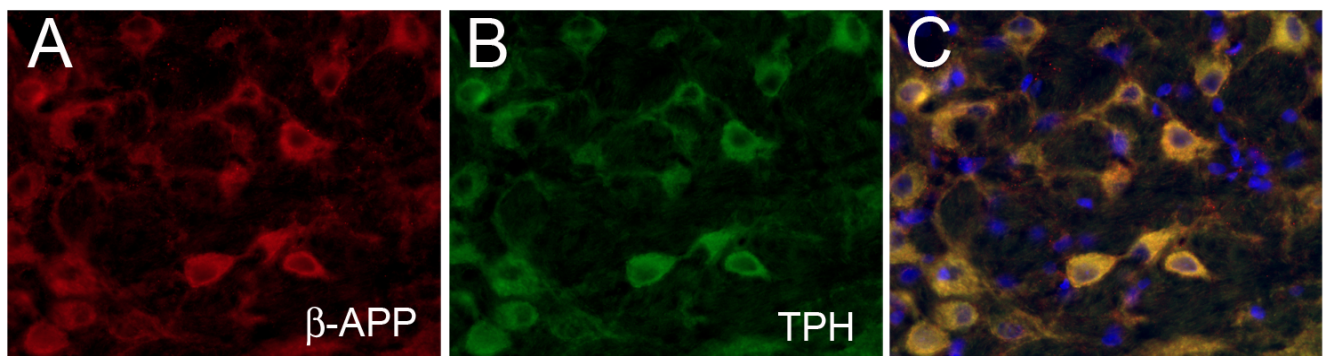
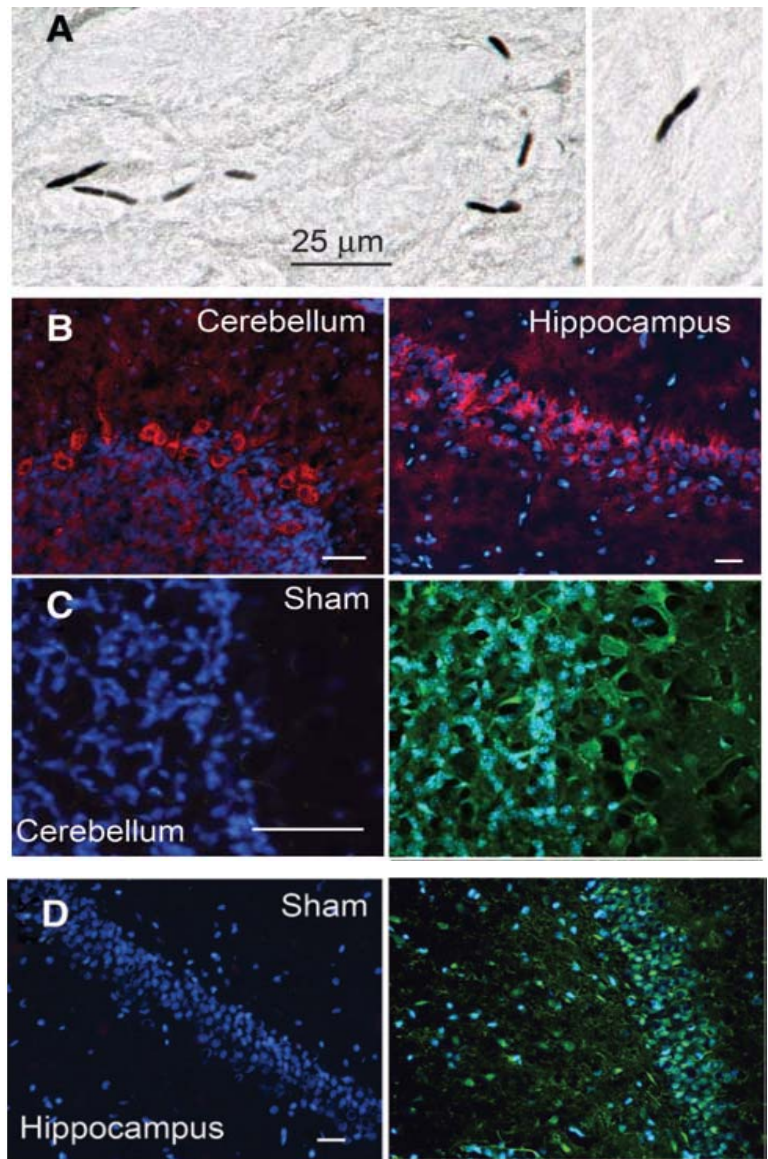


Figure 30: dcBI causes up-regulation of the β -APP in serotonergic neurons of the raphe system. Sections double labeled for β -APP (A, red) and Tryptophan hydroxylase (B, green), enzyme involved in serotonin synthesis, and superimposed image on C show that raphe magnum serotonergic neurons are selectively vulnerable to the blast injury.

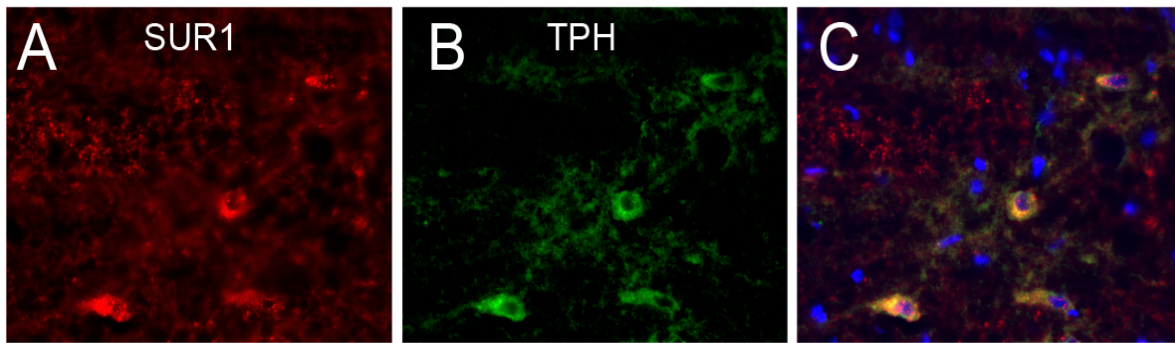


Figure 31: dcBI causes up-regulation of the SUR1 in serotonergic neurons of the raphe system. Sections from the rat brain 24 hours after dcBI double labeled for SUR1(A, red) and Tryptophan hydroxylase (B, green), and superimposed image on C show that blast causes upregulation of SUR1 in raphe nucleus serotonergic neurons.

Objective 3a: determine the effect of glibenclamide treatment on long-term neurobehavioral outcome from blast-TBI

The determinations whether glibenclamide treatment affects outcome, and whether prophylaxis, early treatment and delayed treatment are associated with different outcomes. The rationale for the study of glibenclamide is reviewed in detail in the original submission and from our extensive studies done in our lab ((21-24)), as well as the data shown in the report under objectives 1a and 1b.

Two different sets of studies were performed using COBIA 24.5cm BDC and 29.5cm BDC, including treatment groups with 1) glibenclamide, 2) vehicle, and 3) sham. Treatment was applied right after the blast-TBI within 3-5 minutes.

Rats underwent blast-TBI (groups 1 and 2), or sham, treated as mentioned above by inserting a subcutaneous pump filled either with glibenclamide or vehicle and followed for up to 28 days. These pumps delivered treatment up to a week. Short and long term neurobehavioral tests were performed on days 1, 3, 7, 14, 21 and 28, and Morris watermaze cognitive function tests were performed from day 14 to day 28 post blast.

Drug delivery

Within 2–3 minutes of Blast-TBI induction, mini-osmotic pumps (Alzet 2002, 0.5 μ l/h; Durect Corp.) were implanted subcutaneously that delivered either vehicle (saline plus DMSO), or glibenclamide stock solution (Sigma-Aldrich). To immediately start the treatment an intraperitoneal injection was followed the pump insertion 1ml/kg body weight. Stock solutions of glibenclamide (Sigma, St Louis, Mo) were prepared in dimethylsulfoxide (DMSO) (5 mg/mL). Solutions for delivery were prepared by adding stock solution to normal saline (NS) and clarifying the solution as needed using a minimum amount of NaOH to a pH approximately 8 to 8.5. Solutions prepared in this

way and stored at 37°C for 48 hours retained >80% efficacy as measured in patch clamp experiments on K_{ATP} channels in insulinoma cells. Infusion doses were delivered using a subcutaneously implanted mini-osmotic pump (Model 2001; 1.0 μ L/h; Durect Corp, Cupertino, CA), which was always implanted immediately after Blast-TBI. Controls were administered vehicle (NS plus DMSO) in the same way.

1) Blast-TBI COBIA 24.5cm BDC (517 kPa)

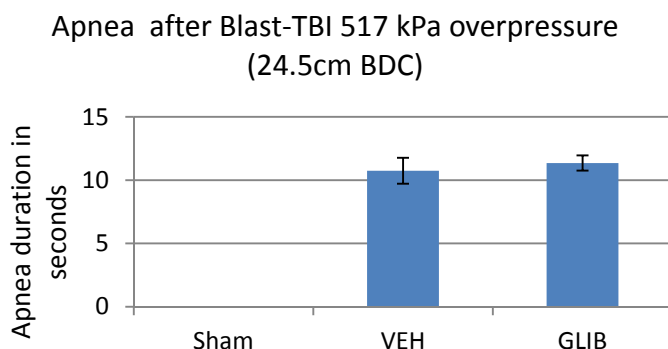


Figure 32: Apnea levels for each group Blast injury. Sham (n=10) animals had no apnea, mean apnea after blast was less in vehicle treatment group (n=11) compared with glibenclamide (n=14) treatment group.

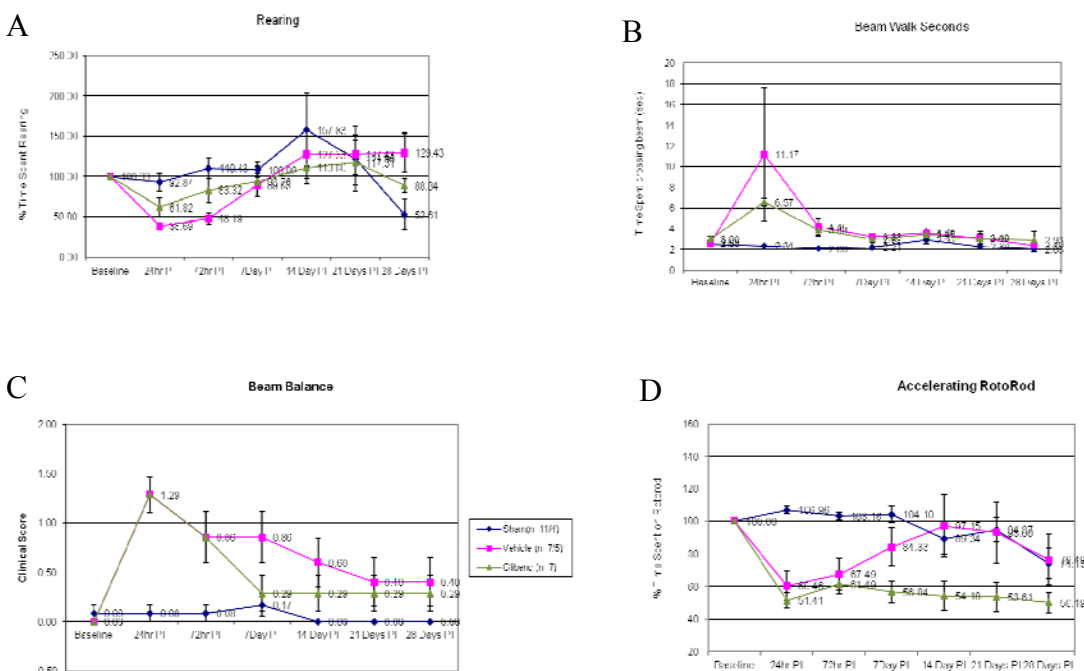
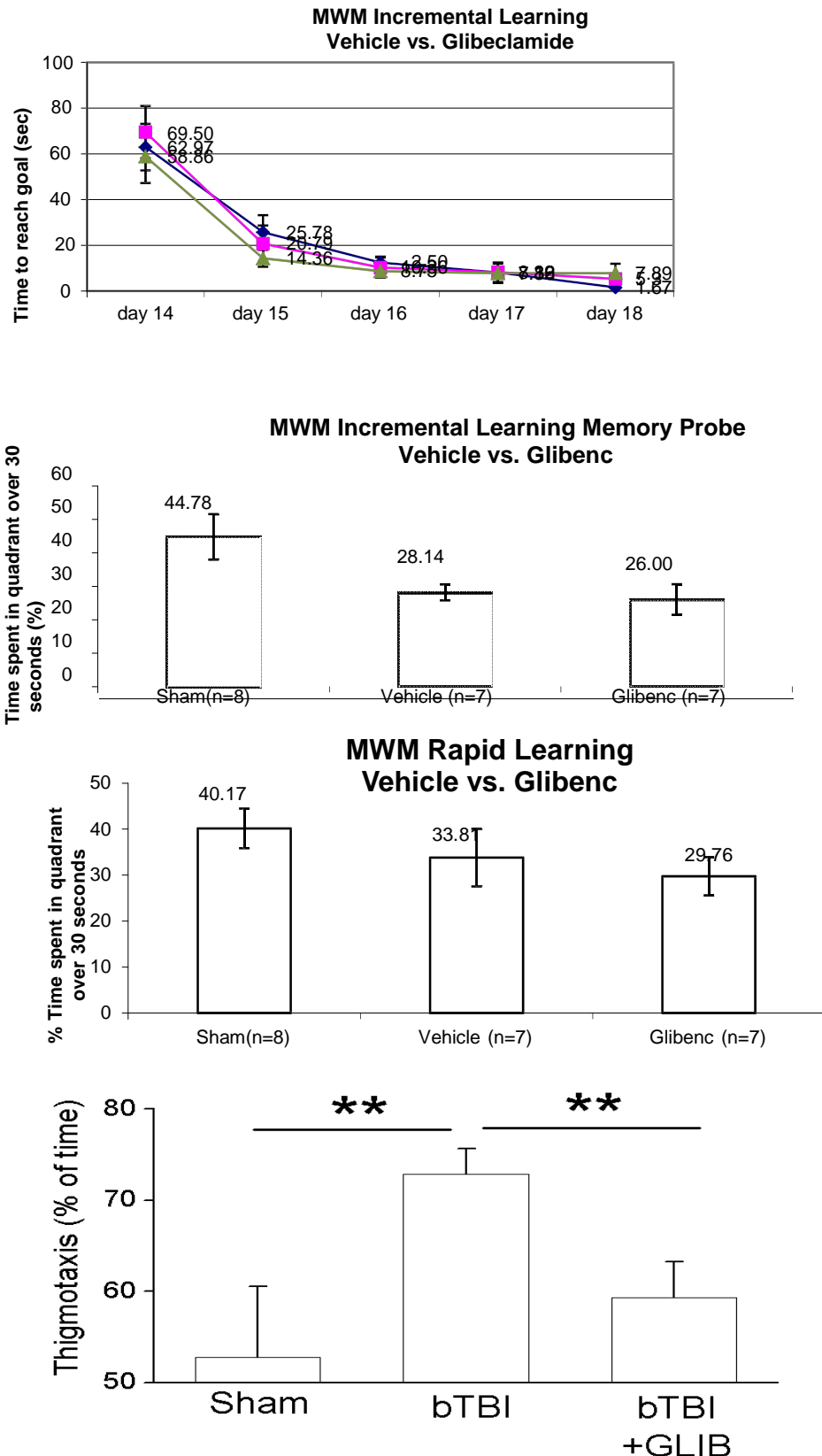


Figure 33: Vestibulomotor behavior between treated and non-treated groups of rats blasted with 24.5cm BDC. A) Spontaneous rearing, B) Beam walk test, and C) Beam Balance and D) Accelerating Rotorod test, up to 28 days post blast exposure and treatment with either vehicle (n=14), glibenclamide (n=7), or sham (n=14). Both blasted groups with or without treatment did badly up to 14 days compared with shams, there was decline in behavior in all groups after 21 days, probably due to heavy weight and/or lack of interest.

Figure 34: Incremental Learning on MWM: A) Incremental Learning post injury day 14-18, there is no significant difference between groups. B) Memory probe on day 19, there is significant difference between sham group compared with Vehicle treated and Glibenclamide treatment, however glibenclamide did not alter the memory of the blasted rats compared with vehicle treated blasted rats. C) Apnea vs. MWM memory probe in rats sham (n=10) o sec., Vehicle (n=11) and Glibenclamide (n=14). D) Similarly there is no difference between the groups in rapid learning memory. E) **Anxiety-related thigmotaxis is elevated in the rats after dcBI.** Open-field thigmotaxis (tendency to remain close to the wall) times are shown for sham rats and rats 2 weeks after blast TBI with vehicle and glibenclamide treatment. Note that elevated thigmotaxis after dcBI is reduced in glibenclamide treated rats.



2) Blast-TBI COBIA 29.5 cm BDC (427 kPa)

Study performed under Good Laboratory like Protocol;(GLP). Prior to beginning the final work on Objective 1c and Objective 1d, all SOPs were written , all equipment was calibrated and certified. All personnel involved in these experiments underwent GLP Training and were certified. Training included Pharmaceutical Training seminars on GLP. GLP training was provided by Jeiven Pharmaceutical Consulting Inc. (Scotch Plains, NJ).

For GLP (like) experiments the 29.5cm BDC was used; which induced 427kPa blast overpressure. The study was done using the COBIA and dcBI method. The average apnea was significantly higher in the glibenclamide treated group (Fig. 35), this probably explains the lack of significant changes in the behavior of the glibenclamide treated and vehicle -treated group. Although we found improvement with the glibenclamide treated rats in vertical exploration up to 28 days (Fig. 36 A), there were no differences with other vestibulomotor tests, beam walk and accelerating rotorod. (Fig. 36 B,C)

In this study Morris Watermaze Test was performed starting at day 14 post blast-TBI: There were no differences in the incremental learning of the three groups; sham (n=15), vehicle treated (n=15) and glibenclamide treated (n=16) rats. (Fig. 37 A). Although there was reduction in the memory probe, rapid learning and thygmotaxis in vehicle treated group, but this difference was not significant (Fig. 37 B,C,D). This might be caused by the higher apnea of the glibenclamide group compared with the vehicle treated group since we already have shown the relationship between high apnea and memory probe (Fig.7 C) and apnea and rapid learning (Fig.8 B).

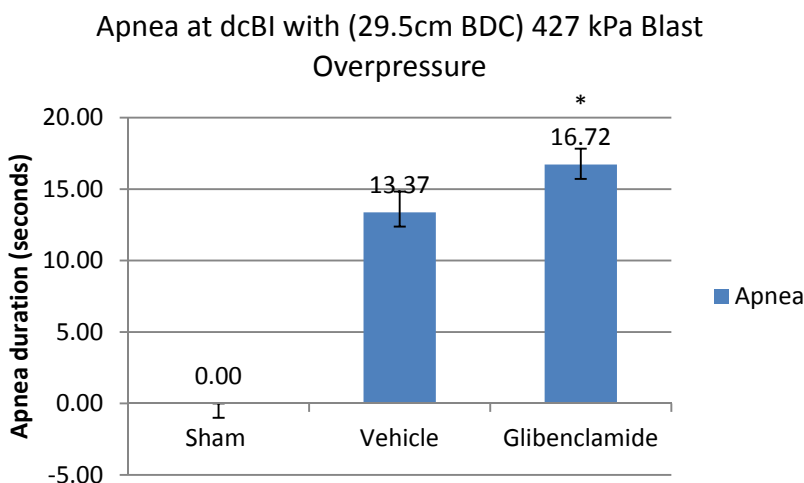


Figure 35: Apnea levels at blast.

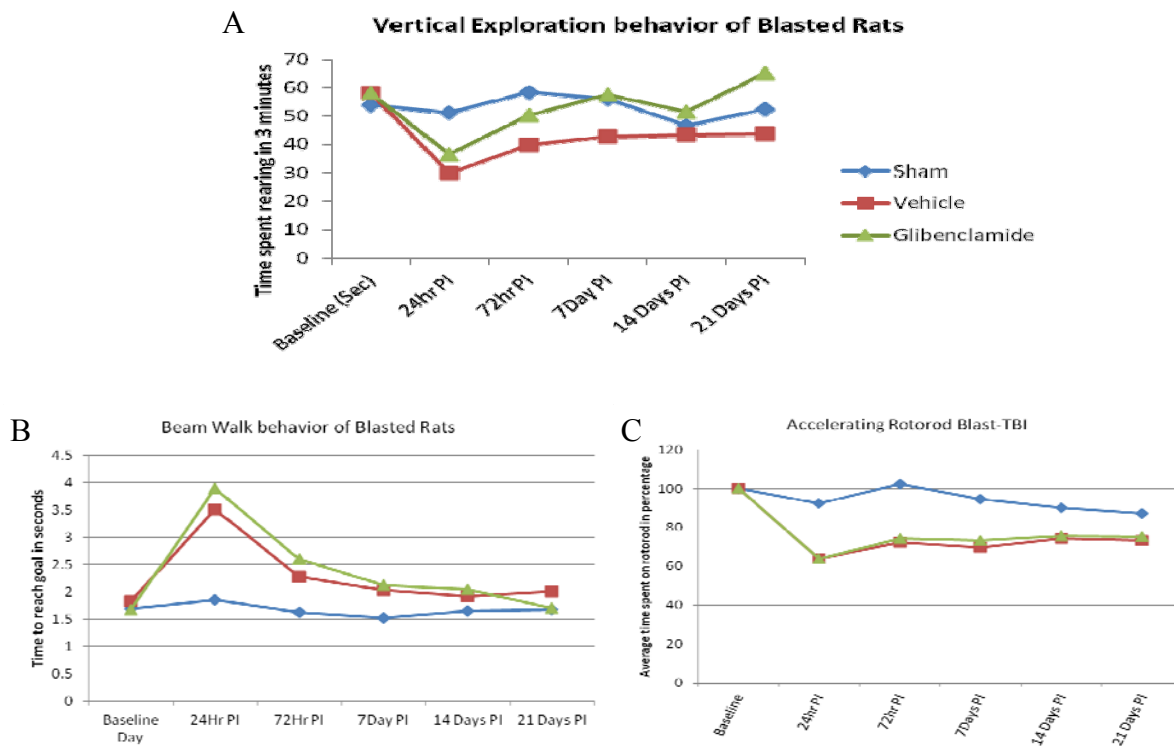


Figure 36: Vestibulomotor behavior between treated and non-treated groups. A) Spontaneous rearing, B) Beam walk test, and C) Accelerating Rotorod test, up to 21 days post blast exposure and treatment with either vehicle (n=15), glibenclamide (n=16), or sham (n=15). Both blasted groups with or without treatment did badly up to 14 days compared with shams, there was decline in behavior in all groups after 21 days, probably due to heavy weight and/or lack of interest.

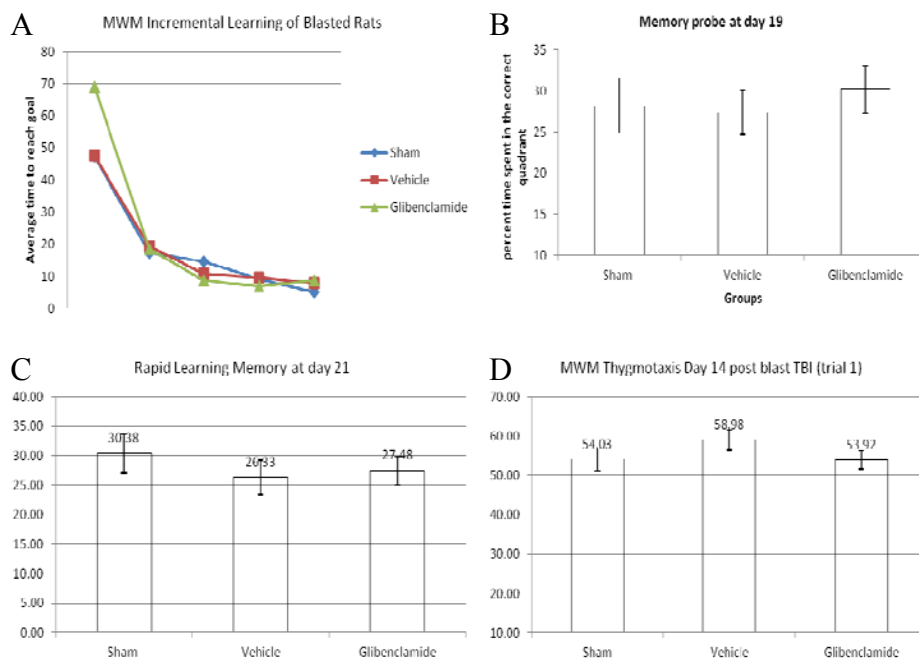


Figure 37: A. Incremental learning 14 days post injury till day 18, no difference in the learning ability of blasted and non-blasted rats. **B. Memory probe after dcBI.** There was no significant difference between the treated and untreated groups in memory probe (day 19) after

incremental learning for 5 days in Morris watermaze. Note that there is slight reduction in vehicle treated rats compared with sham and glibenclamide treated rats. Blast was induced with a 29.5 cm BDC (mild blast). **C. Rapid learning** was not different in those groups. **D. Thygmotaxis** (anxiety measure) day 14 trial 1, notice some elevated levels of thygmotaxis in the blasted vehicle treated rats. Glibenclamide treated rats showed similar levels of thygmotaxis as the sham rats.

Objective 3b: Pre-treatment with glibenclamide rats undergoing Blast-TBI

Pretreatment experiments:

After Improving the COBIA delivery system two separate sets of experiments were conducted on 2 groups of rats, which pretreated with either glibenclamide or vehicle for a week before Blast-TBI, using either the caudal position (blast is delivered caudal to the head mainly towards foramen magnum), or the rostral position where the blast is delivered frontally on superior cerebral.

Pretreatment with Glibenclamide (Blast-TBI Rostral position):

Rats were treated with either vehicle (DMSO) (n=12) or Glibenclamide (n=12) one week before the blast and continued treatment for another week after blast. Treatment pumps were inserted subcutaneously, under proper anesthesia and aseptic conditions a week before the blast. The blast was achieved by using the rostral model, and using BDC 29.5cm (kPa) using charge 4 shells. While under anesthesia pumps were changed containing similar treatments in order to continue another week of the same treatment post blast. The performers were blinded to the treatment codes during the blast and through all the behavior and immunohistochemistry tests and analysis. Pre-training for behavior was performed for baseline, and behavior tests were repeated on 24 hrs, 3 days, 7 days and 14 days post blast. Morris water maze tests were initiated on day 14 after blast and continued till day 28 after which rats were euthanized and brain tissues were harvested for IHC.

Table 3: Physiological data during blast TBI:

Groups	Vehicle	Glibenclamide
N	12	12
Ave Weight	304.48	295.02
Min Apnea(sec)	5.75	7
Max Apnea(sec)	15.41	18.9
Ave Apnea(sec)	9.15	11.55
Ventilation	0	0
pO ₂ at baseline	92.83	93.03
pO ₂ at 30 sec	74.52	70.75
pO ₂ at 1 min	80.46	78.29

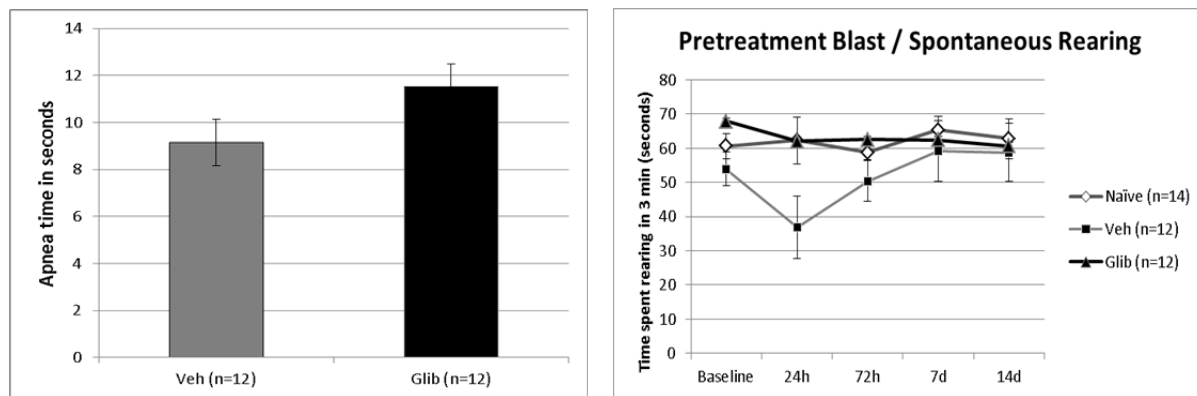


Figure 38: A) Average apnea levels right after blast. (Notice: Glibenclamide treated rats had higher apnea time compared with vehicle treated rats. Higher apnea might correspond to stronger blast levels). B) Oxygen saturation after blast up to 30 min.

Neurobehavioral Function: Pre-Treatment Blast-TBI

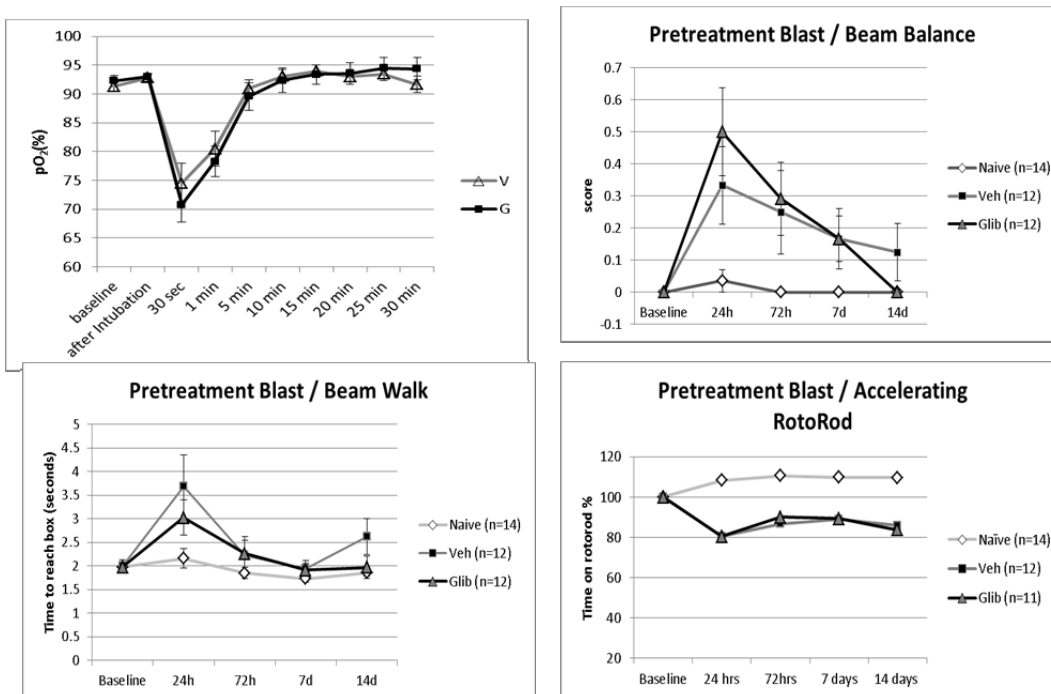


Figure 39. Neurobehavioral function of rats pretreated with either Glibenclamide or Vehicle, similar age matched Naïve rats (n=14) were also included in these tests. A) Spontaneous Rearing shows Glibenclamide treated group performing very similar to the naïve group, and they are significantly different from Vehicle treated group at 24hrs and 3days after blast. B) Beam Balance test also shows similar results as in the spontaneous rearing, where Glibenclamide treated rats recovered faster than the Vehicle treated rats. C) Beam walk data show that rats glibenclamide treated rats recovered faster than the vehicle treated rats notice at day 14. D) There were no differences in accelerating rotorod in either group compared with naïve group. This might probably be because of the higher apnea in Glibenclamide treated group. (Fig.38)

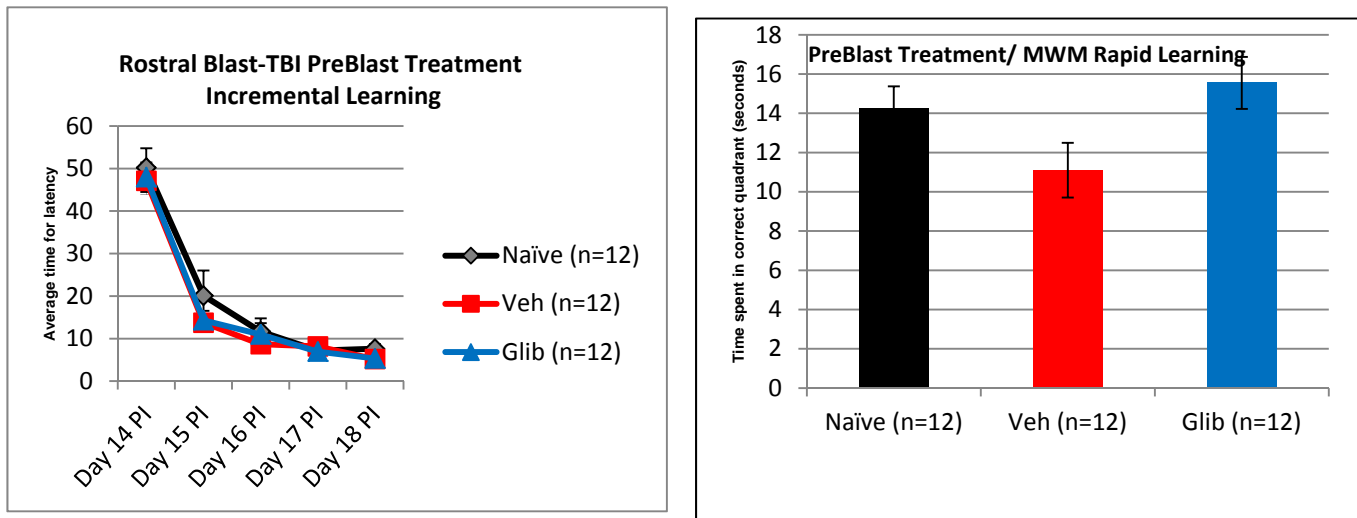


Figure 40. Morris Water maze test A) Incremental Learning, B) Rapid learning at day 28 post blast. There was no difference in incremental learning test, but significant difference between Vehicle treated group and Glibenclamide treated rats at day 28 in rapid learning task. Glibenclamide treated rats behaved as good as the naïves while vehicle treated rats did not remember the location of the platform and spent less time in the correct quadrant in the Morris Watermaze pool.

Summary of animal use:

Total Number	884
Sham	96
Naïve	50
Vestibulamotor Behavior	349
MWM Cognitive	196
Immunohistochemistry	140
Miscellaneous experiments.	60

Additionally to the results reported above in SECTION II and SECTION III (see SUPPORTING DATA) we are reporting Blast TBI model data directly related to the scope of the grant, however they were not specified in in original objectives. Although directly related to the project these studies were partially funded by the sources not related to this project.

Objective 4: in normal human volunteers, determine the safety of oral glibenclamide as it might be used as prophylaxis against blast-TBI.

The SUR1 blocker, glyburide, in normal human volunteers. This activity has been transferred to the University of Washington, St. Louis, due to the fact that the investigator responsible for this experiment has moved there as faculty.

Rationale for Study and Study Design

This pilot study seeks to support the hypothesis that glyburide administered at the lowest dose (1.5 mg/dL daily) to healthy subjects is safe both physically and cognitively. The results of this study will provide the necessary foundation to study this on a larger scale to determine the feasibility of using Glyburide in warfighters either prophylactically or for treatment of brain injury.

The Study Design is a Phase 1 clinical trial (2:1 drug vs. placebo). Subjects enrolled were be randomly assigned (2:1) to receive either Glyburide, 1.5 mg daily (with breakfast) by mouth vs. matching placebo for 7 days while under careful medical monitoring in an inpatient Clinical Research Unit (CRU) within the Center for Applied Research Sciences (CARS) at Washington University's Medical Campus. Randomization was used to avoid bias in the assignment of subjects to treatment, to increase the likelihood that known and unknown patient attributes (e.g., demographics and baseline characteristics) are evenly balanced across treatment groups, and to enhance the validity of statistical comparisons across treatment groups. Subjects participated in an informed consent process, and those wishing to take part werel be asked to undergo a comprehensive interview detailing their past medical history and formal physical examination. If a subject was deemed appropriate by the team, he/she was be asked to perform an exercise test (treadmill for 30 minutes) and undergo laboratory assessments to further determine eligibility. Individuals who did not meet inclusion criteria based on screening activities were notified immediately and were compensated for their time. Volunteers meeting all eligibility criteria were scheduled for the week long in-patient evaluation. Each subject underwent a battery of physical, cognitive, and laboratory tests in addition to receiving oral glyburide or placebo each day for one week.

STUDY PROCEDURES AND ASSESSMENTS

Please refer to the Study Schedule (**SUPPORTING DATA**, Appendix A) for a description of the specific laboratory and clinical assessments being performed by study day.

ASSESSMENT OF EFFICACY AND SAFETY

Details regarding the adverse event reporting and DSMB plan can be found in Appendix (**SUPPORTING DATA** Appendix B).

Choice of Dose of Study Drug to be Tested:

The amount of glyburide to be used in the humans is based on the dose used in our rodent models. In rats (~0.3 kg), we use an infusion of 200 mg/hr subcutaneously, which delivers ~16 µg/kg/day. In humans (~70 kg), we plan to give 1.5 mg po QD, which, assuming 50% absorption from the gut, delivers ~12 µg/kg/day.

Results:

Thirty-seven patients agreed to participate in the study. Of the 37 who consented, 16 were screen failures. 21 participants completed the study (13 male, 8 female). 14 participants were randomized to treatment (oral glyburide 1.5 mg/day) and 7 were randomized to placebo. The mean age of participants was 26 in the treatment group and 25 in the placebo group.

Safety:

A total of 45 adverse events (AEs) occurred during this study. 40 of the AEs were experienced by 13 patients in the treatment arm and 5 AEs occurred in 3 patients in the placebo arm. Of the 40 adverse events in the treatment arm, 24 of them were related to low blood glucose values (48 -69 mg/dl). 3 of the 5 AEs reported in the placebo group were also related to low glucose values (60-69 mg/dl) and occurred in 3 different subjects. Of the 14 patients in the treatment group, 10 patients had an AE related to low glucose. None of the participants with low glucose values were symptomatic. There were no serious adverse events in the entire study group. However, one patient had study drug held on days 6 and 7 due to unexplained elevated ALT and AST levels (per the recommendation of the DSMB who met ad hoc to review all of the participant's laboratory values). These elevations were not considered to be related to study drug, but the PI and DSMB wanted the participant to remain on study to follow him for any additional safety concerns and to address them appropriately. The study participant did not experience any additional adverse events during his remainder of study participation and refused further medical work up to evaluate his abnormal ALT and AST levels (i.e. possible viral association, etc.). Once the results were unblinded, it was discovered that this participant had received Glyburide but his glyburide analysis revealed no correlation.

8 additional AEs experienced by study participants were related to intravenous line or venipuncture site erythema and/or ecchymosis. Finally, 2 patients (one patient in each study arm) complained of vertigo/dizziness during their treadmill exercise test. Both of the episodes resolved without sequelae.

Most important to this investigation was the determination that there was not a statistically significant difference between the number of patients experiencing a low blood glucose value in the treatment arm (71%) compared to the placebo arm (43%) [$p=0.2$]. However, participants in the treatment arm were more likely to experience more than one low blood glucose value than their counterparts.

Treadmill exercises

All participants were able to complete their 3 treadmill exercise tests per day for their entire 7 day study participation without experiencing any serious adverse events. Two patients (1 patient in each arm) experienced dizziness/vertigo during a treadmill exercise. The patient in the treatment arm complained of dizziness on study day 2 during his second treadmill exercise, however he was able to complete the exercise and felt as though his vertigo was related to watching the television screen while on the treadmill. The patient in the placebo arm of the study experienced dizziness at the end of his second treadmill exercise on study day 4, but this dizziness quickly resolved without intervention. Both events were unrelated to low glucose values.

Mini-Mental Exam and Cantab Cognitive Performance

None of the patients in the entire study group exhibited a decrease in their Mini-Mental Status Exam scores during the study period. Although there were some minor differences in individual cognitive performance as measured by Cantab in 2 patients, we found this to be not significant. Overall analysis of the entire study population was clinically significant, though this pilot study was under powered to appropriately measure a difference between the 2 groups. Appendix D.

Quantification of Glyburide in Human Plasma

Blood samples were collected daily after study drug administration and were stored in a – 80° freezer for measurement at the conclusion of the study, in order to maintain the blind. A pre-validated LC-MS/MS method to analyze glyburide in human plasma was selected by an expert in the field, Dr. David Scherrer.

The LC-MS/MS method for quantification of glyburide in human plasma was developed by Dr. Scherrer and his team at the Diabetic and Cardiovascular Disease Center, Washington University in St. Louis. The sample analysis was performed using developed method data accepted based on pre-set GLP criteria.

During the validation, blank human plasma was fortified with glyburide, to prepare calibration standards and quality control (QC) samples. A protein precipitation procedure was used to extract glyburide from 0.05 mL of human plasma. The extracts were separated by column-switching high-performance liquid chromatography (HPLC) on a SecurityGuard Gemini C6-Phenyl (4 x 3 mm) and Gemini C6-Phenyl column (5µm, 50 x 2 mm). Glyburide was monitored by an Applied Biosystems Sciex 4000QTRAP tandem mass spectrometer (MS/MS) equipped with an electrospray ion source in the positive ion mode and multiple-reaction monitoring (MRM) detection with precursor → product ion pair of 494.2 → 369.1 for glyburide, 499.2 → 374.1 for d3-glyburide (internal standard), respectively. The calibration curve consisted of eight standards of different concentrations, each in duplicate, ranging from 2 to 1000 ng/mL of glyburide. The lower limit of quantification is 2ng/mL. The calibration curve was established by a weighted ($1/\text{concentration}^2$) linear regression of the peak area ratio of the analyte to that of the internal standard. The following conditions should be met in developing a calibration curve: less than 20% deviation from nominal concentration for LLOQ and

less than 15% deviation from nominal concentration for standards other than LLOQ. At least four non-zero standards should meet the above criteria, including the LLOQ and the calibration standard at the highest concentration.

A clinical sample analytical batch consisted of calibration standards in duplicate, a blank, a blank with internal standards, low QC (LQC), middle QC (MQC) and high QC (HQC) (multiples of three QC should be at least 5% of the number of unknown clinical samples) and unknown clinical samples. The standard curve covered the expected unknown sample concentration range, and the samples that exceeded the highest standard were diluted and re-assayed. In the dilution sample re-assay, a diluted QC in triplicate was also included in the analytical run. The results of the QC samples provided the basis of accepting or rejecting the run. At least 2/3 QC samples should be less than 15% deviation from their respective nominal value. One third of QC samples may be outside the 15% deviation from their respective nominal value, but not all at the same concentration.

Results:

All the standard and QC samples in clinical sample analysis passed the pre-set criteria and data were accepted. The data of clinical samples are provided in Appendix C.

The level of glyburide present in the bloodstream was found to have no correlation with episodes of hypoglycemia.

KEY RESEARCH ACCOMPLISHMENTS: Bulleted list of key research accomplishments emanating from this research.

1. We developed, constructed and implemented a cranium only blast injury apparatus (COBIA) for production of standardized and reliable rat model of “dose dependent” blast-TBI (bTBI) to study the direct transcranial effects of blast on the brain, independent of indirect transthoracic effects
2. Detailed anatomical evaluation revealed that cranium only blast impacts brain-blood barrier transiently, immediately after the blast. BBB disruption was detected as early as 15 min after bTBI and lasted for up to 24 hours.
3. Long term impact of the blast is manifested predominantly in the brain tissues at the density boundaries, with elevated markers of the neuroinflammation, neurodegeneration and neuronal cell death.
4. COBIA bTBI resulted in the transient vestibulomotor abnormalities and long term spatial memory deficits.
5. After COBIA bTBI Sur1 and TRPM4 RNA and protein up-regulation was detected as early 4 hours after the blast consistent with de-novo expression of the SUR1 regulated NC_{Ca-ATP} channel
6. Studies (including GLP-compliant protocol) with chronic administration of the SUR1 antagonist showed that post-bTBI Glyburide does not alter blast-induced long term cognitive deficits but improves anxiety-like behavior. In contrast prophylactic treatment with Glyburide improved performance in spatial memory task related to the hippocampal function.
7. Study on the human volunteers showed that Glyburide is safe drug to be used for potential prophylaxis against blast –TBI.

REPORTABLE OUTCOMES: Provide a list of reportable outcomes that have resulted from this research

Presentations

“Cranium-only Blast Injury Apparatus (COBIA): A Reproducible Model for Sublethal Blast Traumatic Brain Injury with Delayed Cognitive Deficits”. Williams, A; Bochicchio, G; Driscoll, I; Keledjian, K; Simard, P; Gerzanich, V; Scalea, T; Simard J.M.

Presented at:

American College of Surgeons -Committee on Trauma, State of Maryland annual meeting, November, 2010. First place basic science

American College of Surgeons -Committee on Trauma, Region 3 annual meeting, December, 2010

Second place basic science Gary P. Wratten Surgical Symposium, May 2011

“Direct Cranial Blast, Novel Rodent Model of Blast Traumatic Injury.” Seminar at Johns Hopkins University Applied Physics Laboratory, August 11, 2011

"Molecular, Neurobehavioral and Cognitive Evaluation of the Direct Cranial Blast Injury Model." Kaspar Keledjian, Cigdem Tosun, Volodymyr Gerzanich, J. Marc Simard. 16th Annual VAMHCS Research Day, April 23 2012 at the Baltimore VA Medical Center, Baltimore, MD.

"Molecular, Neurobehavioral and Cognitive Evaluation of the Direct Cranial Blast Injury Model." Kaspar Keledjian, Cigdem Tosun, Volodymyr Gerzanich, J. Marc Simard. National Capital Area TBI Research Symposium, May 22, 2012 at Natcher Conference Center of the National Institutes of Health, Bethesda, MD.

“Exposure of the Thorax to a Sublethal Blast Wave causes Perivascular Neuroinflammation.” Simard JM, Keledjian K, Pampori A, Tosun C, Schwartzbauer G, Ivanova S, Gerzanich V (2012). Military Health System Research Symposium 13-16 August 2012, Fort Lauderdale, Florida.

"Selective Vulnerability of the Foramen Magnum Region to Blast TBI." Adam Pampori, Kaspar Keledjian, Cigdem Tosun, Volodymyr Gerzanich, J. Marc Simard. The 17th annual VAMHCS Research Day, May 6, 2013 at the Baltimore VA Medical Center, Baltimore, MD.

“Selective vulnerability of the foramen magnum region to blast-TBI.” Pampori, A; Keledjian, K; Tosun, C; Gerzanich, V; Simard, JM (2013). *Presented at the 2013 University of Maryland Medical Student Research Day.* 1st place: Best Poster Award

“Selective vulnerability of the foramen magnum region to blast-TBI.” Pampori, A; Keledjian, K; Tosun, C; Gerzanich, V; Simard, JM (2013). *Congress of Neurological Surgeons 2013 Annual Meeting.*

"Selective Vulnerability of the Foramen Magnum Region to Blast TBI." Adam Pampori, Kaspar Keledjian, Cigdem Tosun, Volodymyr Gerzanich, J. Marc Simard. National Capital Area TBI Research Symposium, Apr. 29-30 2013 at Natcher Conference Center of the National Institutes of Health, Bethesda, MD. Oral presentation.

"Invivo Diffusion Kurtosis and MR Spectroscopy Changes Following a Novel Direct Cranial Blast TBI." Jiachen Zhuo, Kaspar Keledjian, Adam Pampori, Volodymyr Gerzanich, J. Marc Simard, Rao Gullapali. National Capital Area TBI Research Symposium, Apr. 29-30 2013 at Natcher Conference Center of the National Institutes of Health, Bethesda, MD. Oral presentation.

"Glibenclamide treatment as a prophylaxis against blast-TBI in rat blast model." K. Keledjian, A. Pampori, J. Karimi, C. Tosun, V. Gerzanich, J.M. Simard. The 18th annual VAMHCS Research Day, May 19, 2014 at the VA Medical Center, Baltimore, MD.

Manuscripts:

Published manuscripts relevant to this project which acknowledge DoD grant support

- (1) Kuehn R, Simard PF, Driscoll I, Keledjian K, Ivanova S, Tosun C, Williams A, Bochicchio G, Gerzanich V, Simard JM. Rodent model of direct cranial blast injury. *J Neurotrauma* 2011;28(10):2155-69. PM:21639724; PMCID:
- (2) Simard JM, Woo SK, Schwartzbauer GT, Gerzanich V. Sulfonylurea receptor 1 in central nervous system injury: a focused review. *J Cereb Blood Flow Metab* 2012;32(9):1699-717. PM:22714048; PMCID:PMC3434627
- (3) Simard JM, Woo SK, Gerzanich V. Transient receptor potential melastatin 4 and cell death. *Pflugers Arch* 2012;464(6):573-82. PM:23065026; PMCID:PMC3513597
- (4) Kurland DB, Tosun C, Pampori A, Karimy JK, Caffes NM, Gerzanich V, Simard JM. Glibenclamide for the Treatment of Acute CNS Injury. *Pharmaceuticals (Basel)* 2013;6(10):1287-303. PM:24275850; PMCID:PMC3817601
- (5) Ryu JH, Walcott BP, Kahle KT, Sheth SA, Peterson RT, Nahed BV, Coumans JV, Simard JM. Induced and sustained hypernatremia for the prevention and treatment of cerebral edema following brain injury. *Neurocrit Care* 2013;19(2):222-31. PM:23468135; PMCID: pending
- (6) Woo SK, Kwon MS, Ivanov A, Gerzanich V, Simard JM. The sulfonylurea receptor 1 (Sur1)-transient receptor potential melastatin 4 (Trpm4) channel. *J Biol Chem* 2013;288(5):3655-67. PM:23255597; PMCID:PMC3561583
- (7) Simard JM, Pampori A, Keledjian K, Tosun C, Schwartzbauer G, Ivanova S, Gerzanich V. Exposure of the Thorax to a Sublethal Blast Wave Causes a

Hydrodynamic Pulse That Leads to Perivenular Inflammation in the Brain. *J Neurotrauma* 2014. PM:24673157; PMCID: pending

- (8) Stokum JA, Kurland DB, Gerzanich V, Simard JM. Mechanisms of Astrocyte-Mediated Cerebral Edema. *Neurochem Res* 2014. PM:24996934; PMCID: pending

CONCLUSION: Summarize the results to include the importance and/or implications of the completed research and when necessary, recommend changes on future work to better address the problem. A "so what section" which evaluates the knowledge as a scientific or medical product shall also be included in the conclusion of the report.

Three major conclusions derive from this study:

1. The results of this study show that in animal model that cranium only delivery of the blast leads to transient (up to 24 h) disruption of the Brain Blood Barrier. Neurobehavioral tests show transient (up to 2 weeks) vestibulomotor and long term cognitive deficits. These abnormalities correlate with long term changes in the brain manifested as upregulation of the neuroinflammatory markers.
2. SUR1/TRPM4 channel, molecular target of the sulfonylurea Glibenclamide, is prominently upregulated as early as 3 hours after the blast. Prophylactic treatment with non-hypoglycemic low-dose of Glibenclamide shows beneficial effects on the long term cognitive deficits induced by the blast TBI.
3. Study on human volunteers confirms that Glibenclamide is safe to be taken as a potential prophylactic for blast TBI.

REFERENCES: List all references pertinent to the report using a standard journal format (i.e. format used in *Science*, *Military Medicine*, etc.)

Reference List

1. M. B. Aboutanos, S. P. Baker, *J. Trauma* **43**, 719 (1997).
2. H. G. Belanger, T. Kretzmer, R. Yoash-Gantz, T. Pickett, L. A. Tupler, *J. Int. Neuropsychol. Soc.* **15**, 1 (2009).
3. G. V. Bochicchio *et al.*, *Am. Surg.* **74**, 267 (2008).
4. R. M. Coupland, D. R. Meddings, *BMJ* **319**, 407 (1999).
5. R. M. Coupland, H. O. Samnegaard, *BMJ* **319**, 410 (1999).
6. E. R. Frykberg, J. J. Tepas, III, *Ann. Surg.* **208**, 569 (1988).
7. I. Cernak *et al.*, *J. Trauma* **40**, S100 (1996).
8. I. Cernak, J. Savic, D. Ignjatovic, M. Jevtic, *J. Trauma* **47**, 96 (1999).
9. I. Cernak *et al.*, *World J. Surg.* **23**, 44 (1999).
10. C. J. CLEMEDSON, *Acta Physiol Scand.* **37**, 204 (1956).
11. D. DENNY-BROWN, R. D. ADAMS, ., *J. Neuropathol. Exp. Neurol.* **4**, 305 (1945).
12. G. A. Elder, A. Cristian, *Mt. Sinai J. Med.* **76**, 111 (2009).
13. I. Cernak, Z. Wang, J. Jiang, X. Bian, J. Savic, *J. Trauma* **50**, 695 (2001).
14. A. C. Courtney, M. W. Courtney, *Med. Hypotheses* **72**, 76 (2009).
15. J. B. Long *et al.*, *J. Neurotrauma* **26**, 827 (2009).
16. S. I. Svetlov *et al.*, *J. Trauma* **69**, 795 (2010).
17. J. M. Simard, S. K. Woo, S. Bhatta, V. Gerzanich, *Curr. Opin. Pharmacol.* **8**, 42 (2008).
18. M. Chen, J. M. Simard, *J. Neurosci.* **21**, 6512 (2001).
19. M. Chen, Y. Dong, J. M. Simard, *J. Neurosci.* **23**, 8568 (2003).
20. J. M. Simard *et al.*, *Nat. Med.* **12**, 433 (2006).

21. J. M. Simard *et al.*, *J. Cereb. Blood Flow Metab* **29**, 317 (2009).
22. J. M. Simard *et al.*, *J. Neurotrauma* **26**, 2257 (2009).
23. J. M. Simard, T. A. Kent, M. Chen, K. V. Tarasov, V. Gerzanich, *Lancet Neurol.* **6**, 258 (2007).
24. J. M. Simard *et al.*, *J. Clin. Invest* **117**, 2105 (2007).
25. H. Kunte *et al.*, *Stroke* **38**, 2526 (2007).
26. M. Chavko, W. A. Koller, W. K. Prusaczyk, R. M. McCarron, *J. Neurosci. Methods* **159**, 277 (2007).
27. D. F. Moore *et al.*, *Neuroimage.* **47 Suppl 2**, T10 (2009).
28. W. C. Moss, M. J. King, E. G. Blackman, *Phys. Rev. Lett.* **103**, 108702 (2009).
29. R. Kuehn *et al.*, *J. Neurotrauma* **28**, 2155 (2011).
30. A. V. Kalueff, A. Minasyan, P. Tuohimaa, *Behav. Brain Res.* **165**, 52 (2005).
31. A. V. Kalueff, A. Minasyan, P. Tuohimaa, *Behav. Brain Res.* **165**, 52 (2005).
32. T. Bast, I. A. Wilson, M. P. Witter, R. G. Morris, *PLoS. Biol.* **7**, e1000089 (2009).
33. R. Gerlai, J. Roder, *Neurobiol. Learn. Mem.* **66**, 143 (1996).
34. S. W. Scheff, S. A. Baldwin, R. W. Brown, P. J. Kraemer, *J. Neurotrauma* **14**, 615 (1997).
35. S. W. Scheff *et al.*, *J. Neurotrauma* **22**, 719 (2005).
36. H. J. Thompson *et al.*, *Restor. Neurol. Neurosci.* **24**, 109 (2006).
37. R. Hajikhani *et al.*, *Adv. Clin. Exp. Med.* **21**, 307 (2012).
38. J. Haller, M. Alicki, *Curr. Opin. Psychiatry* **25**, 59 (2012).
39. S. H. Pinheiro, H. Zangrossi, Jr., C. M. Del-Ben, F. G. Graeff, *An. Acad. Bras. Cienc.* **79**, 71 (2007).
40. H. S. Ghazi-Birry *et al.*, *AJNR Am. J. Neuroradiol.* **18**, 219 (1997).

SUPPORTING DATA: All figures and/or tables shall include legends and be clearly marked with figure/table numbers

SECTION II:

In this section we are reporting Blast TBI model data directly related to the scope of the grant, however they were not specified in in original objectives.

Although directly related to the project these studies were partially funded by the sources not related to this project.

During the experiments of the Blast-TBI we found it necessary to conduct additional experiments and tests in order to better understand the blast injury mechanisms in our COBIA model.

1) We studied the brain alterations after direct cranial blast through magnetic resonance imaging up to 28 days after blast. (Details are in publication X)

2) We studied the transthoracic effect of blast on the brain, by developing a similar apparatus as in COBIA, which transmits blast waves directly to the thorax. Thoracic Only Blast Injury Apparatus (TOBIA). (Details are in publication Y)

3) We studied the mild repetitive blast-TBI in rodents to further validate the COBIA model in repetitive blast injury.

- 4) We further investigated the transvascular transmission of the blast wave and its effect on brain injury through the jugular vein. (JOBIA) (Details are in Publication Y)
- 5) We developed modification for COBIA to direct the blast either caudal or rostral on the skull. (Details are in publication Z)
- 6) In order to understand the treatment delivery window of time we evaluated the blood brain barrier (BBB) leakage after blast-TBI. (Details are in publication Z1)

1)MRI and MRS studies. We investigated brain alterations using diffusion kurtosis imaging (DKI) and proton magnetic resonance spectroscopy (^1H MRS) following dcBI. Microstructural and metabolic changes in dcBI rats were investigated at baseline, 24-hours, 7-days, 14-days, and 28-days after bTBI at 7 Tesla. Among six rats, three rats received 427 kPa, one received 462 kPa and two received 517 kPa. The overpressure blast did not create any MR visible injuries using conventional sequences even at 28 days. The reduced MD and increased MK in the cortex and cerebellum at 14 to 28 days post injury may be an indication of cell swelling and possible cytotoxic edema. (Fig. 3) Increased MK at 28 days may also indicate a delayed microglial activation or activation that elevate high enough to be detectable through changes in MK and also through changes in key metabolites such as NAA. NAA is a neuronal osmolyte and a source of acetate for lipid and myelin synthesis in oligodendrocytes, and its increase at 28 days suggests existence of active repair process. The alterations of Cr and PCr in CB may indicate a mitochondrial malfunction. Taken together, the results from MRS and MRI are consistent with mTBI using the controlled bTBI model which show delayed structural changes using advanced imaging techniques on animals where conventional MRI is negative.

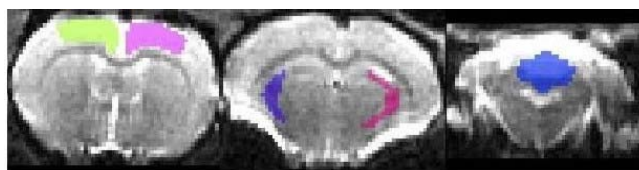
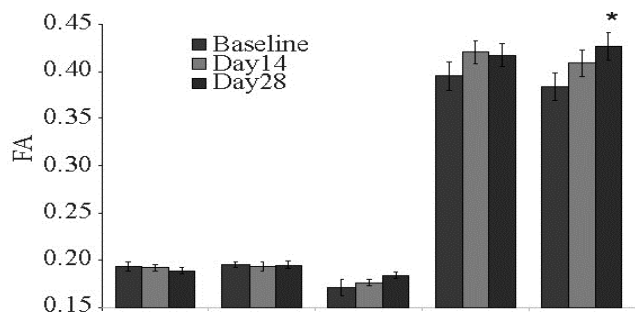


Figure Y1. Regions of interest used for MD, FA, MK calculations in DTI experiment. Somatosensory cortex (left), internal capsules (middle), and cerebellum (right).



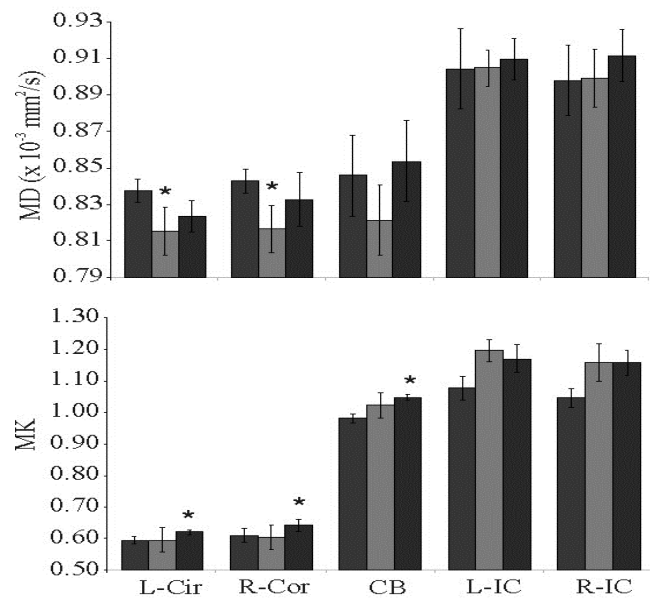
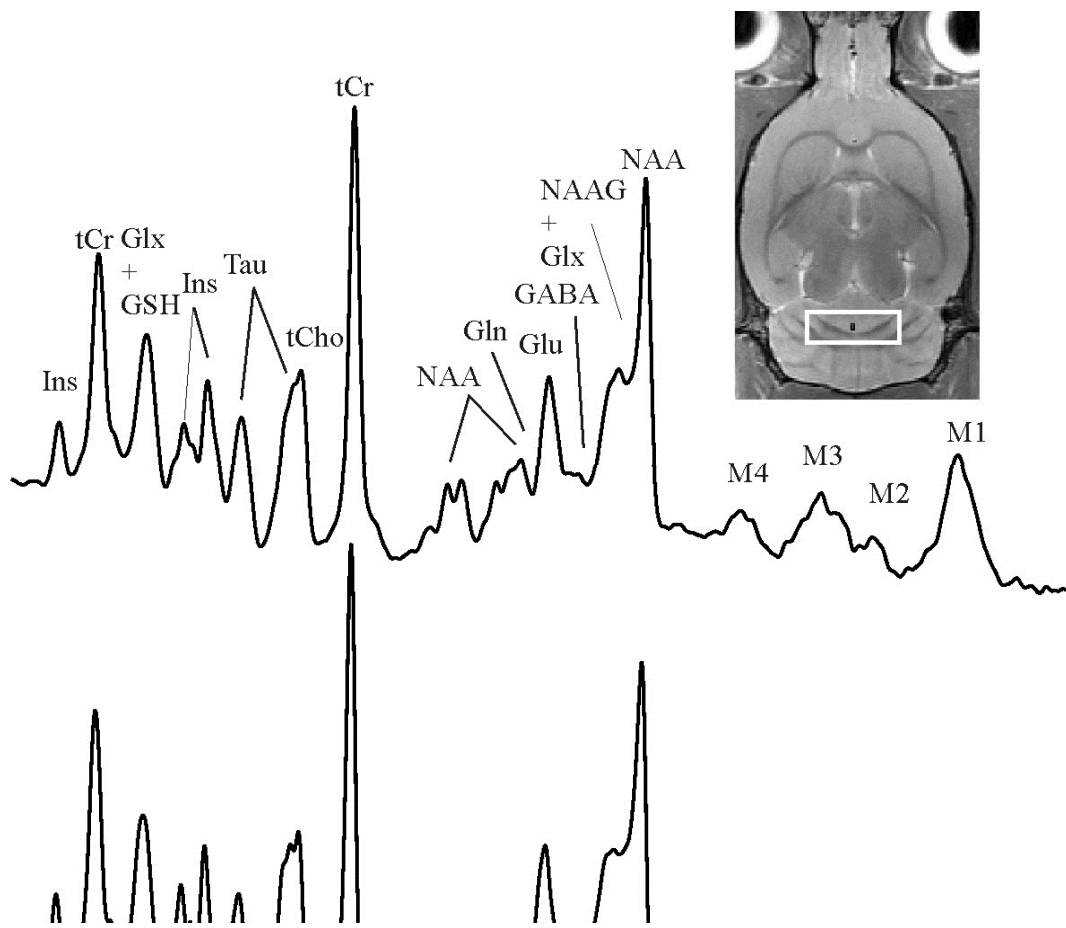


Figure Y2. Regional FA, MD, MK values for baseline and post dcBI; data expressed as mean \pm standard error. *P<0.05 compared to baseline.



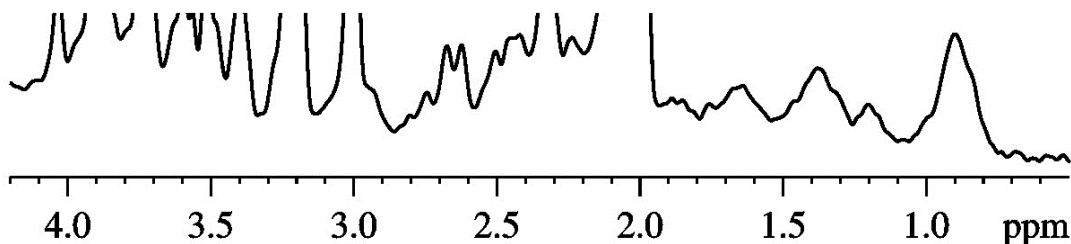


Figure Y3. *In vivo* high resolution proton spectra and corresponding voxel location in cerebellum from a rat at baseline and day 28 after dcBI. It is noted that NAA (NAA.tCr) increased at day 28 compared to baseline. GABA= γ -aminobutyric acid, Glu=glutamate, Gln=glutamine, Glx= Glu+Gln, Ins myo-inositol, NAA=*N*-acetylaspartate, Tau=taurine, tCho=total choline, NAAG=*N*-acetylaspartateglutamate.

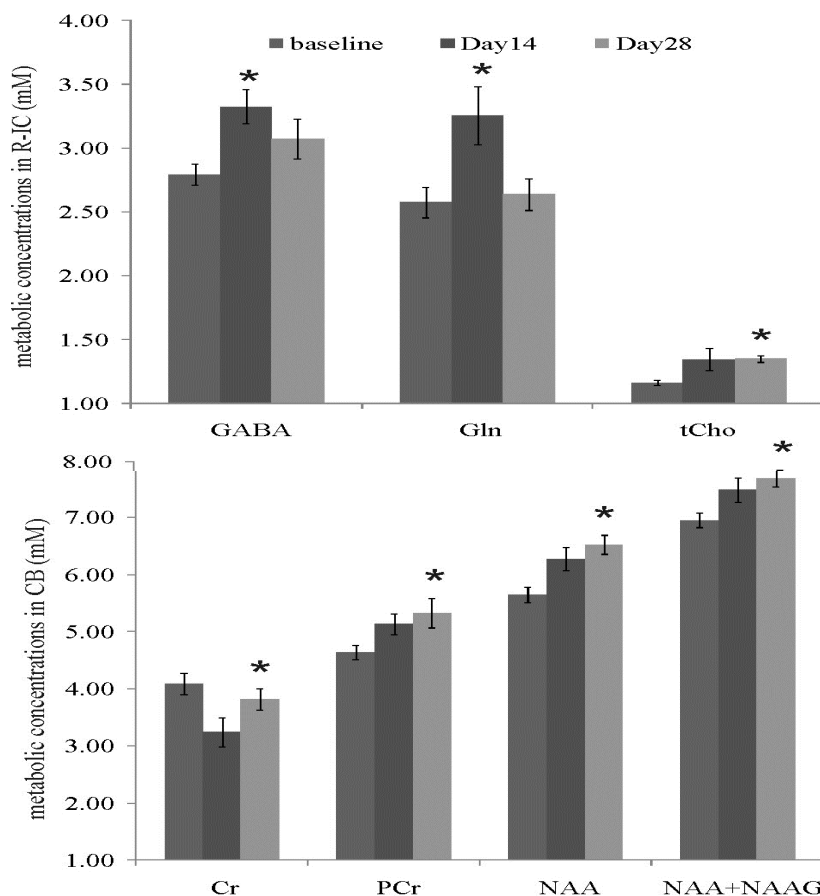


Figure Y4. Regional metabolic concentrations for baseline and post dcBI, data expressed as mean+ standard error. * $P < 0.05$ compared to baseline.

This work was presented as a poster at

- 1) The International Society for Magnetic Resonance in Medicine (ISMRM) 21st annual Meeting and Exhibition under the title: "Diffusion kurtosis and proton MRS changes following mild TBI from blast overpressure using a novel direct cranial blast injury model". Salt Lake City, UTAH April 20-26 2013.
- 2) The 10th annual world congress of SBMT on Brain, Spinal cord mapping, & imaging guided therapy, "In vivo Diffusion Kurtosis and MR Spectroscopy

Changes Following a Novel Direct Cranial Blast Injury Model”. Baltimore Convention Center, Maryland May 12-14 2013.

Presented as an oral presentation at

- 3) The National Capital Area TBI Research Symposium 2013. “In vivo Diffusion Kurtosis and MR Spectroscopy Changes Following a Novel Direct Cranial Blast Injury Model” NIH, Bethesda, Maryland, April 29-30, 2013
- 4) Neurotrauma 2013 Symposium “Temporal Changes Following a Direct Cranial Blast Injury Model using Diffusion Kurtosis Imaging and MR Spectroscopy.” in Nashville, Tennessee on August 4-7.

2) Repetitive mild Blast TBI (Rep. mb-TBI)

Rats (n=5) were subjected to mild dcBI every 3-4 days for a maximum of 5 times. Blast overpressure used 290 kPa, SpO₂ levels returned to baseline values after 5 mins post mild dcBI (Fig. x). The apnea duration was minimal compared with sub-lethal dcBI rats. Fig. X2 represents the average apnea duration in seconds at each Blast day. We conducted also behavior tests with vertical exploration (Fig.X3) and Morris Watermaze stress test (thymotaxis) and compared them with 4 naïve uninjured rats (Fig.X4). We found some decline in the vertical exploration activity in the injured rats. Long term consequences have yet to be determined in future experimental studies in repetitive mild dcBI probably with the modified versions of COBIA (position B vs position C).

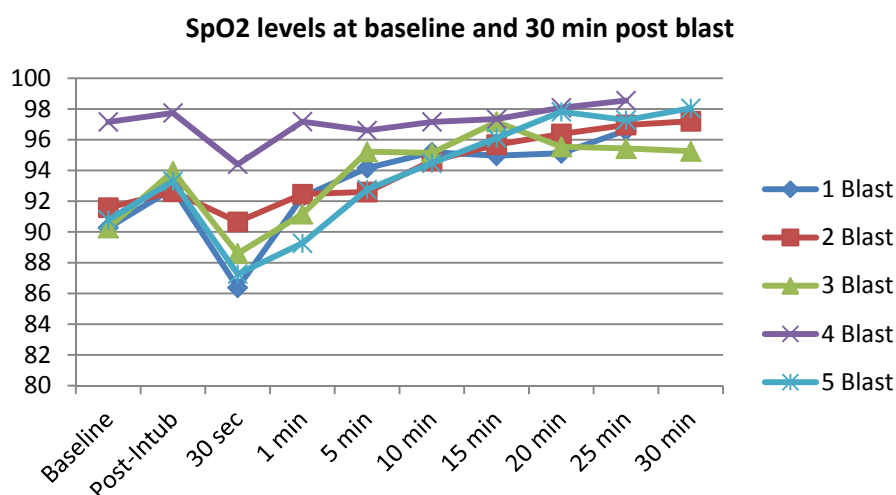


Figure X1. Plot of the oxygen saturation during the initial 30 min following mild dcBI (290 kPa) in 5 injured rats. The plot represents the average numbers of 5 consecutive blasts.

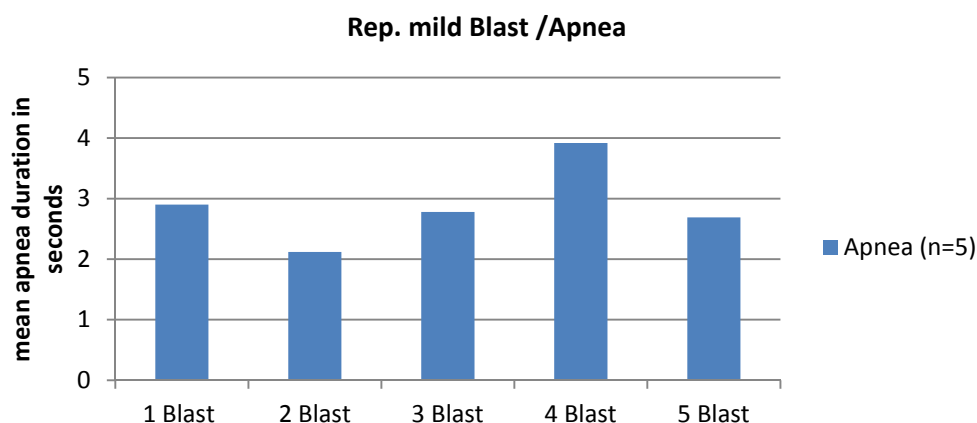


Figure X2. Graph of average apnea after mild dcBI for 5 rats at 5 blasts.

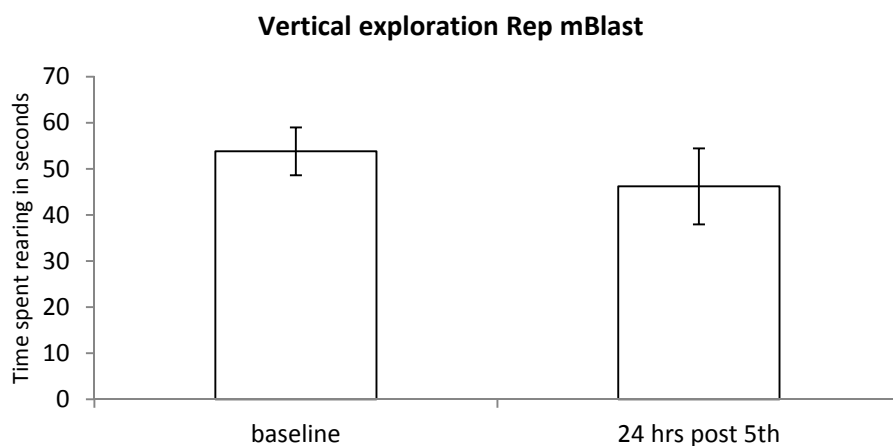


Figure X3. Performance in vertical exploration at baseline and 24 hrs after the 5th mild dcBI.

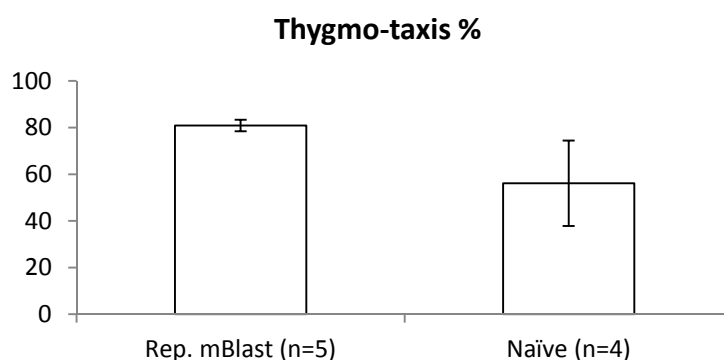


Figure X4. Time spent swimming around the periphery of the pool at the first trial of MWM 24 hrs after last blast. Bars represent \pm SE.

3) Thoracic Only Blast Injury Apparatus:(TOBIA)

Overall, **direct cranial blast injury (dcBI)**, did not result in widespread or generalized extravasation of IgG, cerebral edema and brain swelling. We speculated that vascular dysfunction would be more likely when kinetic energy from the blast wave is transferred to the brain via the transthoracic/transvascular route. This led us to conduct series of experiments to explore the manifestations of **indirect cranial blast injury (icBI)**, which is believed to result from the transthoracic/transvascular mechanism of *Primary* blast injury. For these experiments, we constructed a **Thoracic-Only Blast Injury Apparatus (TOBIA)**, a modification of COBIA. TOBIA allows delivery of the blast wave directly to the thorax, with the head of rat outside of the blast chamber and away from the path of the blast wave (Fig. Z1). For sham injury, the above procedures were performed, except that the cartridge was not detonated. Two other controls also were studied:

- (i) blast exposure as above with TOBIA in rats after ligation of the right internal jugular vein (IJ);
- (ii) blast exposure with the rat positioned immediately adjacent to the BDC-thorax interface of TOBIA, out of line with the collimated blast wave, so that it would not receive a direct impact (“non-impact-TOBIA”).
- (iii) Blast exposure of the catheterized internal jugular vein, so that the overpressure will be transferred to the brain through the fluid filled catheter inserted into the internal jugular vein. JOBIA (Jugular vein Only Blast Injury Apparatus).

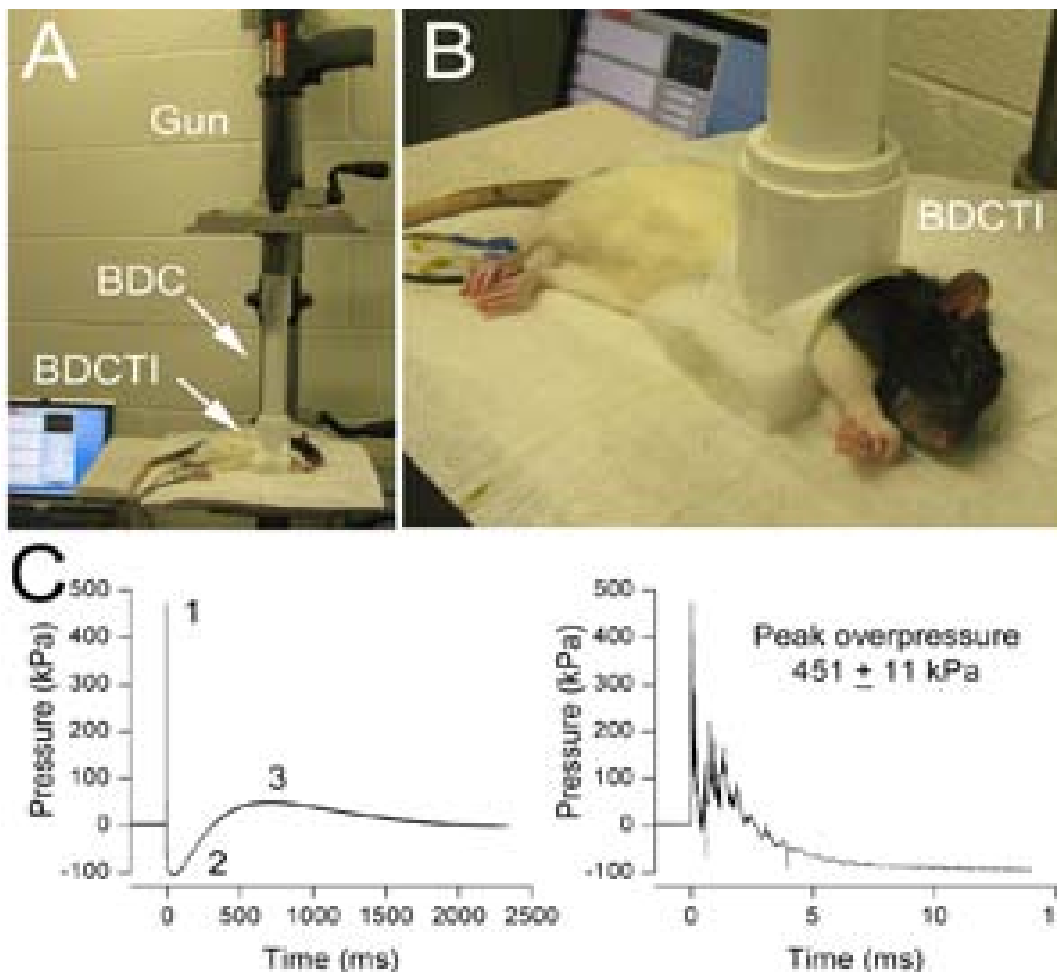


Figure Z1. TOBIA and the blast wave produced by TOBIA. A,B: Overview (A) and close-up view (B) of TOBIA with the rat positioned for blast injury; BDC, blast dissipation chamber; BDCTI, blast dissipation chamber thorax interface. **C:** Blast wave produced by TOBIA shown at low and high temporal resolution; note the specific characteristics of the blast wave, including the initial brief peak overpressure (1), the underpressure (2) and the secondary slower overpressure (3), resemble closely the characteristic features of a free-field explosive blast.

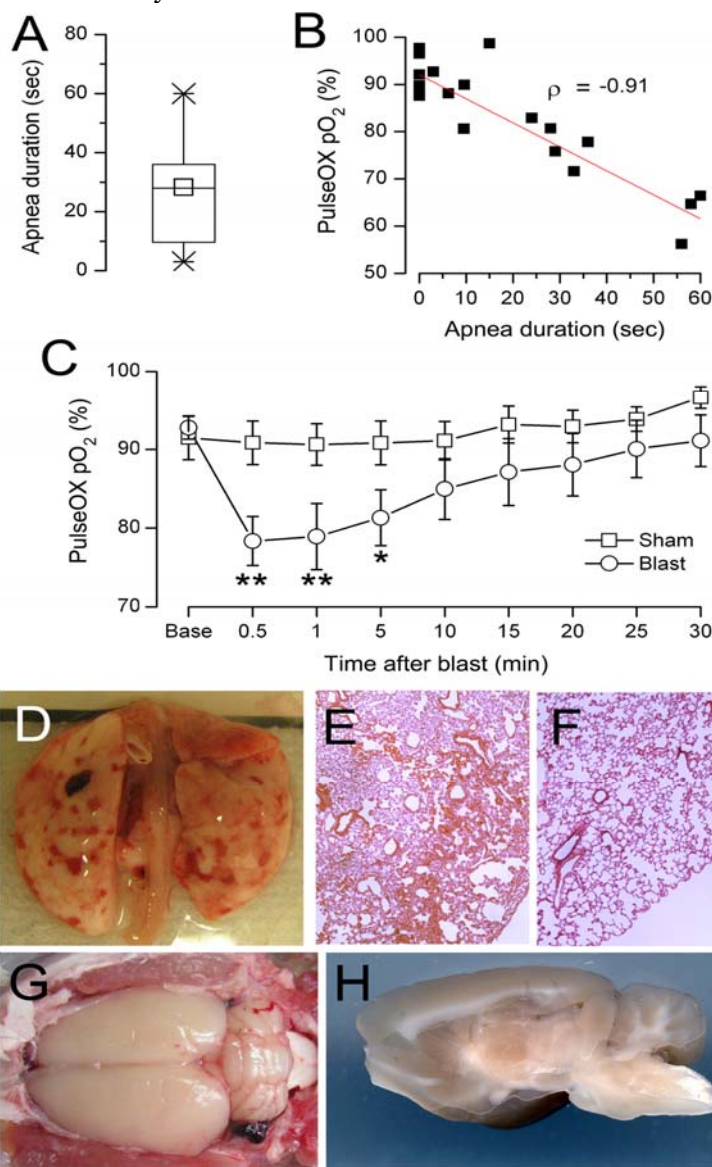


Figure Z2. Blast injury induced by TOBIA is associated with pulmonary but not brain hemorrhagic injury. A,B: Box plot of duration of apnea (A) and relationship between apnea duration and O₂ saturation, measured by pulse oxymetry, in sham-injured (0 sec apnea) and TOBIA-injured rats 1 minute after blast (B); data from 5 and 13 rats in the sham and TOBIA groups, respectively; box plot symbols: box, 25th and 75th percentiles; ×, 1st and 99th percentiles; line, median; small square, mean; ρ , Pearson's correlation coefficient. **C:** Time course of O₂ saturation (mean±SE), measured by pulse oxymetry, in sham-injured (empty squares) and TOBIA-injured rats (empty circles); data from the same rats as in (A); *, $P < 0.05$; **, $P < 0.01$. **D–F:** Images of whole lungs after perfusion (D) and in H&E sections after blast exposure from TOBIA (E), or after sham injury (F). **G,H:** Dorsal (G) and midsagittal (H) views of perfused

brain after blast exposure from TOBIA; in (D–H), the images shown are representative of findings in the same rats as in (A).

SUR1 upregulation after TOBIA Blast

We were exploring the hypothesis that transferring kinetic energy from the blast wave to the brain by way of major blood vessels results in injury primarily to vascular structures of the brain, with cerebral veins, the weakest of the vascular elements, being the most susceptible. These experiments impact directly on our understanding of edema formation in blast-TBI. Given the importance of brain swelling as a cause of death in humans with blast-TBI, a better understanding of the mechanism(s) by which microvessels become dysfunctional is of paramount importance with critical therapeutic implications.

Apnea and lung injury. Non-lethal blast injury induced by TOBIA (451 ± 11 kPa) was associated with apnea that lasted up to 60 seconds and that was accompanied by a commensurate reduction in O₂ saturation (Fig. Z2A,B). O₂ saturation began to recover after 1 minute, but remained depressed up to 30 minutes, compared to sham injured rats (Fig. Z2C). At 24 hours after injury, the lungs showed diffuse patchy hemorrhages bilaterally that were evident on both gross examination and on H&E stained sections (Fig. Z2D–F).

Brain hemorrhage. Non-lethal blast injury induced by TOBIA was not associated with subarachnoid or intracerebral brain hemorrhages in any of the 12 rats examined (Fig. Z2G–I). A small thin frontal subdural hematoma was identified in 1 of the 12 rats.

Perivascular neuro-inflammation

TNF α . Immunolabeling was performed 24 hours after non-lethal blast exposure from TOBIA. Veins were identified as structures >20 μ m diameter that immunolabeled for laminin, were alkaline-phosphatase-negative(40) and that had a single layer of cells in their wall. Co-immunolabeling showed prominent upregulation of TNF α in perivenular tissues throughout the brain, compared to sham control (Fig. Z3A–C). We quantified the abundance of TNF α in perivenular tissues. Analyzing veins in the cortex, hippocampus and hypothalamus showed significant upregulation of TNF α each location, compared to sham controls (Fig. Z3D).

ED-1. We immunolabeled for ED-1, which identifies macrophages as well as activated microglia. In many but not all cases, veins that exhibited prominent upregulation of TNF α also showed ED-1-positive cells in the vessel wall outside of the endothelium (Fig. Z3E–G). In some instances, the morphology of the ED-1-positive cells was more consistent with that of activated microglia than that of invading macrophages (Fig. Z3G).

Sur1 was strongly upregulated in vascular tissues throughout the brain (Fig. Z4). Laminin-positive veins showed prominent upregulation of Sur1 in endothelial cells as well as in perivenular areas (Fig. Z4A–C). Quantification of venular and perivenular Sur1 in cortex, hippocampus and hypothalamus showed significant upregulation compared to sham controls (Fig. Z4A–G). Microvessels in the cortex, thalamus and hippocampus also showed upregulation of Sur1 (Fig. Z4H). Larger arteries at the base of the brain (anterior, middle and posterior cerebral arteries) showed little or no upregulation of Sur1.

4) The transvascular transmission of the blast wave and its effect on brain injury through the jugular vein.(JOBIA)

We studied Sur1 expression following blast exposure with TOBIA in rats after the right internal jugular vein (IJ) had been ligated. We compared Sur1 expression in the hippocampus on the ligated side to that on the non-ligated side. Sur1 was prominently upregulated in hippocampal veins on the non-ligated side (Fig. Z5A). By contrast, Sur1 expression was minimal in hippocampal veins on the side with the ligated IJ (Fig. Z5B). Quantification of Sur1 expression confirmed significantly less upregulation on the side with the ligated IJ (Fig. Z5C).

We examined Sur1 expression in rats subjected to “non-impact blast”, wherein the rat was positioned next to TOBIA so that the collimated blast wave would “miss” the rat. As with sham injured rats (Fig. Z5D–F), and rats with a ligated IJ (Fig. Z5B), Sur1 expression was minimal in the hippocampus of rats with non-impact blast exposure (Fig. 14D).

We conclude that blast injury to the thorax leads to perivenular inflammation, Sur1 up-regulation, and reactive astrogliosis resulting from the induction of a hydrodynamic pulse in the vasculature.

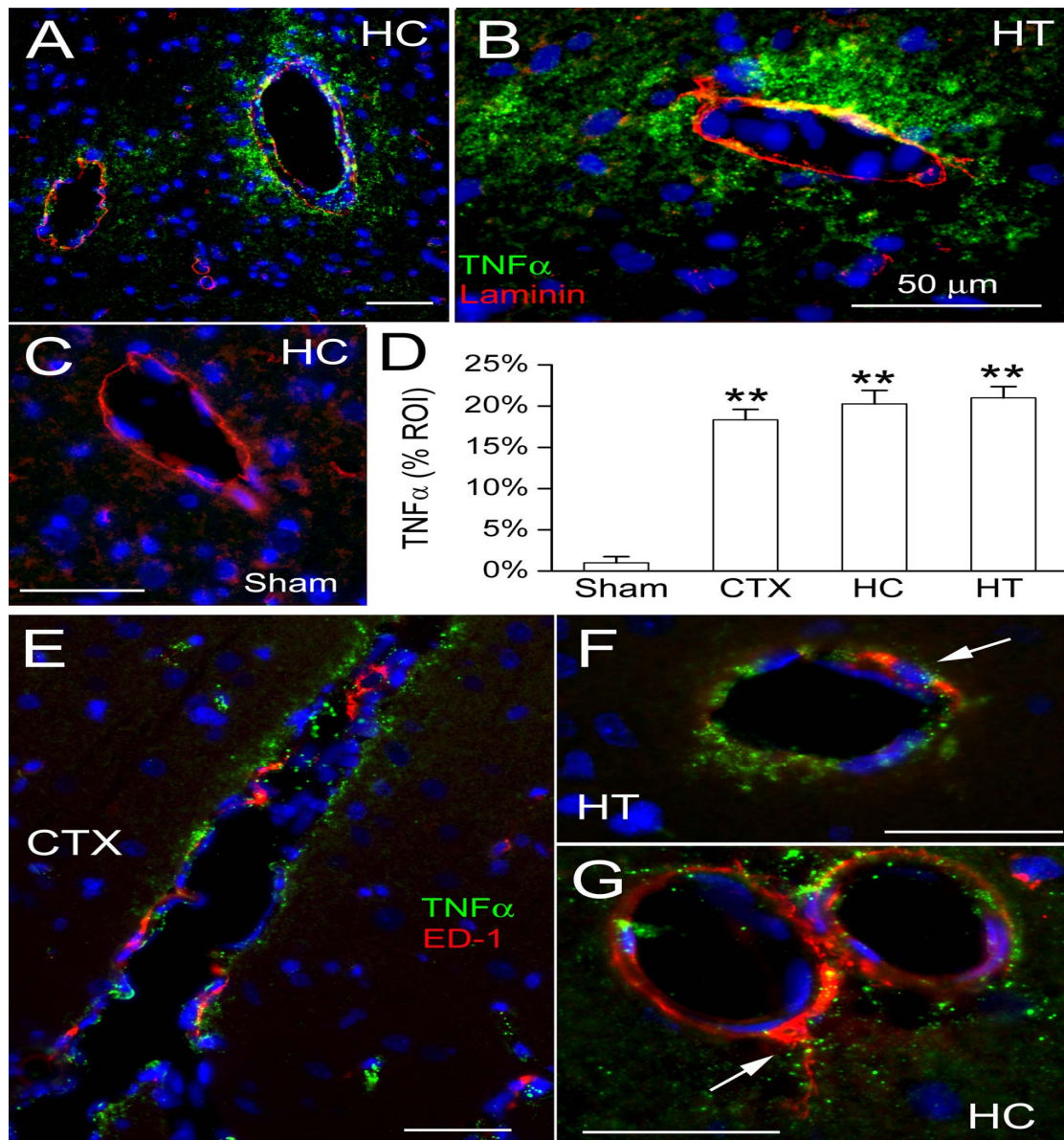


Figure Z3. Blast injury induced by TOBIA is associated with perivenular neuro-inflammation. **A–D:** Co-immunolabeling for TNF α (green) and laminin (red) showing upregulation of TNF α in perivenular tissues after blast injury induced by TOBIA in hippocampus (HC) (A) and in hypothalamus (HT) (B), but not in a sham injured rat (C); the bar graph (D) shows the abundance of perivenular TNF α in cortex (CTX), hippocampus and hypothalamus, compared to sham (sham data from 3 regions combined); all bars, 50 μ m; **, $P < 0.01$; 5 veins per region from 5 rats in the sham and TOBIA groups. **E–G:** Co-immunolabeling for TNF α (green) and ED-1 (red) showing upregulation of ED-1 in the wall of vessels that also display abundant TNF α upregulation after blast injury induced by TOBIA; the arrows point to ED-1-positive cells outside of the endothelial layer, including one with a thin process typical of microglia (G); the data shown are representative of findings in the same rats as in (A–D).

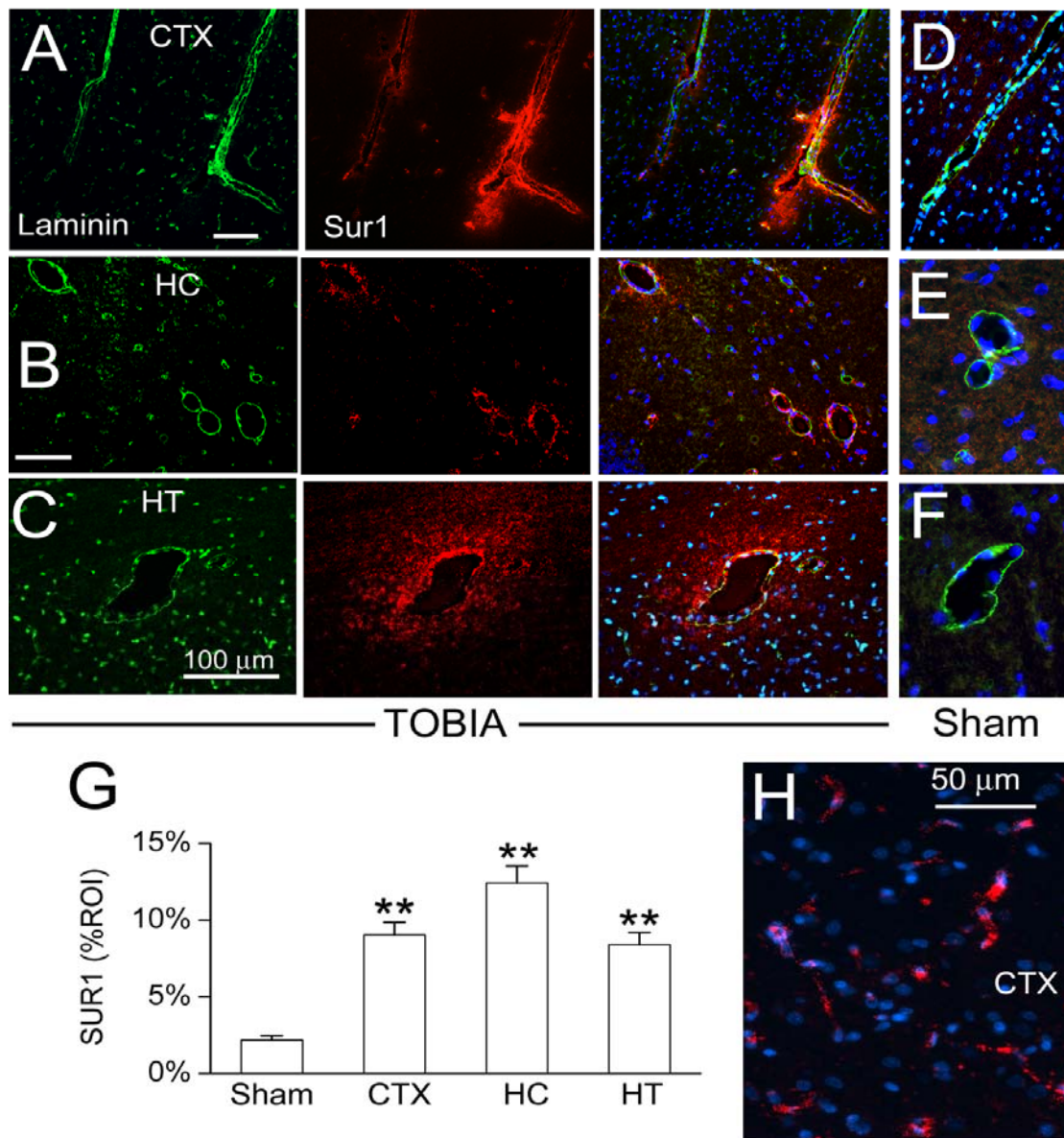


Figure Z4. Blast injury induced by TOBIA is associated with perivenular upregulation of Sur1. **A–C:** Co-immunolabeling for laminin (green) and Sur1 (red) along with superimposed images (right), showing upregulation of Sur1 in veins and perivenular tissues in cortex (CTX) (A), hippocampus (HC) (B), and hypothalamus (HT) (C), after blast injury induced by TOBIA. **D–F:** Superimposed images of sections co-immunolabeled for laminin (green) and Sur1 (red) showing absence of Sur1 in perivenular tissues in cortex (D), hippocampus (E), and hypothalamus (F) after sham injury. **G:** Bar graph showing the abundance of Sur1 in perivenular tissues of the regions indicated after blast injury induced by TOBIA versus sham injury (sham data from 3 regions combined); 5 veins per region from 5 and 8 rats in the sham and TOBIA groups, respectively; **, $P < 0.01$. **H:** Section of cortex immunolabeled for Sur1 showing Sur1 upregulation in elongated structures consistent with microvessels; the data shown in (H) are representative of findings in 3 rats.

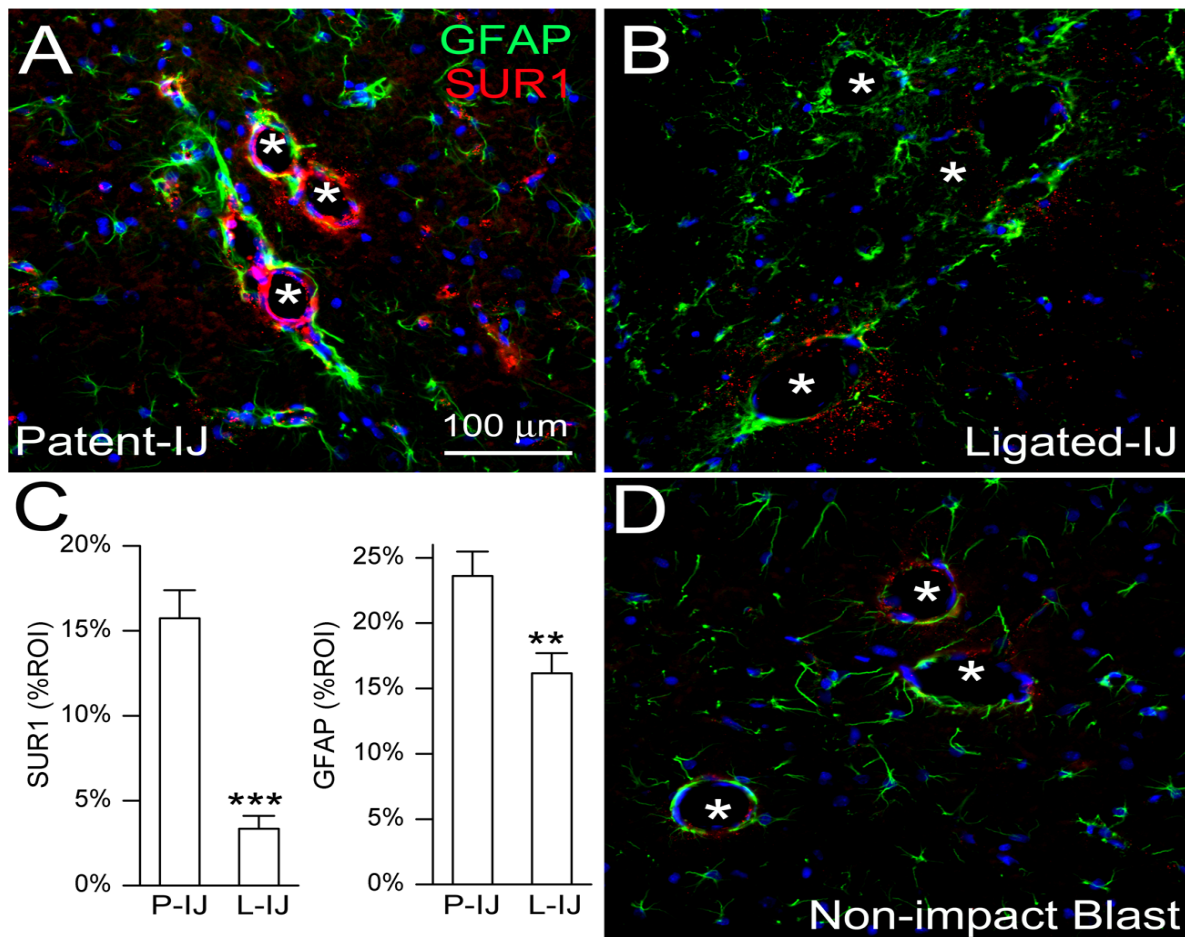


Figure Z5. Perivenular injury with TOBIA requires patency of the internal jugular vein. **A–C:** Co-immunolabeling for GFAP (green) and Sur1 (red), showing prominent upregulation of Sur1 in veins, and upregulation of GFAP in perivenular tissues of the hippocampus on the side with a patent IJ (A), compared to weak expression on the side with a ligated IJ, after blast induced by TOBIA; asterisks denote veins; the bar graph (C) shows a quantitative analysis of Sur1 and of GFAP in or around hippocampal veins from the side of the patent (P-IJ) versus the ligated (L-IJ) internal jugular; **, $P < 0.01$; ***, $P < 0.001$; 17 and 26 veins from patent-IJ versus ligated-IJ sides, respectively, in 2 rats. **D:** Co-immunolabeling for GFAP (green) and Sur1 (red), showing weak expression of Sur1 in veins and of GFAP in perivenular tissues of the hippocampus following non-impact-blast by TOBIA; the image shown is representative of findings in 4 rats.

Conclusion. Overall, our data on the time course of upregulation and downregulation of SUR1 and TRPM4 protein suggest that the SUR1-regulated $\text{NC}_{\text{Ca-ATP}}$ channel is involved in the pathogenesis of the blast-TBI as early as 2 hours after the blast and continues to be expressed up to 1 week after blast. Thus, these data indicate that newly expressed SUR1 presents itself as a potential therapeutic target for sulfonylurea drugs such as glibenclamide for up to 1 week after blast-TBI. Data on TOBIA Blast injury suggest that vascular pathology observed in Blast TBI is mediated predominately via transthoracic route.

Working with COBIA blast injury we discovered that serotonergic neurons in raphe nucleus exhibit enhanced vulnerability to the cranial blast wave. Given the importance of the 5-HT neurons of the raphe system to numerous neuropsychological functions, our observations of pathological involvement of raphe neurons attributable to COBIA blast injury suggests a possible clue that may help explain the propensity of victims of blast injury to suffer psychiatric disturbances.

Results of the experiment with TOBIA provide evidence that the transthoracic/transvascular mechanism is indeed an important mechanism of blast-TBI, and that it leads to brain injury that is distinct from that induced by direct exposure of the cranium to blast. Protection of the brainstem (position B) during blast-TBI has a protective effect on long term behavior in COBIA blast injury, induces milder subdural hemorrhage and neuronal damage, as well as secondary neuronal damage.

Jugular Only Blast Injury Apparatus: JOBIA

In order to study the hypothesis that blast overpressure travels through the vasculature after blast, we developed a model which directly induces blast inside the jugular vein. A rat jugular catheter is inserted into the right jugular vein directed to the brain and tied; the catheter is filled with normal saline, and connected to a vascular port (fig. Z6) the blast is directed to the port which in turn will transfer the blast overpressure to the catheter and the brain vessels. 24 hrs after vascular port blast, brain was harvested and analyzed immunohistochemically. (Fig. Z3-5)



FigureZ6. Jugular Catheter inserted and attached to a large vascular access port (Harvard Apparatus).

SECTION III:

Through the process of the dcBI we noticed that the location of the blast area on the cranium had different outcome in different rodents with similar age/weight, the blast wave tended to preferentially injure tissues at density boundaries, especially at

cerebrospinal fluid (CSF)-brain density boundaries, which also altered our data concerning treatment. Glibenclamide treatment groups had much higher blast impact when compared with untreated or vehicle treated groups which was evaluated by the apnea and seizures after blast-TBI. This in itself induced our interest to further modify our direct cranial blast model to induce blast injury at a similar location in all rodents using the same BDC and powerload factors. After thorough evaluation we noticed that the more the blast was caudal to the rat head (blast impact on cerebellum and brainstem, with the cervical spine included/ CSF-brain boundary) the higher the apnea and mortality (Fig 45) compared with rostral blast impact where even with very high blast overpressures rats had milder outcome with very minimal mortality and milder short term behavioral changes.

COBIA modified

Due to inconsistent mortality rates with the same overpressure BDC and followed by unequal behavior changes in the injured rats, we further re-evaluated the COBIA method by repositioning of the rat head where the blast will be impacted either caudally, foramen magnum (FM) (**position C**) or rostral to the head (**position B**) (Fig. 41), in order to induce consistent blast injury to the brain. We found the benefit of protection of the brainstem during dcBI. Apnea in Position B rats is much lower than in position C. Mortality in position B was almost null compared with position C where we achieved mortality rate of 50% in 427kPa overpressure BDC chamber, which was the lowest available in the series with power level 4.

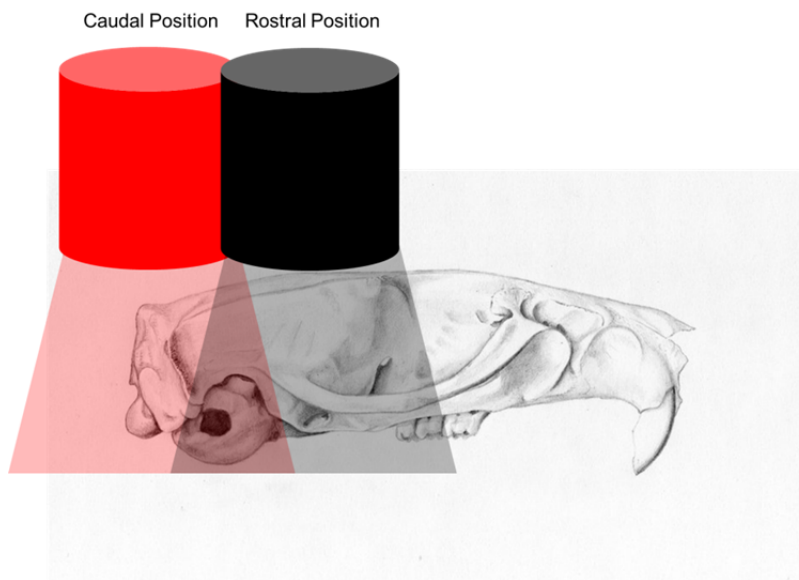


Figure 41. Comparison of the B and the FM blast positions.

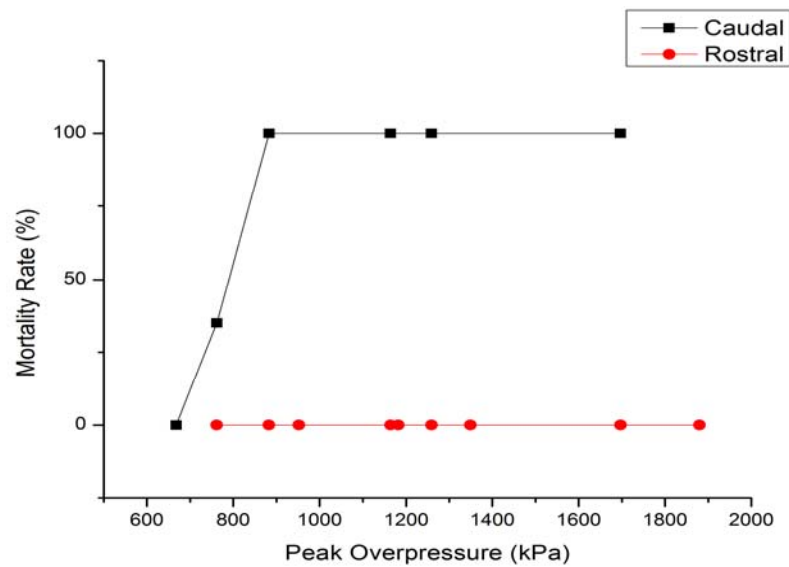


Figure 42. Mortality rate of both FM and B positions is dependent upon peak overpressure. The B blast position (red circles) had no mortality up to 1880 kPa. The FM position had an LD50 of 785 kPa.

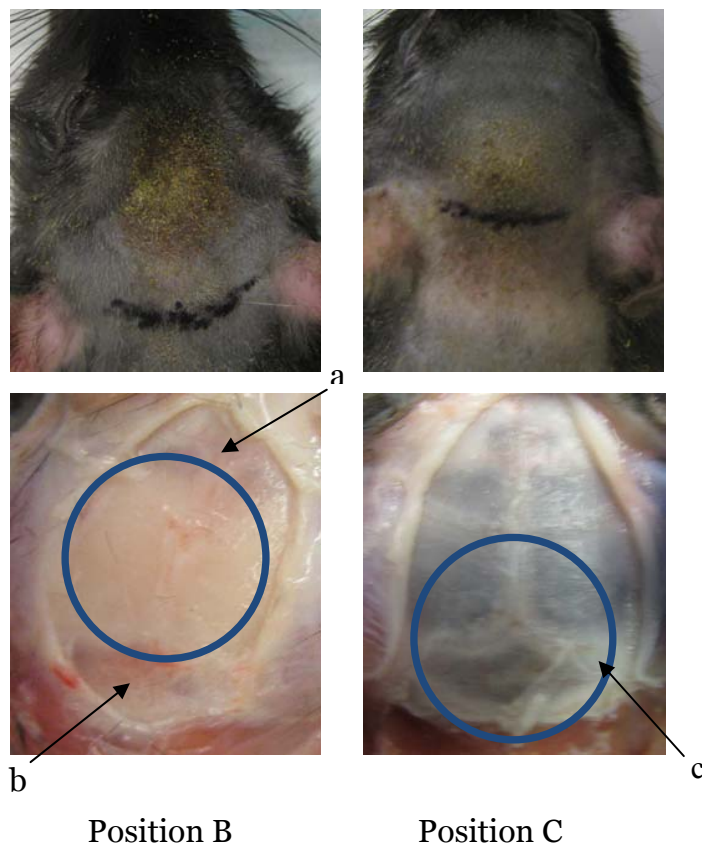


Figure 43. Blast-TBI of a rat head: BDC positioned Rostral (position B)-mild subdural hemorrhage frontal cerebral (a), and near cerebellum (b). BDC positioned caudally (position C)-massive subdural hemorrhage covering cerebra, cerebellum, and cervical spine (c). Circle represents the blast area.

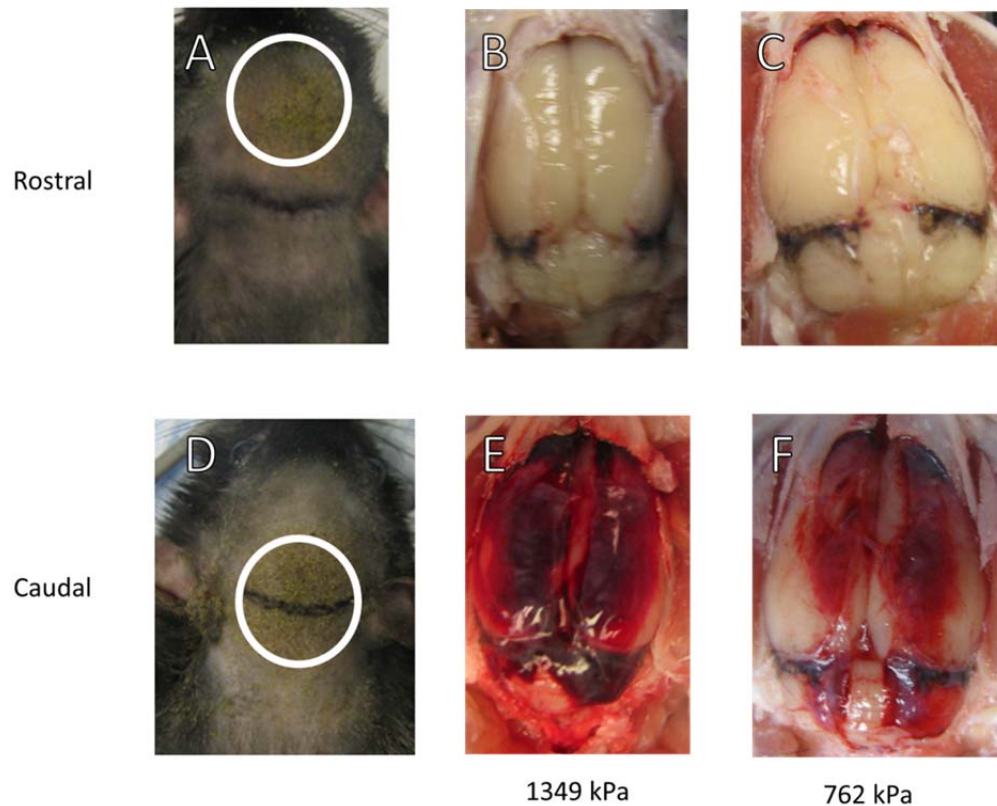


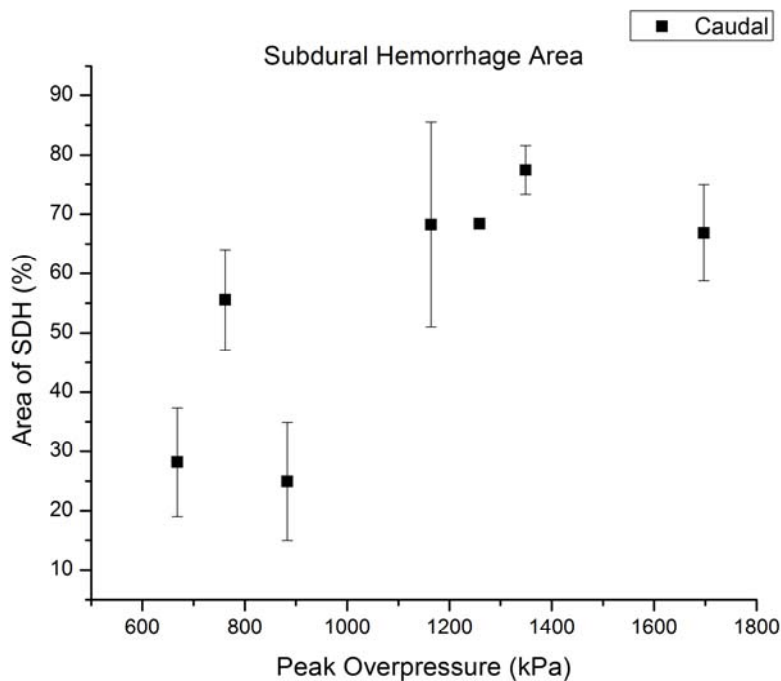
Figure44. FM blast injury causes subdural hemorrhages. Animals in the top row (**A-C**) were blasted in the B position, while animals in the bottom row (**D-F**) were blasted in the FM position. The first image (**A,D**) was taken immediately post-blast injury, and the occipital crest was manually palpated and marked with black permanent marker. The second and third images (**B-C,E-F**) were taken during necropsy 24 hours post-blast. Animals in B and E were exposed to a peak overpressure of 1349 kPa, while animals in C and F were exposed to a peak overpressure of 762 kPa.

Problem encountered

We noticed if the blast was induced caudal to the rat's head, it was more deadly than if it was rostral, and the macroscopic pathology was more severe in the caudal which accompanied with massive subdural hemorrhages covering cerebra, cerebellum and cervical spine. (Fig.44) vs rostral when there was mild to moderate subdural hemorrhage on cerebellum and on frontal cerebral (Fig.44). This might explain the non-significant results with the glibenclamide treatment groups, as we noticed the apnea in the glibenclamide treated rats was significantly higher in the 29.5cm BDC Blast-TBI group compared with the same intensity blast vehicle treated group (Fig. 35). There was also higher apnea in the 24.5cm BDC blasted glibenclamide treated group compared with the same intensity blasted rats treated with vehicle. (Fig. 32)

Resolution of the problem

We further established two different blast positions, B (rostral) and C (caudal) to establish the benefit of protecting the brainstem no matter what intensity levels were used to induced blast-TBI (Fig. 44). We studied the apnea and mortality between these groups using high intensity levels of blast. We further studied the early (5 days) histological changes in the brain tissues of these groups. (Fig. 50, 51). The position B group rats did not have mortality even with the highest levels of blast (1372 kPa) and the subdural hemorrhage was minimal along the cerebellum and frontal cerebral, very mild on medial cerebral (fig 44); while the mortality rate with position C (caudal) was 100% with most of the BDCs studied, we had 50% mortality with this position only with the 427kPa level of blast. This was even further with the pulse oximetry up to 30 min after blast (Fig.46), and throughout the behavioral tests; accelerating rotorod (Fig. 47), beam walk and beam balance (Fig.48), and much later on the cognitive Morris watermaze tests (Fig. 49).



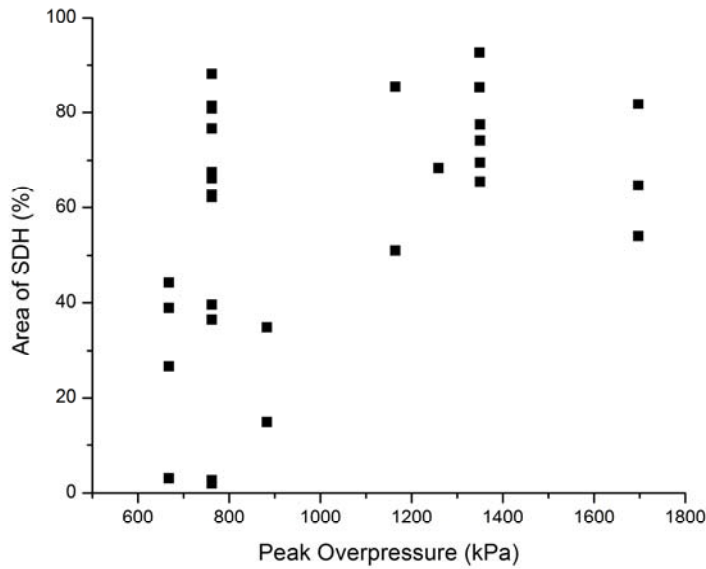
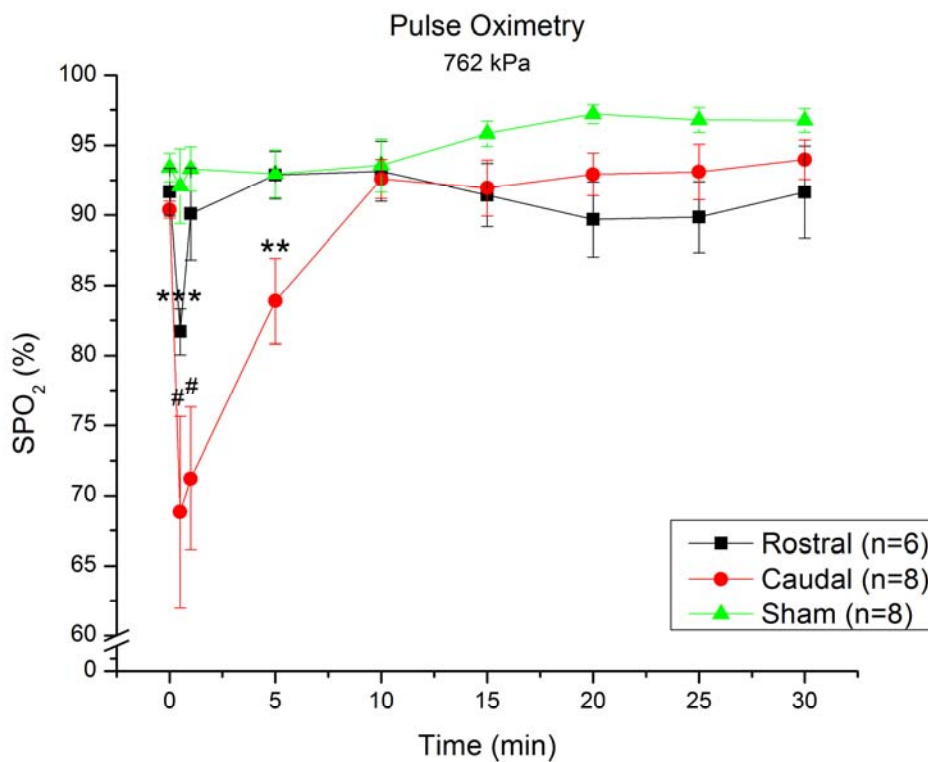


Figure 45. Subdural Hemorrhage area over the superior cortex and cerebellum regions was quantified using images obtained during ne



hours post-injury. crowsy 24

Figure 46. Oxygen saturation levels in the FM group are significantly depressed for 5 minutes post-blast injury compared to sham and B groups. Compared to B, the FM group has depressed oxygen saturation at 30 seconds, 1 minute, and 5 minutes ($p < 0.001$, $p < 0.0001$, $p < 0.01$ respectively).

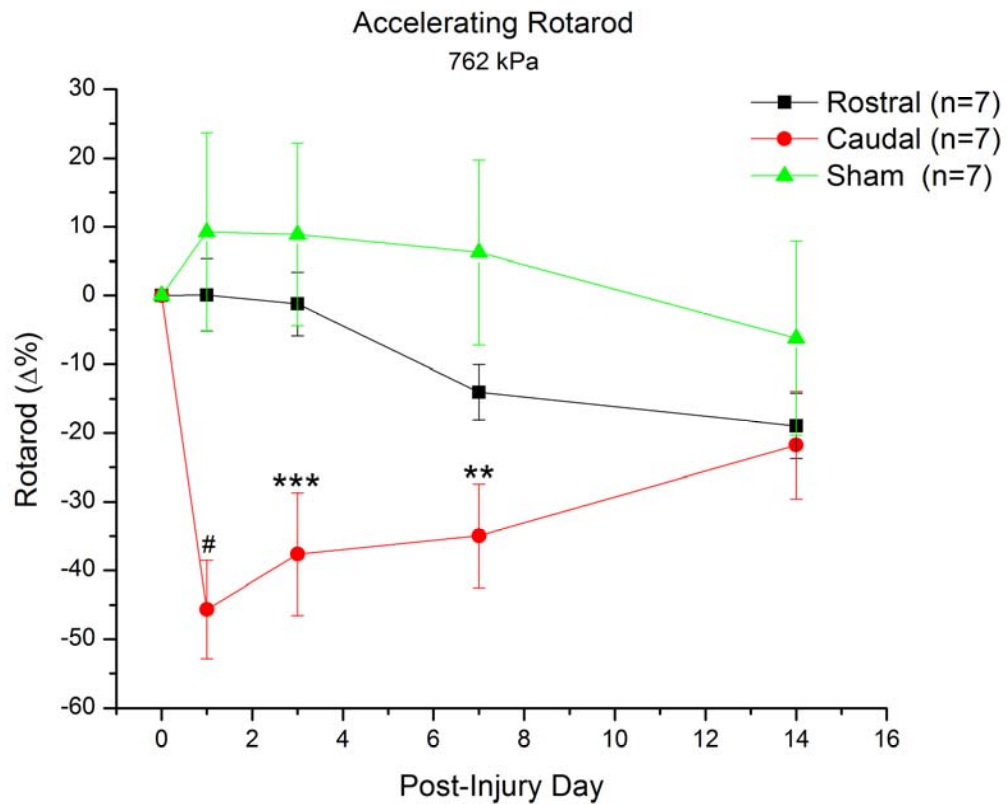


Figure 47. Animals injured in the FM position showed accelerating rotarod deficits up to 7 days post-injury.

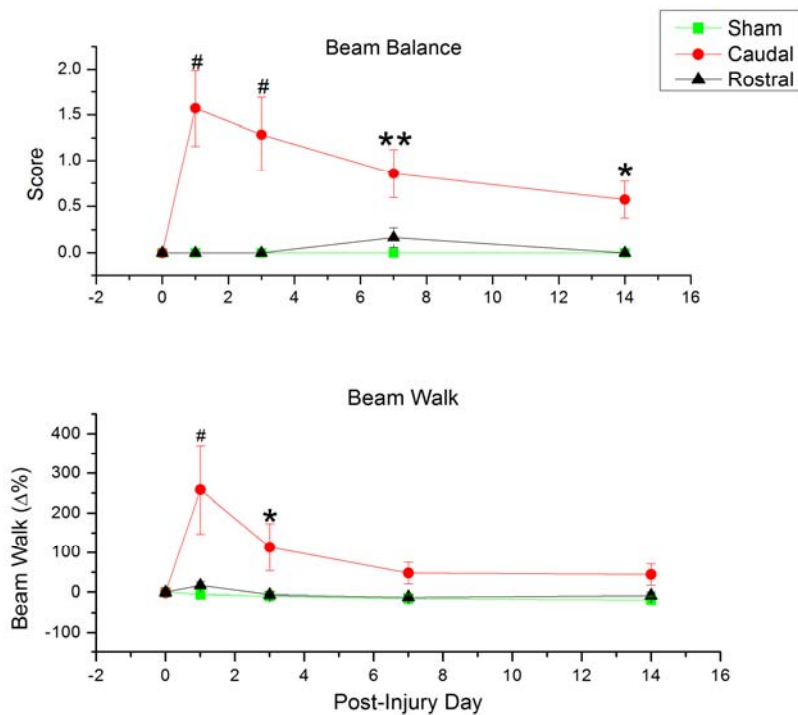


Figure 48. Animals in the FM group had beam walk deficits up to 3 days post-injury, and beam balance deficits 14 days post-injury.

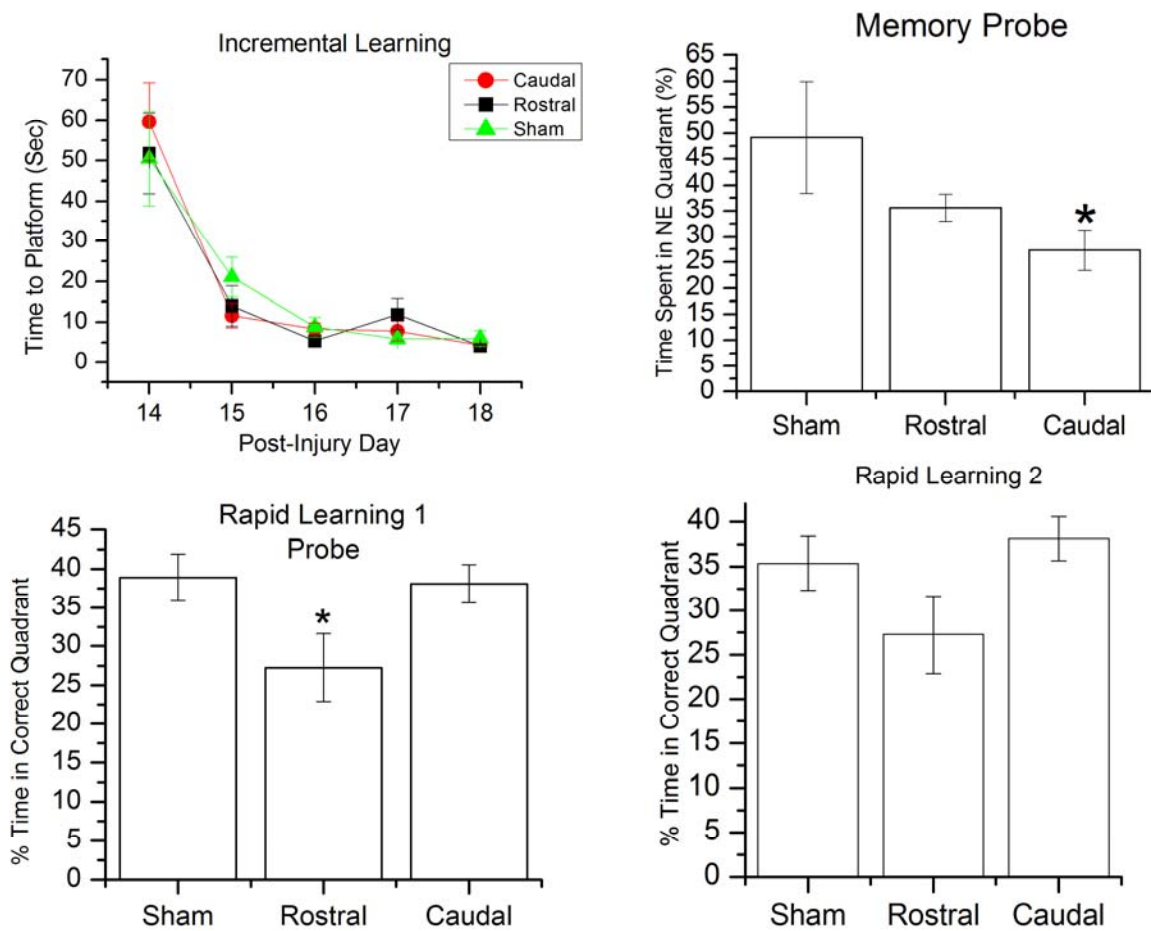
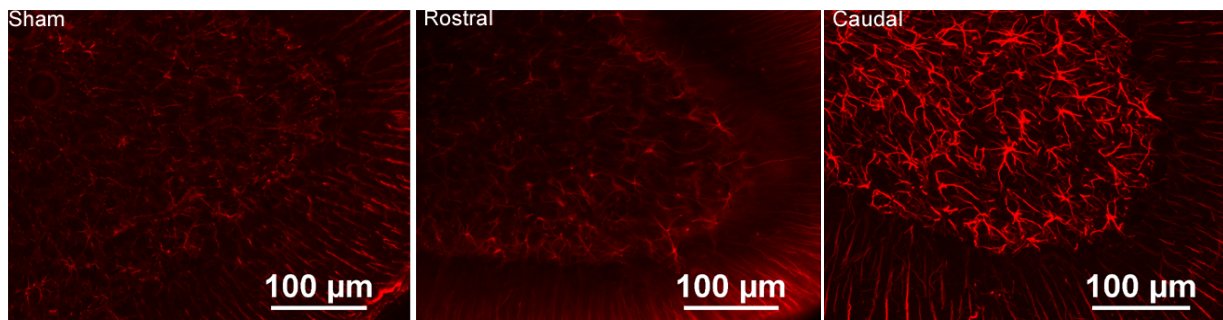


Figure 49. FM injured rats show decreased recall during the memory probe of the Morris Water Maze, but do not show decreased acquisition times during incremental learning. B injured rats show rapid place learning deficits 21 days post-injury. * $p < 0.05$

Immunohistochemical Analysis: Reactive astrogliosis 5 days post Blast TBI (Rostral vs Caudal)

A



B

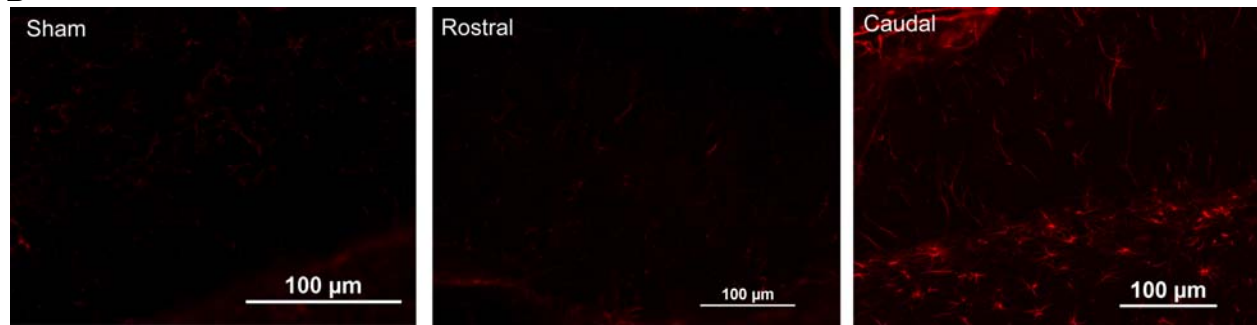


Figure 50. Immunohistochemistry 5 days post Blast-TBI caudal vs rostral positions, immunolabelled with GFAP. A) Cerebellum of sham, rostral and caudal Blast-TBI. B) Hippocampus of sham, rostral and caudal Blast-TBI.

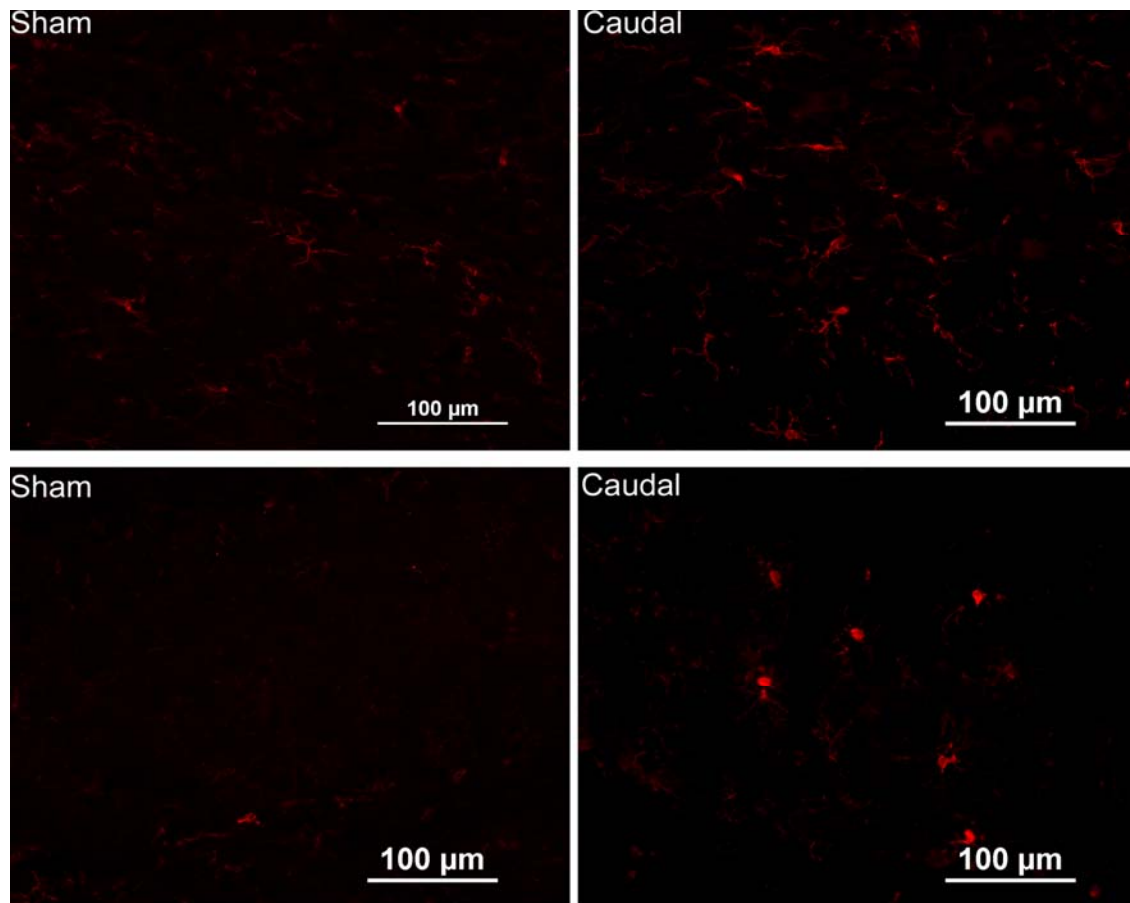


Figure 51. Immunohistochemistry 5 days post Blast-TBI sham vs. caudal Blast-TBI position, immunolabelled with GFAP. A) Brainstem of sham and caudal Blast-TBI. B) Hippocampus of sham and caudal Blast-TBI.

Appendix A. Glyburide Study Schedule of Events

Glyburide Study Schedule of Events (all procedures are for **RESEARCH PURPOSES** only)

Glyburide Study Schedule of Events

	Pretreatment Phase			Treatment Phase	Treatment Day 7	Study Day 8
Study Day	Pre-Screening^a	Screening Visit	Day 0	Days 1 to 6	Day 7	Day 8 **6 AM
<u>Informed Consent</u>		<u>X</u>	<u>X</u>			
<u>Inclusion/Exclusion Criteria</u>		<u>X</u>				
<u>Medical History and Demographics</u>		<u>X</u>				
<u>Blood Sample Collection</u>		<u>X^b</u>		<u>X^g</u>	<u>X^g</u>	
<u>Urinalysis (for toxicology & analysis)</u>		<u>X</u>	<u>X</u>			
<u>Serum Pregnancy Test</u>		<u>X</u>				
<u>Urine Pregnancy Test</u>			<u>X</u>			
<u>Physical Examination^c</u>		<u>X</u>		<u>X</u>	<u>X</u>	
<u>ECG</u>		<u>X</u>		<u>X</u>	<u>X</u>	
<u>Treadmill Activity</u>		<u>X^d</u>		<u>X^h</u>	<u>X</u>	
<u>Randomization</u>			<u>X</u>			
<u>Study Drug (Glyburide or Placebo) Administration</u>				<u>X</u>	<u>X</u>	
<u>Study Assessment</u>				<u>Xⁱ</u>	<u>Xⁱ</u>	
<u>Blood Sugar Measurement</u>				<u>X^j</u>	<u>X^j</u>	
<u>Cognitive/Dexterity Tests (CANTAB tests)</u>		<u>X^e</u> <u>*baseline</u>			<u>X^e</u> <u>*completion</u>	
<u>Provide Planned Meals (per dietary dept. schedule)</u>				<u>X^k</u>	<u>X^k</u>	
<u>Provide Planned Snacks/Beverages (with study medication as needed and at bed time)</u>				<u>X^k</u>	<u>X^k</u>	
<u>Assess for Adverse Events</u>		<u>X</u>	<u>X</u>	<u>X</u>	<u>X</u>	<u>X</u>
<u>Pharmacokinetic Sample</u>				<u>X</u>	<u>X</u>	
<u>IV placement</u>			<u>X^f</u>			
<u>IV Discontinuation</u>						<u>X</u>
<u>Study Discharge</u>						<u>X</u>

*****ALL PROCEDURES BEING PERFORMED DURING THE STUDY ARE FOR RESEARCH PURPOSES ONLY.**

^a Prescreening consists of a phone call in which participants respond to recruitment advertisements about the study by calling the research contact information and are provided with a description of the study and statements that describe what is required for study participation. No participant information will be collected.

^b Laboratory assessments include the following: complete blood count, electrolytes, liver function, kidney function, uric acid, cholesterol, iron, Hgb A1C

^c Physical Exam will consist of vital signs and a head to toe assessment.

^d Treadmill for 30 continuous minutes at a minimum of 4 RPMs to assess for ability to participate in this type of strenuous activity throughout the study. Subjects will not be included if unable to endure this activity (i.e. experience fatigue, dizziness, or chest pain during this exercise test).

^e Subjects will undergo neuropsychological testing using CANTAB during screening (baseline) and on Study Day 7 or Study Completion for subjects who are withdrawn early from study.

^f IV will be placed for blood sample collection on Study Day 1 and will be replaced as needed.

^g Laboratory assessments include the following: complete blood count, electrolytes, liver function, kidney function, uric acid, cholesterol, iron, and glyburide level.

^h Subjects will be scheduled to exercise at a moderate pace (at a minimum of 4 RPMs) on the treadmill for 30 continuous minutes in the morning and after lunch (see procedures section for specific details) and for 15 continuous minutes after dinner while on study.

ⁱ Study assessments will include observing for any signs and symptoms of distress (i.e. pallor, shaking, confusion, dizziness, chest pain, etc.) measuring vital signs (temperature, heart rate, blood pressure) and a neurological assessment using the Mini Mental Status Exam (MMSE).

^j Blood sugars will be measured (collected from IV in place, or by fingerstick or phlebotomy for circumstances where the IV is not working properly or has to be replaced) at scheduled intervals 4 times per day, including at bedtime, and as needed (subject feels dizzy, sweating, etc., bedtime glucose trending down or low).

^k Subjects will be asked to complete a food diary detailing everything they have eaten and had to drink and the amount they consumed of each food/drink during each study day (including snacks).

Appendix B. Glyburide Stopping Rules/AE Reporting
Glyburide Healthy Human Subjects Study Data Safety Monitoring Plan
and Stopping Rules

Patient safety is of paramount importance in this trial and there is an extensive set of procedures in place for monitoring adverse events. These procedures are as follows:

I. Research Monitor

For research determined to be greater than minimal risk, DoDI 3216.02 requires that the IRB approve, by name, an independent research monitor with expertise consonant with the nature of risk(s) identified within the research protocol. We have appointed Jessica Smith, MD to the role of the Research Monitor. Dr. Smith is a physician within the Department of Anesthesiology and Critical Care. Her duties will include but may not be limited to the following:

1. Discussing the research protocol with the investigators;
2. Be the Data Safety Monitoring Board (DSMB) Leader and schedule meetings;
3. Speak with human subjects to ensure ongoing understanding of study related procedures and their continued interest in participating or withdrawing from study, serving as their advocate;
4. Shall have authority to stop a research protocol in progress, remove individual human subjects from a research protocol, and take whatever steps are necessary to protect the safety and well-being of human subjects until the IRB can assess the monitor's report;
5. Shall have the responsibility to promptly report their observations and findings to the IRB or other designated official and the HRPO

II. Data Safety Monitoring Board (DSMB)

A Data Safety Monitoring Board (DSMB) appointed by Dr. Bochicchio, Principal Investigator of the study, will meet once a month and as needed to review the progress of this study (e.g., enrollment, site performance) as well as data on the safety of both arms of the study. The Research Monitor, Jessica Smith, MD will lead the DSMB meetings. Before the study begins, the DSMB (in consultation with the study statistician and PI) will decide the content of the reports to be presented to the board and the frequency and timing of interim efficacy and futility analyses. Using guidelines established by the DSMB and the investigators before the study begins, the DSMB may recommend termination of the study if the treatment arm (study drug arm) is found to be unsafe. Additionally, the DSMB may recommend modifications to the protocol if a correctable safety issue is identified. After each meeting, the DSMB Leader (Jessica Smith, MD) will prepare a report to be submitted to the study principal investigators, Drs. Grant Bochicchio and J. Marc Simard, which will describe the safety review that

took place at the meeting and whether or not there are any safety concerns. This report will be provided to the IRB according to their policies and procedures.

We have appointed a very qualified physician to lead the DSMB as the Research Monitor. Dr. Jessica Smith will review all adverse events in the study as they occur. In addition, Dr. Smith will specifically monitor the serial glucose levels of the first 5 patients receiving study drug for any abnormal glucose levels or any change in cognition (i.e. dizziness, confusion, etc.) experienced by participants.

Dr. Smith will report safety concerns that arise during the trial to the PI and study team. Dr. Smith will direct the monthly meetings of the DSMB and will discuss any concerns about adverse events with the DSMB.

III. Principal Investigators

Drs. Bochicchio and Simard will be informed of the DSMB's monthly assessment of study performance and safety.

IV. Data Safety Monitor Board Members:

* Dr. Jessica Smith, Research Monitor and DSMB Leader (Clinical Instructor, Anesthesia)

Dr. Lee Skrupky (Clinical Pharmacy Specialist, Critical Care)

Beth Taylor (Nutrition Support Specialist MS, RD, CNSD, FCCM)

V. Events to be Reviewed by DSMB:

- All adverse events (AEs), regardless of relationship to study drug will be reviewed once a month by the DSMB.
- All SAE's will be reviewed by the PI and Data Safety Monitor within 24 hours of their occurrence.
- All ***Unexpected , Serious Adverse Events*** (SUA'S) thought to be related to study drug **will be reported to the PI and Data Safety Monitor and IRB immediately**. Emergency medical treatment will be provided as necessary and study participation will be placed on hold pending outcome of the event.

STOPPING RULES: Subjects who experience Unanticipated Serious Adverse Events will be temporarily placed on hold from study drug administration until the etiology of the event and the relationship to the study drug are evaluated. Subjects who experience ***Unanticipated Serious Adverse Events (SUA's) determined to be RELATED to study drug will be withdrawn from the study***. If any subject experiences a SUA/s, or if a permanent injury or disability/death occurs, the trial will be stopped pending further review with the Research Monitor, PI, and IRB. This is necessary due to the extensive safety data already available which has detailed all expected adverse events observed in subjects receiving glyburide. Therefore, any occurrence that would be Unexpected and Serious in nature

would be extremely rare and would warrant a full investigation to protect the safety and welfare of participants. In addition, **the Research Monitor shall have authority to stop this research protocol in progress, remove individual human subjects from this research protocol, and take whatever steps are necessary to protect the safety and well-being of human subjects until the IRB can assess the monitor's report.**

Appendix C.

Glyburide concentration (ng/mL) in clinical sample

<u>ID</u>	<u>#</u>	<u>Day 1</u>	<u>Day 2</u>	<u>Day 3</u>	<u>Day 4</u>	<u>Day 5</u>	<u>Day 6</u>	<u>Day 7</u>
1245-01	2	< LLOQ (2 ng/mL)	< LLOQ (2 ng/mL)	< LLOQ (2 ng/mL)	< LLOQ (2 ng/mL)	71.7	14.5	< LLOQ (2 ng/mL)
1245-05	2	< LLOQ (2 ng/mL)	< LLOQ (2 ng/mL)	< LLOQ (2 ng/mL)	< LLOQ (2 ng/mL)	< LLOQ (2 ng/mL)	< LLOQ (2 ng/mL)	< LLOQ (2 ng/mL)
1245-10	2	< LLOQ (2 ng/mL)	< LLOQ (2 ng/mL)	< LLOQ (2 ng/mL)	4.91	5.34	2.73	27
1245-11	2	< LLOQ (2 ng/mL)	2.11	4.17	15.7	6.64	13.9	3.5
1245-16	2	< LLOQ (2 ng/mL)	< LLOQ (2 ng/mL)	< LLOQ (2 ng/mL)	< LLOQ (2 ng/mL)	< LLOQ (2 ng/mL)	< LLOQ (2 ng/mL)	< LLOQ (2 ng/mL)
1245-17	2	< LLOQ (2 ng/mL)	< LLOQ (2 ng/mL)	< LLOQ (2 ng/mL)	< LLOQ (2 ng/mL)	< LLOQ (2 ng/mL)	< LLOQ (2 ng/mL)	< LLOQ (2 ng/mL)
1245-20	2	< LLOQ (2 ng/mL)	2.23	5.14	11.3	7.26	< LLOQ (2 ng/mL)	75
1245-21	2	32.7	30.9	72.4	61.4	9.32	80.2	64.9
1245-23	2	15.9	31.5	77.1	66	19.4	< LLOQ (2 ng/mL)	< LLOQ (2 ng/mL)
1245-25	2	< LLOQ (2 ng/mL)	8.43	18.1	14.7	17.2	42.9	10.4
1245-28	2	6.24	< LLOQ (2 ng/mL)	5.95	45.7	2.55	55.7	4.51
1245-29	2	< LLOQ (2 ng/mL)	< LLOQ (2 ng/mL)	< LLOQ (2 ng/mL)	< LLOQ (2 ng/mL)	< LLOQ (2 ng/mL)	< LLOQ (2 ng/mL)	< LLOQ (2 ng/mL)
1245-33	2	< LLOQ (2 ng/mL)	< LLOQ (2 ng/mL)	< LLOQ (2 ng/mL)	< LLOQ (2 ng/mL)	< LLOQ (2 ng/mL)	< LLOQ (2 ng/mL)	< LLOQ (2 ng/mL)
1245-34	2	< LLOQ (2 ng/mL)	5.05	8.34	< LLOQ (2 ng/mL)	22.5	91.2	57.9
1245-37	2	< LLOQ (2 ng/mL)	2.81	10.8	6.95	6.03	7.68	3.32
1245-41	2	6.18	21.2	53.3	31.3	23.5	9.2	6.81
1245-42	2	4.96	54.2	14.9	36.4	74.2	33.7	39.4
1245-43	2	< LLOQ (2 ng/mL)	< LLOQ (2 ng/mL)	< LLOQ (2 ng/mL)	< LLOQ (2 ng/mL)	< LLOQ (2 ng/mL)	< LLOQ (2 ng/mL)	< LLOQ (2 ng/mL)
1245-44	2	< LLOQ (2 ng/mL)	21.5	53.9	9.03	31.9	31.3	23.4
1245-46	2	< LLOQ (2 ng/mL)	< LLOQ (2 ng/mL)	< LLOQ (2 ng/mL)	< LLOQ (2 ng/mL)	< LLOQ (2 ng/mL)	< LLOQ (2 ng/mL)	< LLOQ (2 ng/mL)
1245-48	2	< LLOQ (2 ng/mL)	50.5	4.99	83.2	3.86	58.8	< LLOQ (2 ng/mL)